Addis Ababa University
School of Earth Sciences

Slope Stability and Sensitivity Analysis Based on Monitoring Data:

A case of Colluvial Slope failure in the Abay Gorge, Central Ethiopia.

Advisor: Dr. Zemenu Geremew

Submitted by Mihret Manaye

A Thesis submitted for the partial fulfilment of the requirements for the Degree of Masters of Science (Engineering Geology)

Addis Ababa University
Addis Ababa
May, 2018

Addis Ababa University
School of Earth Sciences

Slope Stability and Sensitivity Analysis Based on Monitoring Data:

A case of Colluvial Slope failure in the Abay Gorge, Central Ethiopia.

Advisor: Dr. Zemenu Geremew

Mihret Manaye

A Thesis submitted for the partial fulfilment of the requirements for the Degree of Masters of Science (Engineering Geology)

Addis Ababa University
Addis Ababa
May, 2018

DECLARATION

Addis Ababa University

School of Graduate Studies

This is to certify that the thesis prepared by **Mihret Manaye**, entitled: "**Slope Stability and Sensitivity Analysis Based on Monitoring Data: A case of Colluvial Slope failure in the Abay Gorge, Central Ethiopia**" and submitted in partial fulfilment of the requirements for the Degree of Master of Science (Engineering Geology) complies with the regulations of the University and meets the accepted standards with respect to originality and quality.

Signed by the Examining Committee:

Chairman _____ Signature _____ Date _____

Advisor _____ Signature _____ Date _____

Examiner _____ Signature _____ Date _____

Examiner _____ Signature _____ Date _____

Abstract

Evaluation of stability and sensitivity of recurrent landslides involving colluvium materials resting on gentle topographic slope has been carried out along multiple profiles in a landslide zone. The aim is to attempt integrating multiple profile stability analysis into semi- 3D stability model by weighting the factors of safety obtained in the 2D case with the cross-sectional area the above the slip surface of each profile. The 2D and semi- 3D models were implemented in Microsoft Excel spread sheet program using the simplified Janbu's method. The selected landslide area is located in the Abay Gorge between the towns of Gohatsion and Dejen, on the northern side of the Gorge.

In total, 6 profiles which were aligned approximately parallel to the axis of the landslide from head to toe were evaluated. As the materials are colluvial and deep seated the depth to the slip surface, based on monitoring wells installed in the site, were used to back calculate shear strength parameters using stability charts of Janbu. The back analysis gave residual effective shear strength parameters of (5.7 KPa, 12.6^0) for profile 8; (5.2 KPa, 11.6^0) for profile 9; (3.3 KPa, 11.9^0) for profile 10; (0 KPa, 11.6^0) for profile 11; (3.6 KPa, 11^0) for profile 14; (1.7 KPa, 12.2^0) for profile 15 and (0.3 KPa, 11.8^0) for profile 16.

The Simplified Janbu's method of 2D stability analysis at conditions of back analysed shear strength values and the determined water level from site investigation for each profile gave 2D factors of safety as: 1.94, 1.37, 0.84, 1.03, 0.73, 1.06 and 1.08 for profiles: 8, 9, 10, 11, 14, 15 and 16 respectively. The corresponding semi- 3D factors of safety computed by integrating the 2D factors of safety weighted by the respective cross-sectional area was 1.01.

The influence on stability was assessed based on the sensitivity of the 2D and semi- 3D factors of safety to the independent changes in value of the shear strength parameters and water level, one at a time. Accordingly three selected profiles in the 2D and all the profiles in the semi- 3D cases showed marked sensitivity to changes in friction angle while the factors of safety had lowest sensitivity to the changes in cohesion. The sensitivity to changes in level of water gave intermediate change in both 2D and semi- 3D factors of safety. The low effect of change in cohesion on the factors of safety might be due to the progressive nature of the landslide.

Although simplified and inexpensive methods to analyse the slope stability in semi- 3D approach have been attempted the expected results are not conclusive for various reasons

among which are mixed success with back analysis from slip surface location, and uncertainty in the continuity of the slip surface. Unexpected lower value of the 3D factors of safety might be hence improved by considering solutions to the determination of shear strength parameters and also ascertain continuity of the analysed landslide throughout the model.

Acknowledgment

First of all, I thank the almighty God.

Next, my gratitude goes to my adviser Dr. Zemenu Geremew for his guidance, valuable comments and scientific thinking he tried to instil in me. I had gained a lot in critical reviews and developing scientific perspectives of problems in geological engineering. I am also indebted to Dr Tarun Kumar Raghuvanshi for his valuable advices and lessons in the "Research Methods in Geosciences'', which lessons taught me a lot to immensely improve the thesis. Many thanks are also extended to all staff members of the School of Earth Science, Addis Ababa University for all the instructions I have been provided. I am gratefully to Geological Survey of Ethiopia (GSE), for making their vast resources public and being cooperative.

My special thanks go to my dear, kind and loving husband, Lut, who has always been a constant source of support and encouragement during the challenges in the school and beyond. You are a wonderful husband and really fabulous father to our daughter Hawi. I am truly thankful for having you in my life.

In loving memory of my dear Brother, Yoni

Contents

List of Figures

List of Tables

Annexes

Acronyms

2D two dimensional

3D three dimensional

C: cohesion

ERA: Ethiopian Roads Authority

FoS: Factor of safety

GPS: Global positioning system

GSE: Geological survey of Ethiopia

JICA: Japan International Co-operation Agency

LEM: Limit Equilibrium Method

m a.s.l: meters above sea level

NMAE: National Meteorological Agency of Ethiopia

USBR: United States Bureau of Reclamation

1. Introduction

The study is conducted on the landslides occurring along the main road between Gohatsion and Dejen. These slopes have been subject of several investigative studies and counter measure design studies (Almaz and Tadesse, 1994; Lulseged Ayalew and Yamagishi, 2003; Bisrat Yifru and Fasika Ayehu, 2017; Matebe Meten et al., 2015; JICA AND GSE, 2012). Such studies have generated a good deal of data and information on the activity and extents of the landslides in more detail. This initiates to look into possibilities to carry out non-conventional methods of stability analysis which can be considered an interesting scientific problem to address.

1.1 Problem statement

The main focus of the thesis is to address the following points by testing and comparing with earlier published studies on landslides. An attempt is made to carryout 3D evaluation of selected landslides in the Abay Gorge. The presence of extensive references and data sets in this well-studied area provides suitable setting against which comparisons and references can be readily made between various approaches of analysis (e.g. 3D and 2D analysis) and contribute to develop a more realistic evaluation of the slope stability models which mimic the natural setting. This study however is by no means supposed to be a true 3D modelling which is still at infant stage and more complex rendering it beyond scope of the current study. Nevertheless, other means of estimating factors of safety not restricted to single profiles but multiple profiles in the same landslide can be weighted and combined to give alternative approach to the more complex 3D analysis. Following are the problems to that are anticipated to be answered in the proposed research.

1.2 Research Questions

What simplified approaches can be used to approximate 3D slope stability that can work when monitoring data and investigative data are available for major landslides?

How well do 2D slope stability analysis results compare with the adopted approximate semi-3D stability analysis?

How well do terrestrial monitoring data serve to derive valuable information that can aid in modelling and quantitatively analyse the stability of active landslide?

What counter measure interventions and dynamic natural phenomena significantly affect stability of the landslides studied?

How well can parameters often not representative when tested in the laboratory be acquired from indirect calculation based on other known parameters?

1.3 Objective

General objective of the proposed research is to develop and contrast the conventional slope stability conditions and sensitivity with that of a less used but promising stability assessment in the 3D space.

Specific Objectives

- To implement simple approach to approximate 3D factor of slope stability on selected landslide considering multiple slope profile consideration at every instant of landslide which have sufficient data on subsurface landslide monitoring and physical attributes.
- To carry out back analysis methods for estimating some of the physical parameters not reliably or directly measurable but which can better be constrained by back analysis (shear parameters)
- To compare the results obtained by the approximate 3D factor of safety estimate with that of conventionally obtained 2D slope stability factor of safety assessment (which is based on consideration of the most critical single slope profile).
- To assess sensitivity of developed models to the driving factors of stability using the monitoring data available on the analysed slopes (groundwater, cohesion, internal friction angle).

1.4 Significance of the study

The research is conducted on a selected landslide which has been well constrained in terms of activity, geometry and material properties by previous researchers. The significance of the study is that it gives possibility to test the non-conventional and rarely applied but more realistic approach to landslide assessment. Such approaches have not been attempted in Ethiopia and this can be an opportunity to extend the slope stability assessment into various scientific domains. The study contributes to the current knowledge by testing the theoretical expectations against practical cases. Semi- 3D modelling proposed method generally added important considerations to the better constrain and understand the stability conditions of the

landslides than in case of 2D model. The consideration of multiple slope sections in inhomogeneous material and variable geometry of landslides has better merits in representing the real condition than 2D models. Factors of safety derived using selected slope profiles with highest instability will always result in more conservative values leading to exaggerated instability which in turn leads to unnecessary exaggerated cost of counter measures and amplification of risk. The semi- 3D approach on the other hand is better at giving less conservative value and hence helps to derive a more realistic or economical cost for stabilization or evaluation of risk.

It also demonstrated the adequacy of monitoring data to derive various parameters of the landslides used for the analysis. The implementation of the stability in common commercial software of Microsoft Excel spread sheet program gives the research additional contribution for further use as educational and even practical purposes.

1.5 Adopted Methodology

In the study both secondary and field observation are employed where a number of published and unpublished literature exist. In the research a review of the current knowledge about nature and activity of the landslide in the Abay Gorge was the first task. This helped to capture the geological models already developed for the area by various investigators and incorporate the relevant findings. After selecting most appropriate specific landslide site, a reconnaissance field visit was made for documentation of current state of the landslides and familiarization with the site. The main part of the research was then carried out which concerns analysis and evaluation of monitoring data obtained from the archive of the Geological Survey of Ethiopia and carrying out back analysis, stability analysis and sensitivity analysis in 2D space. This was followed by developing the semi 3D slope stability model after Lambe-Whiteman's example (Lambe and Whiteman, 1969) and carrying out stability and sensitivity analysis for it. The pertinent data from the landslide sites investigation by GSE-JICA was available for public at the library of the GSE in soft and hard copy.

Back analysis are on the other hand was implemented for the shear parameters based on the monitoring and investigative data of the Geological Survey of Ethiopia to derive reliable estimate as the materials involved in the slide are colluvium in nature and not suitable for sampling or testing in the lab. All the information obtained analysed and integrated to implement 2D and semi- 3D stability analysis stability and sensitivity are compared.

Influence of the dynamic parameters such as transient water level fluctuation as a result of rainfall variability, and variation in cohesion and internal friction angle on factor of safety were then tested by carrying out sensitivity analysis for both the 2D and the semi- 3D stability model that is developed. Brief account of the approaches followed is described in the next sub-sections.

Software used in carrying out the research is mainly Microsoft Excel spread sheet program which was developed and used for stability analysis of both the 2D and semi- 3D cases following the Janbu's factor of safety computation. The preparation of the slope geometric model on the other hand involved use of AutoCAD software by overlaying the various datasets including the topographic profile, borehole logs, refraction seismic profiles and monitoring results to construct the slope model. The ArcGIS version 10 software was then employed in extracting pertinent geometric information needed for carrying out the stability analysis where slicing and the geometric parameters were obtained using the spatial analyst and advanced editing tools of ArcGIS 10 version. The detail methodology is given in the chapter dealing with the detail methodology followed.

1.6 Outline of the Thesis

The thesis is structured into 7 chapters. The first chapter gives account of the research problem and set objectives as well as relevance of the thesis work. It also gives highlight of the overall research approach and methodology, as well as limitations and raises questions it tries to answer.

In chapter 2, thorough reviews of governing principles and theoretical background as well as case studies are presented. Only relevant conceptual formulations are described from published literary sources with less emphasis on well-established concepts and derivations of slope stability formulae except basic considerations. All the applied methods of the analysis have been attempted to be accounted in this chapter. The description of the study area then is continued with the main focus on the specific geographic location of the problematic area starting from regional over view for a clear orientation. All physiographic and geological and detail landslide characteristics are described in this chapter. Chapter 4 deals with the detail methodology adopted giving account of step by step procedures followed in the research in the order: preparation of the data set, back analysis, stability analysis in both 2D and Semi 3D cases, followed by sensitivity analysis of both 2D and semi- 3D models developed. The results are presented in Chapter 5 with figures and tables and basic description in the similar

order. The discussion follows in Chapter 6 with comments and aspects of the finding of the research in the scope of the present study again in similar order. Finally Conclusion is given in Chapter 7 summarizing and highlighting on relating the objectives and findings in the context of the current study.

2. Literature review

2.1 Landslides Processes

The term landslide is used in a general sense to describe all types of gravitational movements of earth material. Nevertheless, landslides can be classified according to variety of types and velocities of movement (Rotaru et al., 2007). With regard to velocity they can be any of extremely rapid to very rapid, rapid, moderate, slow, very slow and extremely slow with increasing content of water and fragmentation of the material involved in sliding (Varnes 1958, Cruden and Varnes 1996). Hence Fall, topple, slide spread and flow are in order of increasing speed when they occur, implying similarly increasing degree of risk. They also fall in any of the class in terms of occurrence or activity as active, reactivated inactive and so on (Varnes, 1978; Cruden and Varnes, 1996).

Landslides are parts of natural processes that might be only aggravated as a result of human activities which disturb the slope stability. These phenomena differ according to their shape, size of the displaced mass, moving mechanisms, velocity and other characteristics (Rotaru et al., 2007). They can occur on any terrain given the right conditions of soil, moisture, and the angle of slope. Part of the natural process of the earth's surface geology, landslide serves to redistribute soil and sediments in a process that can be in abrupt collapses or in slow gradual slides (Rotaru et al., 2007; Ayalew et al., 2003). Slope movements can take various mechanisms from rock topple to mudflow, and involve a variety of materials from hard rock to clay, and can result from a variety of triggering phenomena of rapid snowmelt, heavy rainfall, earthquakes or steepening of topographic slope (Rotaru et a., 2007).

A list of precursors is used to infer starting of instability of slopes. This includes emergence of springs, seeps, or saturated ground in areas that have not typically been wet before, new cracks or unusual bulges in the ground, street pavements or sidewalks, soil moving away from foundations, ancillary structures tilting relative to the main house, tilting or cracking of concrete floors and walls, disrupted drainage ditches, leaning telephone or electric poles, trees, retaining walls or fences, offset fence lines, sunken or down-dropped road beds, bulging and cracking of the ground, sudden decrease in stream water level in while under rain are all precursors indicating emergence of landslides (Ayalew et al., 2003; Rotaru et al., 2007).

There are three main conditions that control occurrence of mass wasting processes (Zaruba and Mencl, 1969) which can be visualized in the Figure 2-1.

(i) Slope gradient: The steeper the slope of the land, the more likely that mass wasting will occur.

(ii) Slope consolidation: Sediments and fractured or poorly cemented rocks and sediments are weak and more prone to mass wasting.

(iii) Water: If slope materials are saturated with water, they may lose cohesion and flow easily.

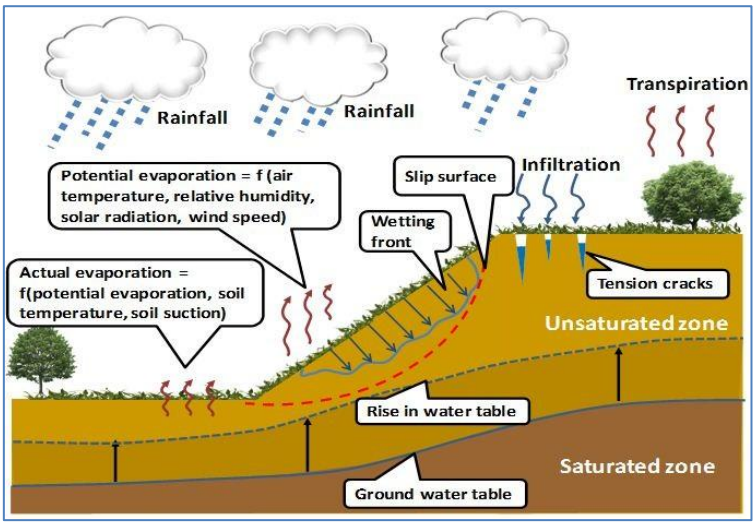

Figure 2-1 Schematic portray of slope system leading to instability (Rahardjo et al., 2012)

2.2 Landslide Monitoring

Landslide monitoring fall into two categories depending on the type of parameters that are monitored (JICA AND GSE, 2012). These are inducing factors monitoring and land slide displacement monitoring. The land slide monitoring includes all subsurface and surface physical as well as terrestrial and aerial remote scanning monitoring. Advanced monitoring techniques include use of radar interferometry and GPS data transmission. On the other hand the inducing factors monitoring includes incipient factors such as earthquake tremor, rainfall, groundwater level etc. These are often directly monitored physically except the rainfall that can also benefit from the satellite assisted rainfall data. Brief account of the most common physical based monitoring instruments and mechanisms are given in the next paragraphs as well as in Figure 2-2.

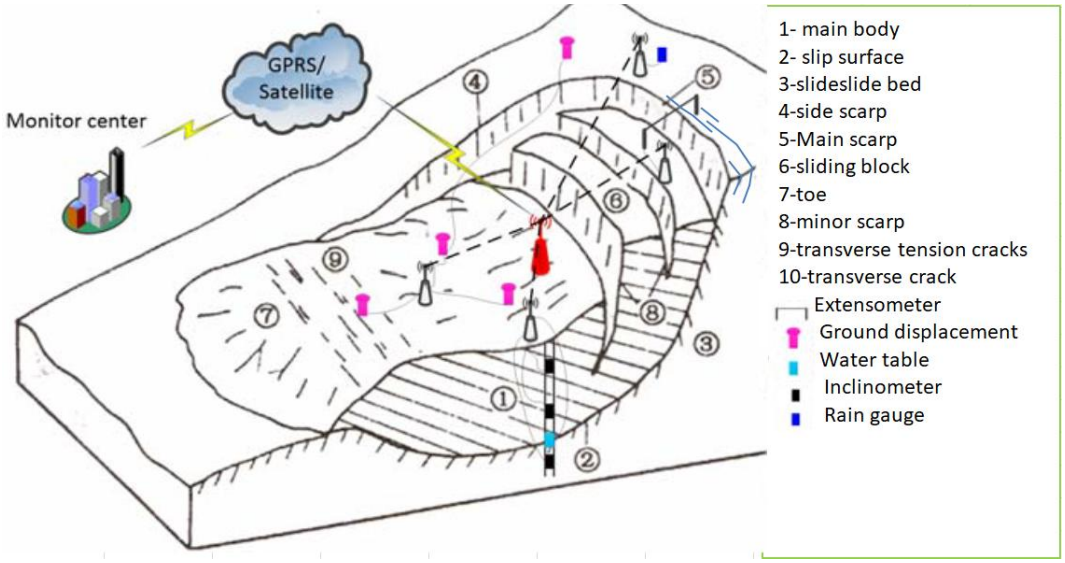

Figure 2-2 Sets of various monitoring data used in landslide investigation (modified after Neng-Pan et al., 2015).

Borehole inclinometer measurement

These are basically flexible aluminium tubes inserted to boreholes immediately after drilling and set to the whole depth (Figure 2-3). The method employs regular measurement of the inclination of the guide pipe that is installed in the borehole. When the guide pipe is installed in an active landslide, the guide pipe is bent by movement of the landslide that would be detected by comparing (subtracting) from the initial measurement. Measurements are taken every few meters of depth along the length (depth) of the pipe. If the guide pipe is not straight at the initial state, initial value of inclination should be measured at the time of installation. The method only works to some extent that pipe bends and is put out of use afterwards. But the data on slip surface is well apparent in active landslide including rate of displacement if measurement is made frequently and regularly (Savvaidis, 2003, JICA and GSE 2012).

Borehole Strain gauge

Similar to Inclinometer except that the strain gauge measures directly the stress at the various depth through installed electric pressure sensor transducers that transmit the pressure through wires to a switch board and data log on top of the borehole. As such the strain gauges provide far more data as compared to Inclinometer as they can still render useful after great extent of displacement (Savvaidis, 2003, JICA and GSE 2012).

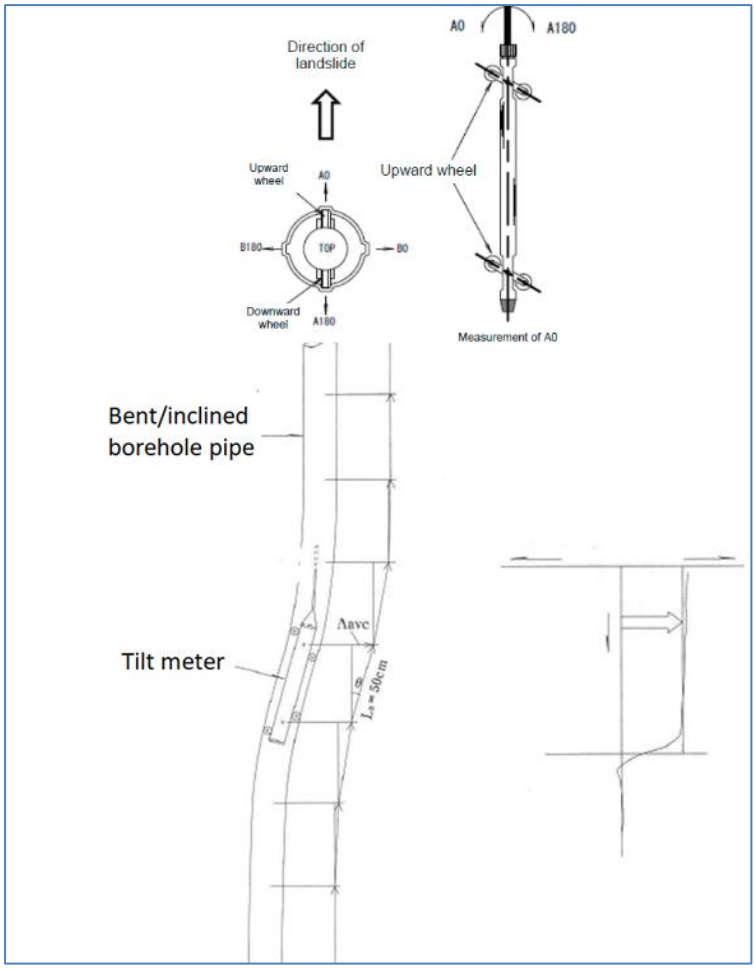

Figure 2-3 Demonstration of working mechanism of Inclinometer.

Borehole extensometer

Borehole extensometer is used to measure displacement incurred as a result of overall slope movement through extension of a special wire that is extended from the bottom anchored part at the bottom of the borehole to the top of the borehole where the wire is attached to a spindle that rotates up on extension of the wire (Figure 2-4). The displacement corresponds to overall displacement and this information cannot give information where the displacement took place and hence has not much use for determining slip surface but it can give information about the activity of the landslide (Savvaidis, 2003, JICA and GSE 2012).

A much similar mechanism is the surface extensometer which instead of being installed down borehole is fitted across surface cracks such as across tension cracks on crown of landslides. One end has to always rest on the unstable part of the ground and the other on the surface of the sliding mass.

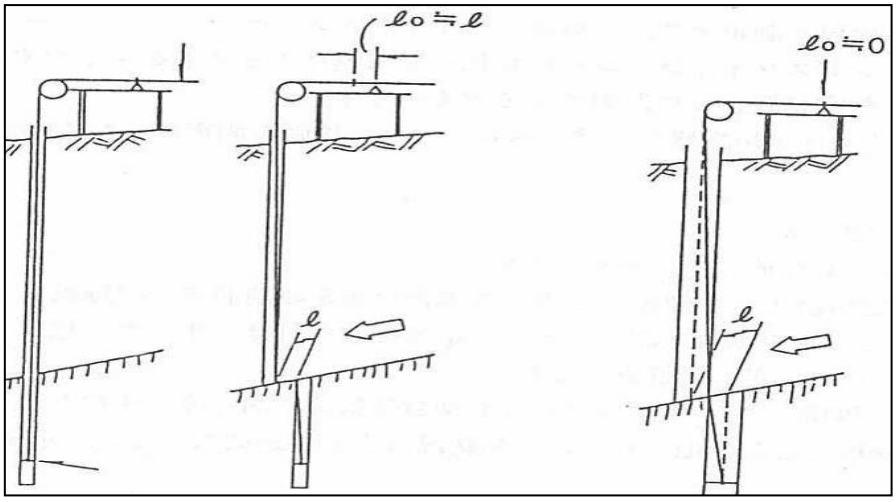

Figure 2-4 Demonstration of working mechanism of Borehole extensometer.

GPS survey

This method is to measure movement on the ground surface using GPS. The advantage is that the stations can be shifted around to follow the landslide activity. Nevertheless stations need to be fixed after the initial measurement until enough data has been acquired from particular station which can then be shifted again and used in similar manner lasting at least for whole cycle of the season. The advantage is that the data is able to be tele-transmitted and works well even at night or bad weather which is an advantage since early warning systems can rely on the data in bad weather when landslides are more likely to occur (Savvaidis, 2003; JICA and GSE 2012).

Groundwater monitoring

Groundwater level monitoring involves installing water level gauges well below the expected depth of critical water level. The fluctuation in the borehole corresponding to the piezometer line at the borehole is continually measured and transmitted to the data logger on top of the borehole. This is very important to link activity of the landslide with precipitation and inclinometer or extensometer derived displacement data where threshold levels of displacement and effective counter measures can be designed following the long term monitoring (Savvaidis, 2003; JICA and GSE 2012).

Rain fall is another triggering factor which affects the landslide through the influence of raising groundwater level or increasing the wetting front. Automatic Rain Gauges are nowadays very common and can detect rainfall at practically any time interval of every second to several hours' frequency. Since most are digital and automatic the data analysis and integration is also much efficient (JICA and GSE 2012).

2.3 General approach and Principle of Slope Stability Analysis

Landslides are defined as downward and outward movement of slope-forming materials composed of natural rock, soils, artificial fills, -or combinations of these materials (Varnes, 1958). Slope stability analysis techniques have been used to study landslides for more than four decades assuming simplified conditions or time effective analysis techniques such as the 2D limit equilibrium method (Reyes and Parra, 2014). The limit-equilibrium techniques are the most commonly-used analytical methods to investigate the stability of landslides, which consider the material of the sliding body as rigid body (Janbu, 1954; Bishop, 1955; Morgenstern and Price, 1965; Spencer, 1967; Guo and He, 2011). The Fellenius' method was further developed by researchers assuming the different conditions of inter-slice forces, such as Janbu (1954), Bishop (1955), Morgenstern and Price (1965), Spencer (1967). Limit equilibrium methods are widely applied to analyse the stability of two-dimensional landslides. These methods can be classified into circular methods (e.g. Swedish circle and friction circle methods), non-circular methods (e.g. log-spiral procedure), and methods of slices (e.g. Bishop's method; Janbu's method; Morgenstern and Price method; and Spencer's method (Kalatehjari and Ali, 2013).

2.3.1 2D LEM Slope stability models

The analysis of slope stability problem requires consideration of equations based on constitutive laws. The field equations are formulated by use of equilibrium equations while the later relates to description of soil behaviour. As the soil is inhomogeneous and complex in properties and even more complicated if considered in saturated conditions, several assumptions are made to justify treatment of soil as plastic material and perform classical stability analysis (Albataineh, 2006).

The soil is hence assumed to have properties that conveniently can be expressed by shear strength parameters of cohesion (c) and internal friction angle (φ). What is more, these parameters are that are assumed to be uniform for the whole considered soil mass based on the notion that the soil are assumed behave as plastic material which can be represented by Mohr-Coulomb failure criterion. Nevertheless this is contrary to the reality as the soil has a complex behaviour that can only be closely approximated by constitutive laws.

Once the assumptions are applied the plastic state of soil are used in Mohr-Coulomb's failure criteria either as a whole rigid body and analysed as single body or sliced into partitions of

the rigid body and evaluated separately to finally integrate at the end (Figure 2-5). The equilibrium between the sliding mass and the foot wall can have any shape from planar to circular or irregular. In the equilibrium shear stresses (τ) are calculate and compared with available shear resistance (τ_f) (Eq. 1). This is what is evaluated and used to indicate stability of slope as factor of safety.

$$F = \frac{\tau_f}{\tau} \qquad \text{(Eq. 1)}$$

In the slice method **t**he volume affected by slide is subdivided into a convenient number of slices. If the number of the slices is *n* the problem presents (6n-2) unknowns while the number of equations is (4n). The force components involved in typical slice is shown in Figure 2-6. This means it is statistically indeterminate to the extent of, i = (6n - 2) - 4n = 2n-2.

The degree of non-determination is further reduced to (n-2) as it is assumed that the "normal forces" are applied at a midpoint of the slice leading to lesser unknown assuming the hypothesis that total normal stresses are distributed uniformly. The various methods that are based on limit equilibrium theory hence differ in the way they handle/overcome the (n-2) degrees of in determination.

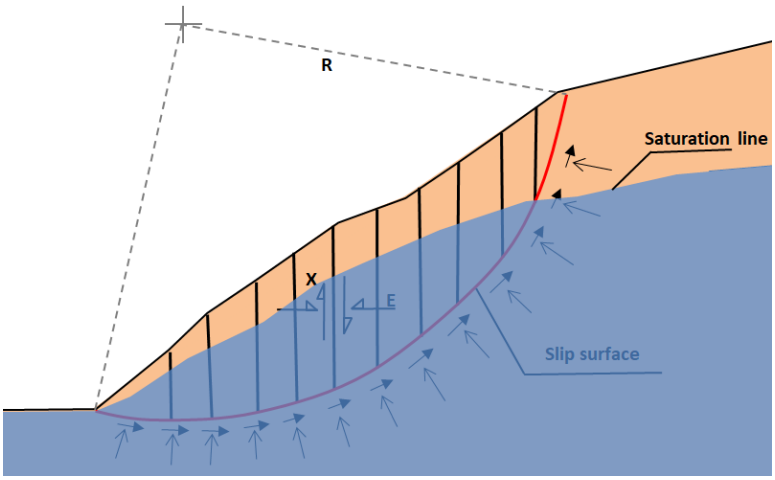

Figure 2-5 Principle of slicing for slope stability analysis

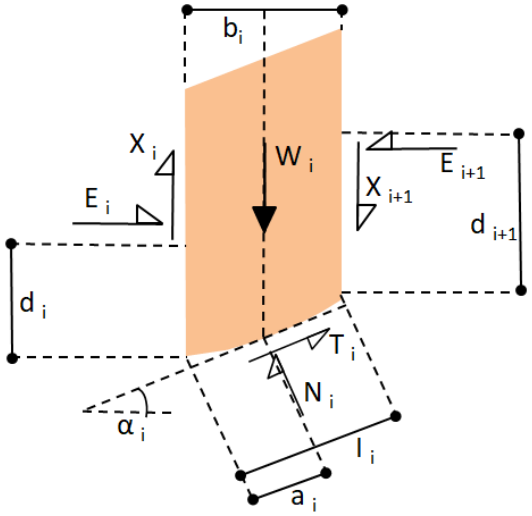

Figure 2-6 Force components of a slice along the slope.

Where,

b_i	slice width (Length)
d_i	hight of slice center (Length)
α_i	inclination of slice base (angle)
a_i	half-length of slice base (length)
l_i	length of slice base (slip surface) (Length)
T_i	shear resistance on slice base (Force)
N_i	normal orce at center of slice (Force)
X_i	interslice shear with the lower next slice (Force)
E_i	lateral force from lower next slice (Force)
W_i	weight of slice (Force)
E_{i+1}	lateral force from upper next slice (Force)
X_{i+2}	interslice shear with the upper next slice (Force)
d_{i+3}	hight of upper next slice center (Length)

For example in Fellenius's method (only valid for circular form of slip surfaces) inter slice forces are ignored and thereby the unknowns are reduced to (2n+1). The available equations are also (2n+1) and hence the factor of safety computed is the simplest one of the available methods (Eq. 2). But the results are highly conservative (Albataineh, 2006).

$$F = \frac{c_i * l_i + W_i * \cos\alpha_i - u_i * l_i * \tan\varphi_i}{\sin\alpha_i} \qquad \text{(Eq. 2)}$$

In Bishop's method on the other hand none of the contributing forces acting on slices are ignored but use is made of two assumptions, force and moment equilibrium. Hence:

$$\mathbf{\Sigma F_y = 0, \Sigma M_0 = 0}$$

Nonetheless, the factor of safety term appears on both sides of the equation which needs to be solved through iteration (Eq. 3).

$$F = \frac{c_i * b_i + \left(W_i - u_i * b_i + \Delta X_i\right) * \tan\varphi_i] * \left[\frac{\sec\alpha_i}{1 + \tan\alpha_i * \frac{\tan\alpha_i}{F}}\right]}{W_i \sin\alpha_i} \quad \text{(Eq. 3)}$$

Nonetheless, due to their simplicity, 2D slope stability models are the most commonly used among practitioners. Three different methodological approaches are commonly applied in the 2D limit equilibrium analysis of slope stability. These are the method of slices, circular methods and non-circular methods (Duncan and Wright, 1980; Abramson et al., 1996).

The method of slices is based on the notion of dividing the slope into different slices and analysing the stability of the failing mass taking into consideration the static equilibrium of the slices individually and the overall equilibrium of the failing mass as whole as well. On the other hand, circular and noncircular limit equilibrium methods consider the equilibrium of the whole failing mass alone (Abramson et al., 1996).

Among the approach utilizing rigid sliding mass method the simplest is a circular analysis called Swedish Circle method. It is used to analyse the short-term stability for both homogeneous and inhomogeneous slopes based on the assumptions that a rigid, cylindrical block will fail by rotation about its centre and the friction angle is zero so the shear strength is assumed to be due to cohesion only (Abramson, et al., 1996). The factor of safety, defined as the ratio of the allowable shear strength to mobilized shear strength, is calculated by summing moments about the centre of the circular surface as:

$$F = \frac{\text{Resisting moment}}{\text{Driving moment}}$$

In the method of slices (Anderson and Richards, 1987), the soil mass above the slip surface is divided into a number of vertical slices and the equilibrium of each of these slices is maintained. The actual number of the slices depends on the slope geometry and soil profile. In order to get the factor of safety by using method of slices, it is necessary to make assumptions to remove the extra unknowns and these assumptions are the main reasons distinguishing the various methods in practice. Nevertheless all the slices method are based on the Mohr-coulomb failure criteria differing only in the way they fulfil either of the force, moment equilibrium or both about the common point of rotation for each slices.

The Janbu's simplified method (Fredlund and Krahn, 1977) is another slice method applicable to non-circular slip surfaces. Janbu's simplified method uses a correction factor, fo, to account for the effect of the inter slice shear forces. The correction factor is related to cohesion, angle of internal friction, and the shape of the failure surface (Janbu et at. 1956). In this method, the inter slice forces are assumed to be horizontal and thus the shear forces are zero. Therefore, the expression obtained for the total normal force on the base of each slice is the same as that obtained by Bishop's method (Bishop, 1955). The factor of safety is product of the uncorrected factor of safety Fo and the correction factor f_o for inter slices forces.

Table 2-1 Comparison of the principal slope stability factor of safety determination methods in 2D (Duncan and Wright, 2005).

Procedure	**Equilibrium Condition Satisfied**	**Shape of slip surface**	**Assumptions**	**Unknowns Solved for**
Swedish Circle (Ø = 0) Method	Moment Equilibrium about center of circle	Circular	• The slip surface is circular. • The friction angle is zero.	1 Factor of safety = 1 Total unknown
Logarithmic Spiral Method	Moment Equilibrium about center of spiral	Log-spiral	• The slip surface is a logarithmic spiral.	1 Factor of safety = 1 Total unknown
Friction Circle Method	Moment and Force Equilibrium	Circular	• Resultant of the normal and frictional component of shear strength tangent to friction circle.	1 Factor of safety = 1 Total unknown
Ordinary Method of slices	Moment Equilibrium about center of circle	Circular	• The forces on the sides of the slices are neglected. • The normal force on the base of slice is Wcosα and the shear force is Wsinα.	1 Factor of safety = 1 Total unknown
Simplified Bishop Method	Vertical equilibrium and overall moment equilibrium	Circular	• The side forces are horizontal (i.e., all interslice shear forces are zero.	1 Factor of safety n Normal force on the base of slices (N) = n + 1 Total unknowns
Janbu's Simplified Method	Force equilibrium (vertical and horizontal)	Any shape	• The side forces are horizontal.	1 factor of safety n Normal force on the base of slices (N), n-1 Resultant interslice forces (Z) =2n Total unknowns

Spencer's Method	All conditions of equilibrium	Any shape	• Interslice forces are parallel (i.e., all have the same inclination). • The normal force (N) acts at the center of the base of the slice.	1 Factor of safety 1 interslice force inclination (θ) n Normal force on the base of slices (N), n-1 Resultant interslice forces (Z), n-1 Location of side forces (line of thrust) = 3n Total unknowns
Morgenstern and Price's Method	All conditions of equilibrium	Any shape	• Interslice shear force is related to interslice normal force by: $X = \lambda f(x) E$ • The normal force acts at the center of the base of the slice.	1 Factor of safety 1 interslice force inclination "scaling factor" (λ), n Normal force on the base of slices (N) n-1 Horizontal interslice forces (E), n-1 Location of interslice forces (line of thrust) = 3n Total unknowns

The factor of safety derived from 2D analysis is by far more conservative and results in excessive design requirement to stabilize. Moreover, the factor of safety differs greatly depending on the profile selected to analyse the stability of the slope again leading to counter measures only suitable to particular slope profile section considered. Therefore, stability analysis by the three-dimensional analysis has paramount importance (Huang and Tsai, 2000; Cheng et al, 2007; Kalatehjari and Ali, 2013).

2.3.2 3D Slope stability analysis approaches

Despite the wide acceptance and standard practice 2D limit equilibrium methods are simplified approaches to slope stability analysis from the reality. By assuming to ignore the side forces it reduces the problems to ones that are determinate and governed by plane-strain conditions. This also entails that the slip surface being treated to be infinitely wide surface. Contrary to this assumption, all slopes in nature have finite widths and therefore this simplification affects the analysis by ignoring the width of the slide mass. In other words 2D limit equilibrium methods are based on simplifying assumptions that reduce the 3D problem to 2D. In the processes the accuracy of the analysis results in varying factors of safety

derivation between the different approaches employed entailing that always comparison of multiple analysis approaches be made (Fredlund and Krahn, 1977; Duncan, 1996).

Three-dimensional analysis methods divide the failure mass into a number of columns with vertical interfaces and use the conditions for static equilibrium on each face of the column giving the 3D factor of safety (Chen, 2003). This results in consideration of 3D shapes of slip surface. Assumptions are always introduced to derive statically determinate solution where a number of methods and assumptions are proposed over the years resulting in numerous versions and types of models (Chen et al., 2003). Several landslides stability models are hence based on extensions of Bishop's simplified, Janbu's simplified, and Morgenstern Price's methods (Cheng and Yip 2007). In these methods the static conditions of limit equilibriums of the columns are satisfied (Kalatehjari and Ali, 2013). There are several ways to do that where some methods do it by either decreasing the number of unknowns or by increasing the number of equations or both (Kalatehjari and Ali, 2013). The sliding mass side wall resistance effect and the lateral variation in geometry of slip surface are taken into consideration in the 3D models which significantly distinguish it from the traditional 2D models. Figure 2-7 shows the forces needed to be evaluated and statically balance while some methods ignore some of these forces or make simplified assumptions (Kalatehjari and Ali, 2013).

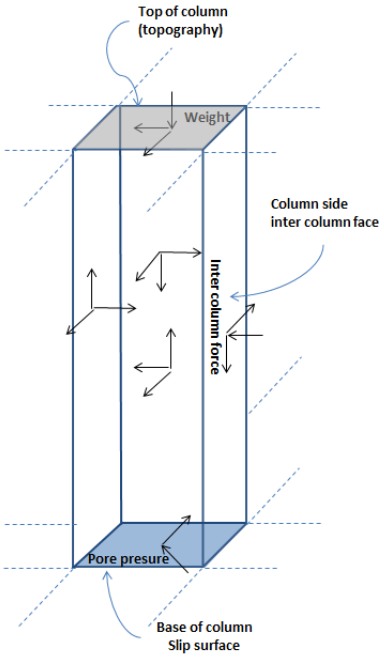

Figure 2-7 Forces involved in solving 3D slope stability analysis.

According to Reyes and Parra (2014) and references therein, the 3D analysis becomes important in cases where the geometry is complex which makes it difficult to select a typical two-dimensional section to analyse for the following reasons: (1) the geometry of the slope and slip surface varies significantly in the lateral direction (2) the material properties are highly inhomogeneous or anisotropic and (3) the slope is locally surcharged.

In addition, the 3D analysis overcome complications due to the interaction of shear strength and/or pore-water pressure (Reyes and Parra, 2014). It is always required to combine the effects of slope geometry and shear strength parameters to determine the direction of movement that leads to a minimum factor of safety or to back calculate the shear strength of the failed slope. In these situations, a 3D analysis may be necessary. A summary of the principal characteristics of existing 3D procedures based on the limit equilibrium method are given in Table 2-2 (Reyes and Parra, 2014).

Table 2-2 Summary of characteristic aspects of the principal 3D slope stability analyses methods (Cited in Reyes and Parra, 2014).

Procedure	Theoretical basis	Slip surface	Factor of safety ratio found (3D/2D)
Anagnosti (1969)	Morgenstern & Price (1965)	Unspecified	>1
Baligh & Azzouz (1975)	Swedish circle (Fellenius 1922)	Cylindrical with conical or ellipsoidal ends	>1
Hovland (1977)	Ordinary method of slices (Fellenius 1927)	Cylindrical with conical ends	>1 for cohesive soils, <1 for cohesionless soils
Chen & Chameau (1983a, b)	Spencer (1967)	Cylindrical with conical or ellipsoidal ends	>1 for cohesive soils, <1 for cohesionless soils
Thomas & Lovell (1988)	Spencer (1967)	Symmetrical	>1 for cohesive and not always for cohesionless soils
Dennhardt & Forster (1985)	Limit equilibrium method	Ellipsoidal	>1
Leshchinsky et al. (1985)	Limit equilibrium method and variational calculus	Spherical and cylindrical	>1
Ugai (1985)	Limit equilibrium method and variational calculus	Cylindrical with curved ends	>1
Hungr (1987)	Bishop (1955)	Rotational with circular central section	>1
Ugai (1988)	Fellenius (1936), Bishop (1955) and	Cylindrical with Spencer (1967)	>1 for cohesive soils, ellipsoidal ends <1 for cohesionless soils

Procedure	Theoretical basis	Slip surface	Factor of safety ratio found (3D/2D)
Gens et al. (1988)	Swedish circle (Fellenius 1922)	Cylindrical with planar or curved ends	>1
Xing (1988)	Ordinary method of slices (Fellenius 1927)	Symmetrical elliptic with circular vertical cut	>1
Hungr et al. (1989)	Bishop (1955) and Janbu's Simplified (Janbu et al. 1956, Janbu 1973)	Symmetrical and rotational	>1
Leshchinsky & Huang (1992a, b)	Limit equilibrium method and variational calculus	Expansion of a log-spiral function	>1
Lam & Fredlund (1993)	General equilibrium method (Fredlund et al. 1981)	Generalized rotational	>1
Huang & Tsai (2000)	Bishop (1955)	Asymmetrical	>1
Hungr (2001)	Morgenstern & Price (1965)	Symmetrical	>1
Chang (2002)	Sliding block analysis	Asymmetrical	>1
Huang et al. (2002)	Janbu's generalized (Janbu 1954, Janbu 1973)	Generalized	>1
Chen et al. (2003)	Spencer (1967)	Generalized rotational	>1
Jiang & Yamagami (2004)	Spencer (1967) and variational calculus	Symmetrical rotational	>1
Cheng and Yip (2007)	Bishop (1955), Janbu's simplified (Janbu et al. 1956, Janbu 1973) and Morgenstern & Price (1965)	Spherical	>1
Zheng (2009)	Limit equilibrium method	Generalized	>1
Sun et al. (2012)	Morgenstern & Price (1965)	Generalized	>1

2.3.3 Simplified Pseudo 3D slope stability modelling approach

Lambe and Whitman (1969) suggested the use of a pseudo 3-D approach to calculate the 3D factor of safety. In this approach the 2D factor of safety is calculated for several parallel cross-sections and then used to find the weighted average factor of safety of the slope in 3D. The Lambe-Whiteman method (Lambe and Whitman, 1969) treats the landslide in terms of multiple profiles rather than column grids. Multiple profiles of the landslide (slope) are separately analysed giving corresponding multiple 2D factors of safety. These are then pulled together by weighting with the corresponding cross-section area of the sliding mass giving the approximate semi- 3D factors of safety as a whole for the considered particular landslide. The cross-section area of the landslide, hence have some influence on the derived factor of safety.

It is common practice to use two sections or three sections to perform the 3D analysis (Nermeen Albataineh, 2006). Cornforth (2004) recommends that this can be done for example in two section by making the sections at the quarter of the widths of the slope or in three sections by making the sections at the two ends of 1/6th widths of the slopes and the centre line resulting in 3 sections (Figure 2-8). This method is a simplification of the 3D analysis and has been in practice for some time (Cornforth, 2004; Kalatehjari and Ali, 2013).

In addition, such assumption will always yield a 2D factor of safety close to the 3D factor of safety and not the real value.

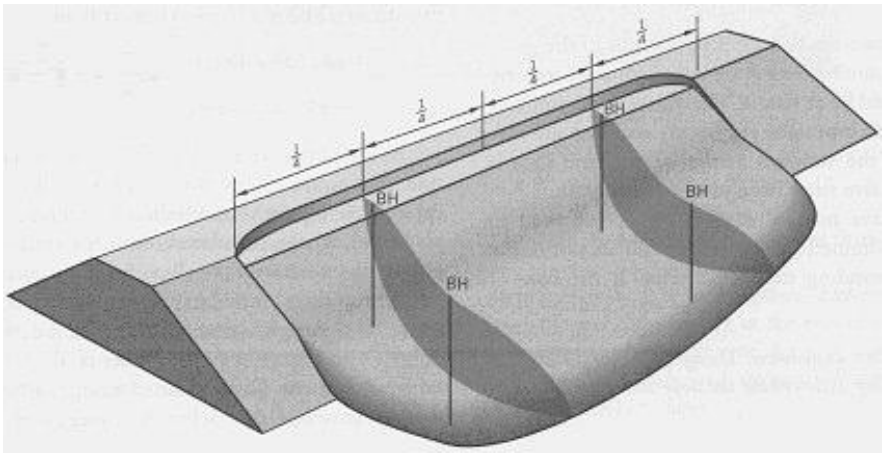

Figure 2-8 3D analysis using cross-sections spaced in typical manner (after Cornforth, 2004)

Coric et al. (2015) demonstrated approximate 3D analysis of slope stability in Serbia utilizing 2D factors of safety derived across a single profile along the landslide assuming an irregular slip surface. The 2D factor of safety was then modified by adding the lateral resisting forces (on either sides) on the interface at the ends of the landslides to arrive at the 3D factor of safety. In the case study internal friction angle mobilized by the slide in the case of 2D stability analysis using Janbu's method were found to be slightly lower than that obtained from the extension to 3D factor of safety. Similarly the factor of safety for the 3D case was slightly higher than that calculated in the 2D case.

Three dimensional (3D) stability analyses have undergone continued improvement where main analysis methods are summarized by Huang and Tsai (2000) and Kalatehjari and Ali (2013). Several software are also commercially available for carrying out 3D slope stability analysis by extending 2D stability methods (Reyes and Dara, 2014). For example, SVSLOPE-3D® allows creating a 3D model by, among other methods, interpolating multiple cross-sections of slope systems (https://soilvision.com/product/svslope). But in this thesis attempt is made to use easily available spread sheet program, Microsoft Excel, by inputting parameters obtained for the landslide and running stability and sensitivity analysis manually as the software are expensive and do not go with the intention of the objective of utilizing the method of multiple profiles analysis but rather depend on the grids of column requiring more data than can be obtained from the field.

One of the sited problems in the case of most 3D model is the effect of side resistance (Akhtar and Timothy, 2017 and references therein) leading to increase in computed factors of safety in the various 3D methods. This means the vertical side faces (profiles) of the slopes pose additional resistance to the whole landslide block which adds to reducing the driving force and subsequently increase in factor of safety calculated by normal 3D approaches. Nevertheless, the effect becomes more significant in cases where the ratio of width of the landslide to depth of the landslide become very low since it would develop more resistance from the increased surface area of side walls to resistance (lateral friction). This situation is demonstrated in Figure 2-9.

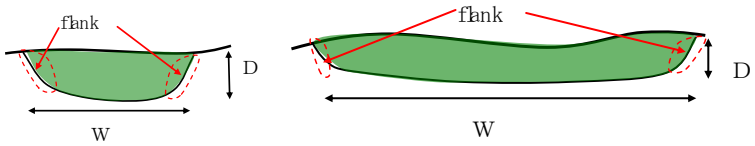

Figure 2-9. Effect of lateral shear resistance on 3D slope stability as viewed in vertical section into the landslide lateral cross section. Lower W/D ratio in the figure to the left and higher W/D ratio in the figure to the right.

2.3.4 Numerical methods of slope stability analysis

The other important and robust approach to slope stability analysis is using of numerical methods such as Finite Element Methods instead of the simplified limit equilibrium method. The main difference between the finite element method (FEM) and the limit equilibrium method (LEM) in slope stability analysis is that the FEM satisfies the equilibrium at any point in the sliding soil mass and the surrounding. The LEM on the other hand satisfies the equilibrium (force or moment) for the sliding mass as a block (Albataineh, 2006). The derived factor of safety in the FEM is believed to be more accurate than the LEM in 2D and 3D analysis as well. The FEM methods however are complex in that they need specialized often expensive software but the out puts are multiple faceted where all deformations, pore water pressure developments etc. are efficiently visualized (Albataineh, 2006).

2.4 Back analysis and Sensitivity analysis

2.4.1 Back analysis

Slope stability analysis required accurate and sophisticated testing of materials to evaluate the performance such as tri-axial tests, ring or direct shear tests with different implications on obtained values. Often it is either not practical due to the nature of materials involved to apply such laboratory tests or too expensive. It is also a question of doubt if the measured parameter will reproduce a true value of the parameters sought such as the shear strength

parameters (Tang et al., 1999; Duncan et al. 2014). Back analysis of failed slopes, especially in disturbed soils and colluviums, are indispensable for the retrieval of best estimates of the shear strength parameters in an inexpensive way.

It is always difficult to obtain intact and representative samples from colluvium for laboratory testing on one hand and difficult to assign appropriate shear strength parameter to it either, as it often contains a range of materials ranging from fines to coarser clast (Karikari and Gyasi, 2000). Hence back analysis in such situations as one with already failed slope offers a good opportunity to utilize in retrieving the mobilized shear strength parameters based on other known and assumed conditions (Duncan, 1996). Nevertheless, complications and errors due to the assumptions made in carrying out back analysis are always eminent and are usually applied with precaution (Duncan et al. 2014).

Back analysis also indispensable for the estimating more realistic physical properties based on known conditions and other properties, it also has its draw back (summarized by Hussain et al., 2010). Some of the causes for this draw back are uncertainties in type of materials distribution in profiles considered for analysis, slope geometry at the time of failure, effect of rainfall, phreatic surface and pore water pressure at failure, role of tension cracks (Hussain et al. 2010).

Typically a landslide analysis is suggested to follow sets of procedures (Hussain et al., 2010, Duncan et al. 2014). Hussain et al. (2010) outline the procedures that should be followed to carry out a proper back analysis which can be summarized into 6 steps: (1) Understanding the subsurface conditions material and landslide morphologic features, (2) Defining representative cross-sections parallel to the direction of maximum movement (3) Defining the type and location of the failure surface based on available data (4) Selecting type of stability (5) Varying the shear strength of the problematic layer until the factor of safety equals approximately unity and retain the obtained shear strength parameters (6) Comparing the back-calculated shear strength parameter (φ') with the results of laboratory strength testing and with empirical correlations to ensure agreement.

Duncan et al. (2014) presents a method where the knowledge of slip surface can be used in back calculating the shear strength parameters. It states that starting with consideration of sets of shear strength parameters for homogenous slope and corresponding estimated critical circles in a typical slope. As the each set of shear strength parameters produce a factor of safety of 1, whereby the critical slip surface is different, a dimensionless parameter, $\lambda_{c\phi}$

defined as function of slope height and sets of assumed c' and φ' values (Eq. 4), is obtained. This parameters is related to the depth of the slip surface and is used calculated the total or effective stress shear strength parameters.

Because each pair of shear strength parameters ($c - \varphi'$ or $c' - \varphi'$) corresponds to a unique slip surface, the location of the slip surface, along with the knowledge that the slope has failed (i.e., $F = 1$), can be used to back-calculate values for two shear strength parameters ($c - \varphi'$ or $c' - \varphi'$) (Duncan et al., 2014).

Often the difficulty could be the factor of safety which can be effectively applied using the sets of charts developed (for example Janbu, 1968). For the a calculation of factors of safety in back analysis Duncan et al. (2014) gives account of charts developed for simple homogeneous soil conditions in $\varphi > 0$ and $c = 0$ and those with $\varphi > 0$ and $c > 0$ as well. These can be used to represent inhomogeneous material distribution by introducing critical circles that subtend the different material layers in the slope profile at varying angle and hence used to weight the contribution in estimation of overall shear parameters (Duncan et al., 2014). To apply this method, after approximating simpler slope geometry resembling the actual slope in question, a trial location of the critical slip surface is made.

The central angle of arc subtended within each layer or zone of soil is measured thereupon weighting the relative contribution of the slope materials in the weighted average parameters (Duncan et al., 2014). Once the average shear parameters are obtained the next step is to find the corresponding shear parameters which will are used to generate the dimensionless parameter, $\lambda_{c\varphi}$. The dimensionless parameter together with the slope angle will then be used to extract another parameter called stability number, N_{cf} (*Figure 4-22*). This value is used to calculate the associated factor of safety for the estimated critical slip surface and the previously obtained average shear parameters (Eq. 10).

2.4.2 Sensitivity Analysis

Often stability conditions are dictated by certain factors more than any other among the geotechnical properties (Cheng and Chiang, 2012). In slope stability after establishing the slope model the response variable of Sensitivity analysis is set to be the factor of safety whereas the reference parameter are the various influencing parameters of the safety factor (Cheng and Chiang, 2012). It is hence imperative to undertake sensitivity analysis for the impact of the various parameters once a working slope model is established. A number of

cases as well as strategies adopted for undertaking slope stability sensitivity analysis with respect to factors driving the slope stability been extensively applied elsewhere in literature (for example in review of Luo et al., 2017). A method followed by Agam (2016) where sensitivity analysis was carried out to compare the performance of Spencer's method and General Limit Equilibrium. By varying each of the parameter in uniform increments, between the minimum and the maximum values, the response of the factor of safety is evaluated in this study following similar strategy of Agam (2016).

2.5 Previous studies

The Nile Gorge otherwise also known by its local name of Abay Gorge has been studied for a range of interests. Few studies have been conducted on potential for petroleum exploration as it forms thick cretaceous sediments with indications for petroleum source rock (Wolela, 2007, 2012, and 2014). The geological evolution, stratigraphy and structural features of the gorge is also studied by combining field and remote sensing data with focus on the Gohatsion-Dejen section (Getaneh Assefa, 1980, 1991; Gani and Abdelsalam, 2006; Gani et al., 2009). Some studies have also focused on the hydrological and groundwater characterization in the Gorge and in the wider entire Abay River catchment (Sileshi Bekele et al., 2008 and references therein; Ahmed Ali, 2014). The slopes along the main road between Gohatsion and Dejen have been also subject of several slope stability investigations and counter measure design studies (Tarekegn Tadesse, 1993; Almaz Gezahegn and Tadesse Dessie, 1994; Lulseged Ayalew and Yamagishi, 2003; Leulseged Ayalew, et al., 2009; JICA and GSE, 2012; Elami, 2013, Matebe Meten et al., 2015; Bisrat Yifru and Fasika Ayehu, 2017). This has led to constraint on the activity and extents of the landslide body in much better detail than anywhere in the country.

Incision rate of the Blue Nile Gorge was analysed based on the geology and morphometry of the drainage basin (Gani et al., 2007; Ismail, 2013). After analysing knick-points along the river course, three consecutively increasing rates of incision were inferred: (1) those associated with uplifting by the two Cainozoic flood basalt eruption events and (2) the latest upon the initiation of the main Ethiopian rift. In fact the present day incision rate has been found to be the highest with 320 mm/Ma or 0.12-0.32 mm/yr which is exponentially raised from previous since the initiation in the Cainozoic (Gani et al., 2007). The role of mass wasting processes as important factors in shaping the abay gorge has been discussed by Leulseged Ayalew and Yamagishi (2004). Considering the volume of removed material in

the gorge they argue that the postulated soil lose by McDougall et al. (1975) is far less to account for the removed material to have been created by the soil loss alone and proposed rock fall and landslides processes to fill the gap (Lulseged Ayalew and Yamagishi, 2004).

The geological units comprising of the Gorge, including the geographic area of the present study, are investigated and mapped by various authors at various scales. Getaneh Assefa (1980, 1991) defined the type locality of the Abay Formation. Jepson and Athearn (1962) carried out detail investigation of the gorge. The 1:2,000,000 scale regional geological map also portrayed the major lithological units in the Abay Gorge area (Mengesha Tefera, et al., 1996). Gani et al. (2006) carried out a combined field based and remote sensing based geological mapping at 1:50,000 scale for the Abay Gorge section. Characteristic features of the stratigraphic sequences have been described by several studies (Almaz Gezahegn and Tadesse Dessie, 1994; Lulseged Ayalew et al., 2009). Continuous accumulation of terrace deposits covering the vast slope breaks in the Gorge forming a range of colluvium is highlighted (Almaz Gezahegn and Tadesse Dessie, 1994; Leulseged Ayalew, et al., 2009; JICA and GSE, 2012). A recent study with emphasis on role of groundwater fluctuation on slope stability conditions highlights the complexity of groundwater level fluctuation and flow direction in the region due to spatial and temporal variability of the groundwater fluctuation (Bisrat Yifru and Fenta Ayehu, 2017).

A number of works utilizing GIS and remote sensing for evaluating the susceptibility and vulnerability of the landslides have been made extensively (Ayalew and Yamagishi, 2003; Henok Wolde Giorgis et al., 2014; Shiferaw Ayele et al., 2014, Meten et al., 2015) including several thesis works (Jemal Saed, 2005; Shiferaw Ayele, 2009; Yoseph Endalamaw, 2010; Samuel Molla, 2011). Some of the studies focused partly or entirely on the probabilistic hazard analysis using susceptibility modelling with regard to role of environmental factors of landslide occurrence (Henok WoldeGiorgis et al., 2014; Shiferaw Ayele et al., 2014; Meten et al., 2015).

One of the earliest comprehensive studies was made by the then EIGS in the early 90's. Geophysical explorations followed by routine engineering geological investigations were carried out including trial pits and boreholes. The investigations found out that overall up to 20m thick unconsolidated materials composed of gravel to cobble sized basaltic rock fragments in a fine matric of sand silt and clay that are highly expansive overlie the bed rocks of the volcanic terrain (Almaz Gezahengn and Tadesse Dessie, 1994). Based on the

consideration of the logging and laboratory test on clay soil horizons together with engineering and morphological mapping of the gorge they attributed the cause of the failures to the saturation of the colluvium mass by the heavy precipitation that traversed down the vertical joints into the underlying expansive clay rich soil resulting in mostly through rotational failure (Almaz Gezahengn and Tadesse Dessie, 1994).

A study by Jemal Saed (2005) focused on the slope stability analysis of the road cut slopes of Gohatsion – Dejen section in the valley. Planar, wedge and circular modes of failures were identified by the study on 9 out of 17 critical slope sections considered. Slope stability all along the old road and new alignment were evaluated at critical slopes based on presence of scarp faces on the slopes, presence of slope distress such as tension cracks and bulging of slope face, adverse orientation of discontinuity and presence of recent rock falls and debris flow. After considering 17 critical slopes meeting the criteria evaluation of the rock slope stability conditions were made on 7 prominent localities including soil slopes falling on both northern and southern road slopes. Although no exhaustive stability analysis was made on the identified soil slopes their characteristic and unstable nature was described. Planar, wedge and circular failure analysis using the SARC model were evaluated for the rock slopes. A synoptic physical attributes of the soils undergoing instability and the analysed rock slopes involved in the instability were also given. According to the study the mapped soil units consist of mainly colluvium and partly residual soils with few alluvial deposits along the tributaries of the main River. The colluvium soils gave high to very high plasticity with inferred volume change reaching more than 25% per the USBR (1974) (Jemal Saed, 2005).

The colluvium soils are also described as unconsolidated and permeable and are cited to be subject to high expansion during prolonged precipitation in the rainy season and shrinkage during the following dry season leading to aggravated instability associated with volume change. The rock mass physical characteristics were reported for the Basalt, Limestne, Gypsum and Sandstones that make up the major lithology in the gorge. The basalt generally has significantly higher intact strength of 163MPa which is generally more than three times the value obtained for the other lithologies.

Shiferaw Ayele et al. (2014) used weighted linear combination (WLC) method of overlay to deal with problems of inhomogeneity and uncertainty of factor maps. The factors considered are geology, groundwater conditions, drainage, slope, geologic structure, aspect, and land use/land cover which were generated from satellite images and digital elevation model while

other discrete data were based on earlier works in the area. They used fuzzy boundary to account for uncertainty in boundaries created during division of factors into classes with varying weight of relative rating. Five levels of hazards were finally produced from the weighted overlay ranging from very low to very high hazard levels where up on validation 67% of the past landslides were found to fall in the high hazard classes.

Rock slopes of the Abay Gorge slopes mainly the gypsum units were analysed by a thesis work (Henok Woldegeorgis, 2008) through stability condition evaluation of selected critical slopes in the valley along the main road in the cut slopes. The study was conducted with the aim of applying causative factors role on instability from historical failed slope in the area. The area studied is the southern slope of the Abay gorge on the Gohatsion side. Landslide hazard evaluation factors (LHEF) were inventoried from the Abay gorge and evaluated with the LHEF scheme and subsequently those ranking higher in susceptibility were further analysed for deterministic stability conditions. This was followed by comparison of possible counter measures to stop the instability. The evaluations were carried out in facets map of the area derived from the combination of topographic and geological uniformity resulting in 139 units. Among the factors slope morphometric, geology and land use land cover were found to have higher role in occurrence of slope instability. At five selected critical slopes of rock mass detail structural slope stability analysis were made whereas at 2 selected sites of critical soil slope stability analysis were made. Nevertheless the shear strength parameters of the soil were based on recommendations of Hoek and Bray (1989), USBR (1974) and secondary data from ERA. Stability for the landslides was carried out using the Bishop method. The factors of safety in all cases were found to be less than one. Further, reported shear strength parameters used by ERA appear to be more conservative than the values adopted in the study although both show factor of safety significantly lower than one.

Slope stability evaluation of selected slopes in the Abay Gorge was also made with emphasis on sensitivity of the stability to change in level of groundwater level by a thesis work of Samuel Molla (2011). The same landslide that occurred at 27 to 28 Km distance from the entry of the valley on Gohatsion town side of the gorge along the main road has been evaluated in the thesis work (Samuel Molla, 2011). Nevertheless, the stability analysis was performed for critical slip surface based on slope model developed using shear parameters obtained from sensitivity analysis rather than determined slip surface. In the case of Samuel Molla (2011), using the SARC model, the cohesion back calculated as 0.3 KPa and the internal friction as 11^0. The values obtained for shear parameters is based on sensitivity of the

factors of safety to combination of cohesion and friction angle where the least varying combination is taken as the representative values for the cohesion and friction angle (Samuel Molla, 2011).

Statistical index and certainty factor methods of bivariate statistics were used to assess part of the Abay Gorge covering areas around the main road between Gohatsion and Dejen in the thesis of Endalemaw Yoseph (2010). Elevation, slope, lithology land cover, proximity to drainage and proximity to road were considered in the analysis based on relations on already occurred historical landslides in the area. Overall the study found out that the instabilities were significantly higher in areas comprised of basaltic lithology when covered by shrub lands and when falling in elevation higher than 2100 m a.s.l, with slope angle of 30-45 degrees. It shows also the areas within 50 m proximity to the road and 50-100 meter from streams were the highest susceptible slope instability where both methods gave reasonably comparable result.

Similar statistical or probabilistic approach has been applied to the same area by a doctoral thesis of Meten (2015) based on multiple causative factors based on the observed relationship between each factor and the distribution of past landslides. The main objective of the study has been in finding the most effective combination of landslide factors to produce the most accurate result when compared to the historical landslides mapped in the same area independently during validation of the outputs. Lithology, slope, land use and distance from lineament when used in the weighting for prediction of slope instability hence gave the optimum accuracy among total of eight factors analysed in the study which included distance from river, topographic profile and plan curvatures and aspect.

Both methods rely heavily on mapping of past landslides which usually are difficult to ascertain for completeness throughout the domains of the various considered causative factors classes. In addition the issue of classifying some of the factors classes into various classes is usually haphazardly made and have serious repercussions on the results. Further the combination of using continuous and discrete data in spatial context is another difficulty to integrate all factors together and no systematic way of handling such difficulties appear although as the study in Meten (2015) tries to overcome such problem using the fuzzy logic approach where each location is given certain level of membership to various classes instead of discrete membership to one of the classes.

Slope cut design criteria has been proposed based on performance of unsupported slope cuts observations in the Blue Nile Gorge along two main roads crossing the river at 180 KM and 285 KM downstream of Bahir Dar town (Lulseged Ayalew et al., 2009). In their finding while heterogeneous slopes needed to be designed based on the consideration of various aspects the hardest rock mass slopes can stand up to 0.25:1 horizontal to vertical cut ratio. The softest and most vulnerable on the other hand are found to be stable at slope cut angles of 1:1 ratio. The study evaluated several slope stability analyses to arrive on the recommended safe cut ratio using Bishop's slip circle method for rotational failures and using the equation elaborated by Rahardjo et al. (1995) for planar slope failures. In the planar slope failures the methodology used is said to best represent the scenario in the Abay Gorge where perched water table develops between the wetting front and the ground surface. For the stability analyses they carried out several laboratory tests and in-situ tests are reported. Undrained shear strength estimates from hand penetrometer tests on colluviums and weathered basalts gave 200 to 400 KPa while direct shear test on samples from the area gave 30 to 75 KPa and internal friction angle of 23^0 to 28^0 (Lulseged Ayalew et al., 2009). On the other hand it is often not the case that any representative value will ever be obtained from testing of samples in case of colluvium the tests have to be used in precaution.

A study was conducted by Geological Survey of Ethiopia (JICA and GSE, 2012) to identify countermeasures for the slope instability of occurring along the main road between Gohatsion and Dejen which is part of the major highway to the north western part of the country. The investigation was carried out by technical assistance of JICA (JICA and GSE, 2012). Extensive survey of the landslide hazards and monitoring wells were sunk at four localities along the road where geophysical and topographic surveys were also integrated. The study utilized more than 40 boreholes for installing monitoring devices and subsurface exploration along with deployment of extensive seismic and electrical resistivity profiling in the area (JICA and GSE, 2012).Comprehensive monitoring and exploratory data have been generated from the study as well as recommendations for counter measures for the slopes to safe guard the main road between Gohatsion and Dejen towns.

The final results suggested role of groundwater as decisive factor and the study ended up recommending draining of the subsurface water through horizontal drilling. Although no in depth slope stability has been carried out to the fullest as the focus was to model the landslides mechanism over recommendation of counter measures were suggested based on fewer stability analysis.

Stability was carried out using Janbu's method and Modified Fellenius method. But since the slip surface is predetermined instead of the critical slip surface a defined surface is used. This information also gave a good estimation for the properties to be determined from back analysis. This was carried out assuming the known geometry of the landslide, the almost zero cohesion as might be expected during the active rainy season and then the internal friction angle was calculated in Geo-Slope studio using Janbu's method. The results obtained compared well with the similar values coming from Neogene Tuff in Japan (JICA and GSE, 2012).

2.6 Conclusion

From the literature it can be seen that the Abay Gorge has attracted many interests for range of purposes including geomorphic evolution, geological evolution and landslide hazards. The geological formations are well constrained by various studies where the relative competence difference between lithologies is apparent. The majority of the works pertain to spatial evaluation of landslide occurrence probability on the basis of various geo-environmental factors. LHHZ has been extensively applied with good success and has highlighted the importance of geological materials and fault line as important contributing factors for occurrence of landslides. On the other hand the geomorphic evolution all suggest active role of landslides and similar mass wasting processes which in geological time scale is much higher than the situation in the past 30 Ma years of the evolution of the Gorge. Accelerated incision rates and deficient sediment yield in comparison to volume of material removed from the Gorge the Abay Gorge are suggestive of importance of landslides and similar mass wasting process in shaping the morphology implying the continued activity.

Nature of the landslide being recurrent and consequently having generally very low cohesion (residual state) is an important point reflected in some of the literatures which is very useful in relation to this study for comparison and evaluation.

The literature also reveals specific deterministic slope stability analysis carried out in the Gorge which is valuable to compare with and consider in carrying out the stability analysis. Some findings and datasets are also obtained from previous published works. A good perspective is gained on the pros and cons as well as the basics of the back analysis methods. Good understandings of the vast slope stability models and the limitations have been gained from the literature review.

3. General overview of the study area

3.1 Location of the study area

The present study area lies in the Abay basin of Central Ethiopia. It encompasses the main road that connects the towns Gohatsion and Dejen, which is found at the borders of the Amhara and Oromia regions. The study area is mainly located on the main road that goes from Addis Ababa to Bahir Dar through Gohatsion and Dejen between 180 Km and 220Km from Addis Ababa. Physiography of Abay Gorge area is shown in *Figure 3-1*.

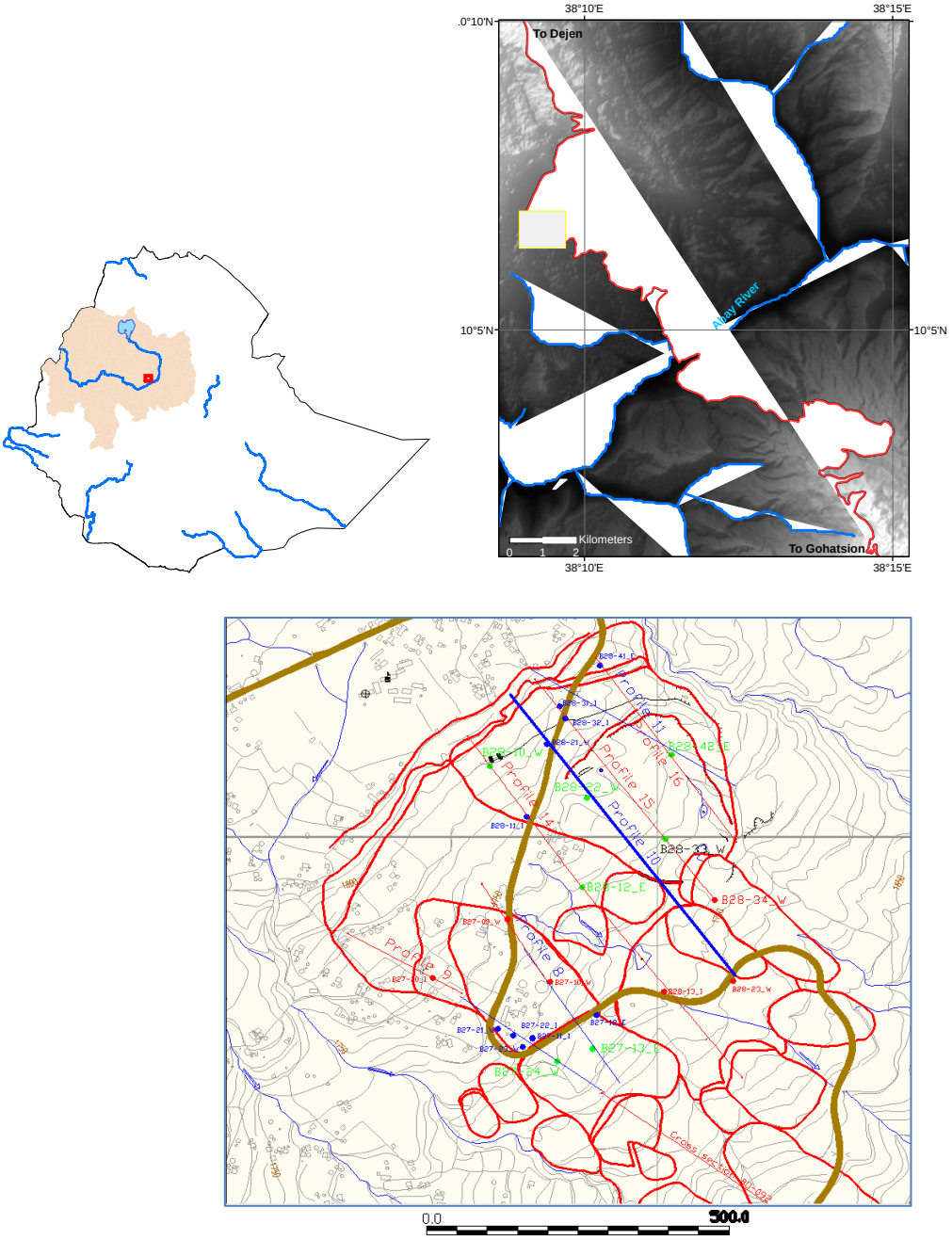

Figure 3-1 Location of the study area and topographic over view

3.2 Climate condition of the study area

Meteorological data from the gauging stations of NMAE indicate the prevalence of two rainy seasons in the Abay Gorge and the surrounding from March to May and from June to October (*Figure 3-2*). Landslides and rock falls in the study area. A total of 4 meteorological stations established by Ethiopian Meteorological Agency are located in the study area located in the towns of Gohatsion, and Dejen and villages of Filiklik and Kurar. In addition one automatic Rain Gauge at elevations corresponding to the sites of Ethiopian Meteorological Agency station at Feliklik and Kurar, and another one at the Bridge of the Aby River crossing were established by Geological Survey of Ethiopia (JICA and GSE, 2012) with hourly data record of rainfall during the project and sporadically continued afterwards.

Most of the rainfall in the study area occurs during the summer season mainly from June to September (Figure 3-2) whereas somewhat low rainfall occurs in November and January. The rainfall peaks in July and August at about 300 to 400 mm per/month while dry spells run from October to May. The mean annual rainfall is generally low ranging from 1100 to 1400 mm (NMAE). There is overall decrease in rainfall between the plateau and lower level of the Valley. The daily maximum precipitation at Dejen is 64 mm/day while AbaySheleko located halfway between the Valley bottom and the plateau on Dejen side is 52 mm/day (NMAE). Historically the rainfall in 1996 is one of the highest recorded at Dejen as 105 mm of daily rainfall (Henok W/Giorgis, et al., 2014). Average annual rainfall record at the two plateau tops of Gohatsion and Dejen are 1185 mm and 1528 mm, while on the middle slope of the Valley at Filiklik (southern slope) is 1268 mm.

The mean monthly maximum temperature is quite uniform around 20^0C from June to December and around 25^0C from January to May (NMAE). The mean monthly minimum temperature on the other hand registers around 10^0C from April to October and around 5^0C from November to March (NMAE). But the temperature near the bottom of the gorge reaches up to 42^0C.

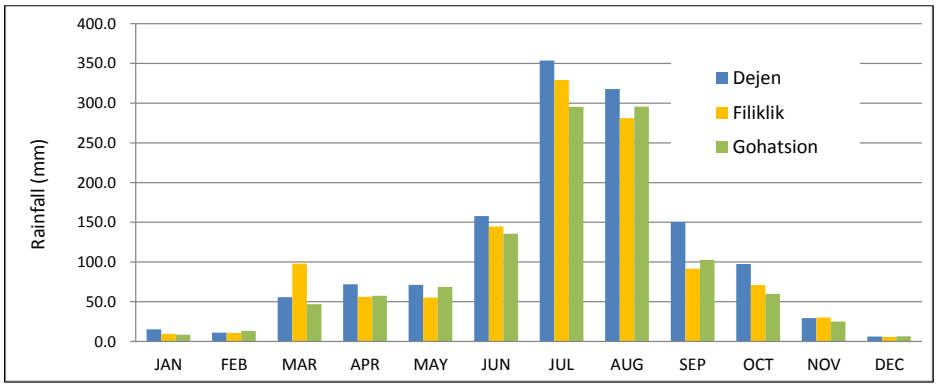

Figure 3-2. Mean monthly precipitation pattern in the area based on data from Meteorological Agency of Ethiopia for the years 2000 to 2017/18 measured at 3 stations.

3.3 Physiography of the study area

The study area falls in the spectacular canyon formed by the deep incision of the Mesozoic and tertiary volcanic series (*Figure 3-3* and *Figure 3-4*). It forms series of terraces and steep slopes controlled by the lithological variations (Almaz Gezahegn and Tadesse Dessie, 1994; Leulseged Ayalew et al., 2009). The flat terraces correspond to the softer and incompetent lithologic layers composed of shale, silt and bioturbated marly limestones in the lower levels of the valley and the tuff layers on the higher level between basalt layers (Gani and Abdelsalam, 2009) as depicted for example in Figure 3-3. The Abay River and its tributaries carved into these formations and drains to the west with perennial tributaries confluent laden with abundant sediments from either side of the valley. The major tributaries are usually characterized by steep-sided, V-shaped valleys all along the tributaries several water falls are also common with varying yield between wet and dry seasons. There is no doubt the entire valley has been and is still undergoing continuous mass wasting process which is only aggravated by the anthropogenic activity (Leulseged Ayalew and Yamagishi, 2004.

Figure 3-3 Physiographic over view of upper levels of the Abay Gorge (left) and middle level of the Abay Gorge (right).

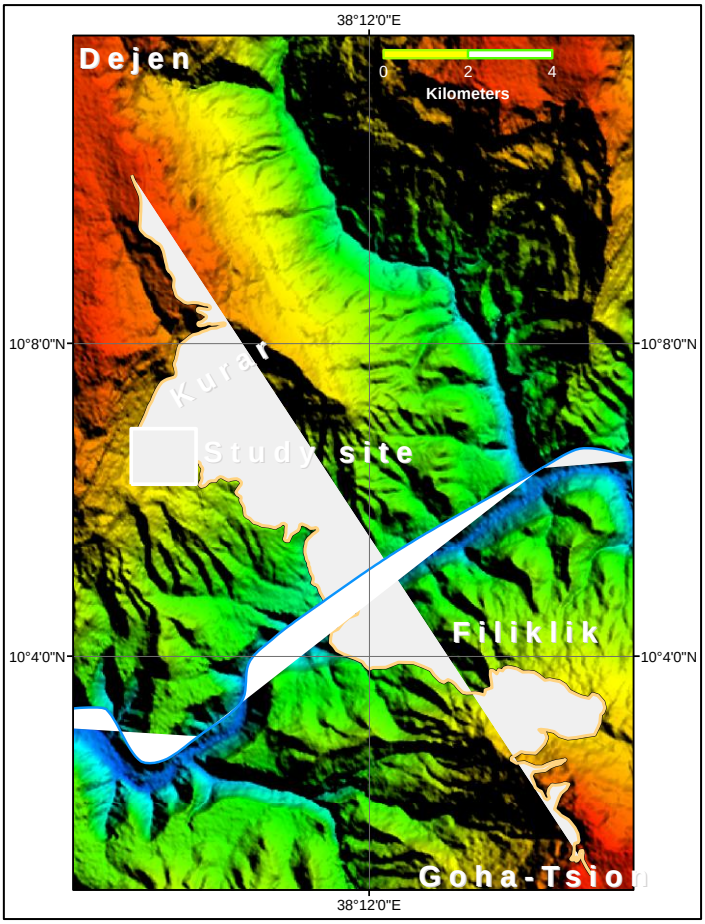

Figure 3-4 Physiographic over view of the study area

Elevation difference between top of the Valley on the Plateau and the canyon floor reaches 1,500 m while the span of the valley from plateau to plateau is about 17 Km. The main Bridge across Abay River is found at about 1,050 m a.s.l. while the highest elevation on the plateau is 2,500 m a.s.l. The valley profile shows alternation of steep cliff forming hard rocks and soft gentler slope forming layers. Large boulders and blocks are commonly scattered all over the valley which are telling of the past history of mass wasting processes.

Streams in the valley slopes more or less flow in dendritic pattern. Two of the major tributaries are found each on either side of the valley. On the southern slope is the stream called Mekentuta River. It forms a water fall at the entrance of the valley from the south near the main Road. On the opposite side of the valley (northern) called Ado Wedeb River.

3.4 Seismicity of the study area

The ‘Seismic Risk Map' produced by Fekadu Kebede and Laike mariam Asfaw (1996) for hundred year return period and 0.99 probability of exceeding shows that the study area falls in a region with Mercalli’s earthquake magnitude scale of 7. Based on the Mercalli

Magnitude scale the estimated horizontal earthquake acceleration is about 0.08g (Johnson et al, 1988 cited in Fekadu Kebede and Laike Mariam Asfaw, 1996). New study on the other hand improved the previous seismicity map for the region of horn of Africa including Ethiopia (Atalay Ayele, 2017) using Probabilistic Seismic Hazard Analysis methods. The study puts the area of the landslide in the Abay Gorge in value ranges below 0.05g Peak Ground Acceleration (Figure 3-5), implying lower risk of seismic hazard.

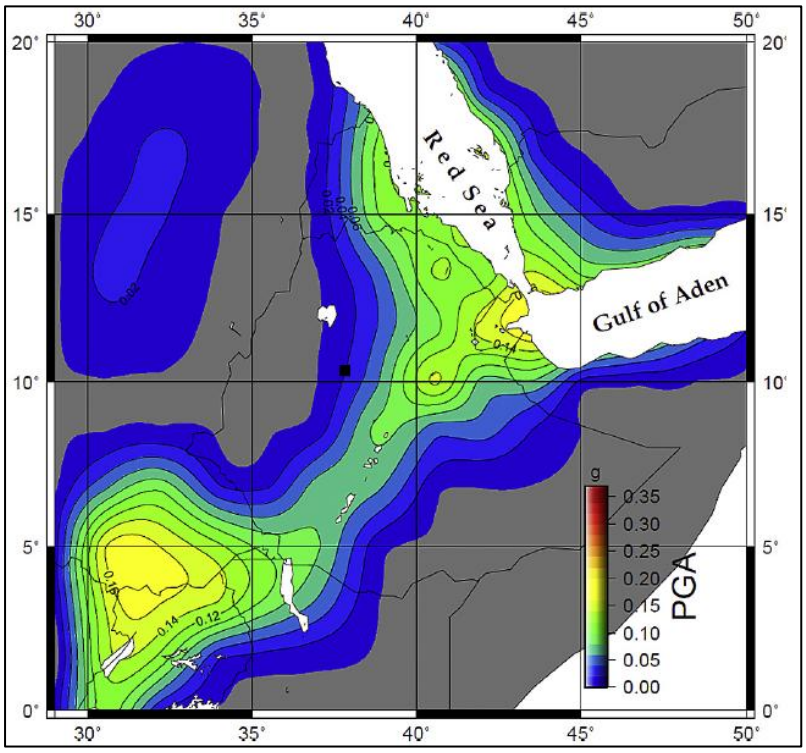

Figure 3-5 Horizontal Peak Ground Acceleration seismic hazard map with exceedance rate of 10% in 50 years for rock sites, study area is represented by dark spot (Atalay, 2017).

3.5 Land use land cover

Shrubs and wood lands dominate the gorge with seasonal green plants flourishing during only the rainy season. But rather intensive farming takes place in most part of the valley except on the few terrains very close to the river. The dominant crop produced in the area is sorghum, wheat, maize, Teff and Sugarcane (Samuel Molla, 2011).

3.6 Regional Geology

The geological setting of Abay Gorge is peculiar where it exposes long geologic time records of the rock formations ranging from late paleozoic sediments to recent quaternary volcanics. According to (Getaneh Assefa, 1980, 1991; Tefera Mengesha, et al., 1996) the rock formations in the Abay Gorge from lowest (oldest) to upper (youngest) are: (1) the Early–

Middle Jurassic Adigrat sandstone (2) Middle Jurassic Abay limestone which also includes shale and gypsum units (Gohatsion Formation) (Getaneh Assefa, 1991) (3) Middle-Late Jurassic Antalo limestone and (4) the younger plateau forming volcanic rocks of Cainozoic flood basalts). Several subsequent studies have since been made with more detail study of the formations in terms of resource exploration, geomorphic evolution and hazard risk studies (for example Leulseged Ayalew et al., 2003, 2004; Gani et al., 2006; Wollela, 2007; JICA and GSE, 2012; Ismail, 2013).

The volcanic rock is found in direct sharp contact with the limestone where predominantly the rocks are of aphanitic basalts alternating with a tuff layers (JICA and GSE, 2012). The basalts are noted to form sub-vertical columnar joints (cooling joints) indicating rapid cooling after eruption. Slopes of the Gorge are covered with continuous accumulation on terraces of extensive and thick colluvium which has repeatedly undergone episodes of major landslides (JICA and GSE, 2012). These form gentle slopes on the areas underlain by limestone and shale while they form steeper slopes on the tertiary volcanic sequences.

Oldest geological structures in the area are results of sedimentary depositional features such as bedding and layering in the sedimentary formations. The strike of the bedding which is gently inclined has NW trend on Goha Tsiyon side and N to NE trend on the Dejen (northern side of the valley) side. The bedding in the limestone beds are almost horizontal, where by sets of two orthogonal sub-vertical extension joints with NW-NNE and NE-NEE trend intersect with. The younger volcanites in the Gorge have horizontal flow layering and alternation bedding with the tuff units while they exhibit well developed extensional joints in with NW and NE trends (Gani and Abdelsalam, 2009; JICA AND GSE, 2012). The prominent secondary tectonic structures in the region are generally dominated by NW and NE trending normal faults, which form prominent and continuous escarpment morphological features along with N-trending lineaments which are also identified in the area based on remote sensing data interpretation and field observation (*Figure 3-6* and *Figure 3-7*) (Gani and Abdelsalam, 2009).

3.7 Local Geological setting

It is interesting to note that the valley developed slightly asymmetrical profile across the gorge where the northern profile is more flattened than the southern sides of the valley (*Figure 3-7*) at the cross section between Gohatsion and Dejen towns (Gani and Abdelsalam, 2006, Lulseged Ayalew and Yamagishi, 2004). Coincidentally, this morphology is reflected

in the presence of more competent cliff forming beds of sediments in the southern side than in the northern side. Some have associated it to the prevalent mass wasting in the northern side of the valley and also to the character of the lithology distribution between the two sides (Lulseged Ayalew et al., 2009). For example a significant thickness of cliff forming limestone on the southern side is absent on the northern side (Lulseged Ayalew et al., 2009).

In the Abay Gorge, around the area of the profile from Gohatsion to Dejen, the formations from oldest (lowest) to the youngest (upper most) are described below. The superficial colluvial deposits in the areas where borings were made point to as much as 20 meter thickness (Almaz Gezahegn and Tadesse Dessie, 1994; JICA and GSE, 2012). The lithological units making up the valley are given in the following description and Table 3-1

Sandstones: Adigrat Formation

Late Palaeozoic to Triassic formations are mainly sandstones. The lower part is basically thinly bedded incorporates greenish silty mudstone and white sandstone alternation of strata. The middle part is characterized by fine to medium grained reddish sandstone which has a reddish tone on visual observation. The upper part is thickly bedded (1-3 meter) and characterized by thick white sandstone and its conglomerate. The unit has gradational contact with overlying siltstone and shale (Getaneh Assefa, 1980, 1991, Almaz Gezahegn and Tadesse Dessie, 1994).

Siltstone, mudstone and shale: Abay Formation

Middle Jurassic age intercalations of siltstone, mudstone and shale beds belong to Abay formation. They have gradational contact with both the over lying limestone and gypsum units as well as the underlying sandstone unit. The thickness of the main unit is about 120 m on the Gohatsion side and about 40 m on the Dejen side (Getaneh Assefa, 1980, 1991; Almaz Gezahegn and Tadesse Dessie, 1994; JICA and GSE, 2012). The siltstone unite is composed as well as of silt and clay particles. The shale is argillaceous clastic sedimentary rock which contains a lot of clay minerals which attains greenish friable beddings (JICA and GSE, 2012).

Lower Limestone and siltstone: Abay Formation

The limestone units are found occupying the area between the underlying shale and overlying gypsum units with thickness of about 70 m thick on both sides of the gorge and contains alternated limestone, siltstone and shale. They form moderately steep cliffs (Getaneh Assefa, 1980, 1991; Almaz Gezahegn and Tadesse Dessie, 1994; JICA and GSE, 2012).

Gypsum: Abay Formation

The thickness of this unit is about 130 m on the Gohatsion side and about 160 m on the Dejen side. Due to susceptibility to weathering the areas underlain by these units are prone to mass wasting. The lower and middle part is principally massive while the upper part is layered (Getaneh Assefa, 1980, 1991; Almaz Gezahegn and Tadesse Dessie, 1994; JICA and GSE, 2012).

Upper Limestone: Antalo Formation

These represent the late Jurassic ages in the area forming steep, cliff forming limestone beds, especially on the Gohatsion side of the valley side. Thickness of bedding decreases down ward in these limestone units (Getaneh Assefa, 1980, 1991; Almaz Gezahegn and Tadesse Dessie, 1994; JICA and GSE, 2012).

Tertiary volcanic unit

The thickness of the formation is over 380 m on both the Gohatsion side and Dejen side and occurs intercalated with pyroclastic layers (JICA and GSE, 2012). The lower part of this unit is characterized by a massive basaltic lava flow associated with colluvial deposit with thickness reaching 70 m while the middle part is composed of basaltic lava and pyroclastic rocks with thickness over 70 m (JICA and GSE, 2012). In the upper part basaltic lava and pyroclastic rocks form cliffs of over 80m high. In all the volcanic beds vertical widely opened joints are developed. These often appear to conduit water from surface to pass down to the less jointed and softer volcano clastic intercalations (JICA and GSE, 2012).

Colluvium is found all along the valley with varying thickness but are mainly concentrated on the terraces of volcanic units, Gypsum beds, and Abay Limestone. Their thickness is more than 20m especially on the Dejen side of the valley where numerous unstable landslides are concentrated (Almaz Gezahegn and Tadesse Dessie, 1994; JICA and GSE, 2012).

Table 3-1 Summary of lithologic section across Gohatsion-Dejen (Modified after Gani et al., 2006)

Age	Lithologic Units	Formation	Lithology	Mean Thickness (m)
Middle Oligocene to Early Miocene	Volcanic Rocks	Cainozoic Flood basalt	Mostly flood basalts with extensive columnar joints and dialation fractures, intercalation of pyroclastic deposits	~ 380

Age	Lithologic Units	Formation	Lithology	Mean Thickness (m)
Middle to Late Jurassic	Upper Limestone Unit	Antalo Limestone	Bedded to massive limestones with alternating layers of lime mudstones, fossiliferous, fossils include mostly brachiopods, gastropods, bivalves	~ 525
Middle Jurassic	Lower Limestone Unit	Abay Limestone	Alternating Limestone and gypsum where limestone increases upward, bedded limestone at base sometimes bioturbated	~ 290
Triassic to Middle Jurassic	Glauconitic Sandy Mudstone Unit Lower Sandstone Unit	Adigrat Sandstone	Upper part interbedded with hummocky cross-Stratified sandstone Coarse to very coarse sandstone, dune trough, less interbedded mudstone, channelized with large accretion surface, granule or pebble pockets, silicified wood, mostly fluvial	~ 250

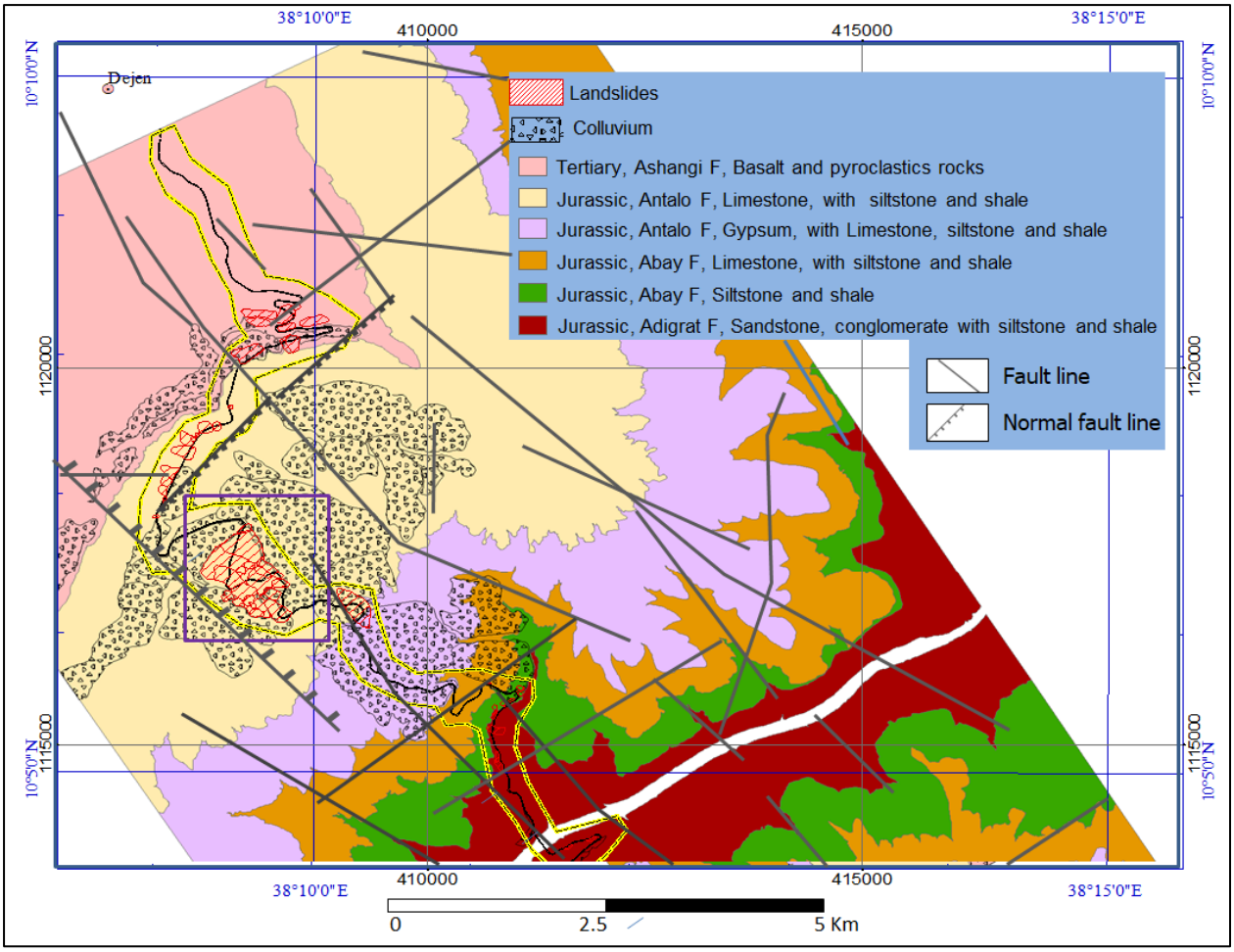

Figure 3-6 Geological map of theAbay Gorge along the Main Road from Gohatsion to Dejen. Pink colored box is location of the study site (Lithology after JICA AND GSE, 2012 and Fault line from Gani and Abdelsalam, 2009)

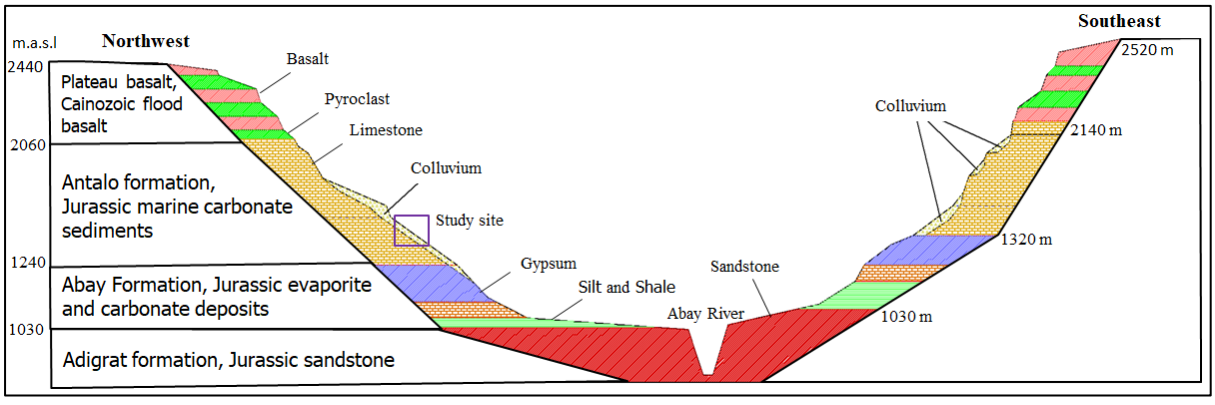

Figure 3-7 geological cross-section of the Abay Gorge parallel to the Millenium (Kessie) Bridge (modified from JICA AND GSE, 2012)

3.8 Description of the Landslide between Chainage 27 Km and 28 Km

Slope stability has long history in the Abay Gorge area. The first encounter in record is that of the collapsed Viaduct near Washa Michael Church at about 5 Km from the gorge entrance on Gohatsion side (south) in 1960. The Viaduct collapsed immediately after completion of

construction due to landslide (Jemal Saed, 2005). It was later discovered that the piers had been founded 12 meter above the bed rock suggesting a very thick unconsolidated colluvium underlying it and eventually collapsing.

The landslide which is the focus of the current study occurs between chaniage 27Km and 28 Km, measured from entrance of the gorge on Gohatsion side. The nearest settlement is the village of Kurar resting near the crown area of the landslide along the main road from Gohatsion to Dejen. Although several zones of instability are recorded on this northern side of the Abay Gorge slopes all along the road, a particularly active and wider slope instability occurs between the chainages 27 km and 28 Km. In this area a number of landslide scarps and individually moving blocks of shallower landslides and deeper landslides have been identified by study of JICA and GSE (2012). The blocks signify apparent difference in activation where several blocks represent different activation history. The morphological classification of the landslides is corroborated further by follow up extensive drilling and subsurface geophysical exploration program (JICA and GSE, 2012). In addition, a extesnive monitoring has been carried out by the installed water level and displacement sensors installed in the boreholes and on the surfaces in the landslide zone (JICA and GSE, 2012).

The area is comprised of sedimentary successions of cretaceous age overlain by Cainozoic volcanic series above 2,100 m a.s.l. In particular the landslide is located on carbonaceous formation of limestone of variably bioturbated and friable nature. It also features thin layers of silt and mudstone rich in carbonate (Figure 3-8f). Most striking feature of the geological material is the colluvium deposit which has substantial thickness as seen from drilled boreholes during the investigation of JICA and GSE (2012) and from field reconnaissance in the gullies. The landslides are mostly noted to be deeper in extent and recurrent in nature following rainy season. No activity of the landslide has been witnessed during the field visit to the area in last week of February, 2018. Nevertheless, the remnants of the recent landslide damage are still evident from the last rainy season.

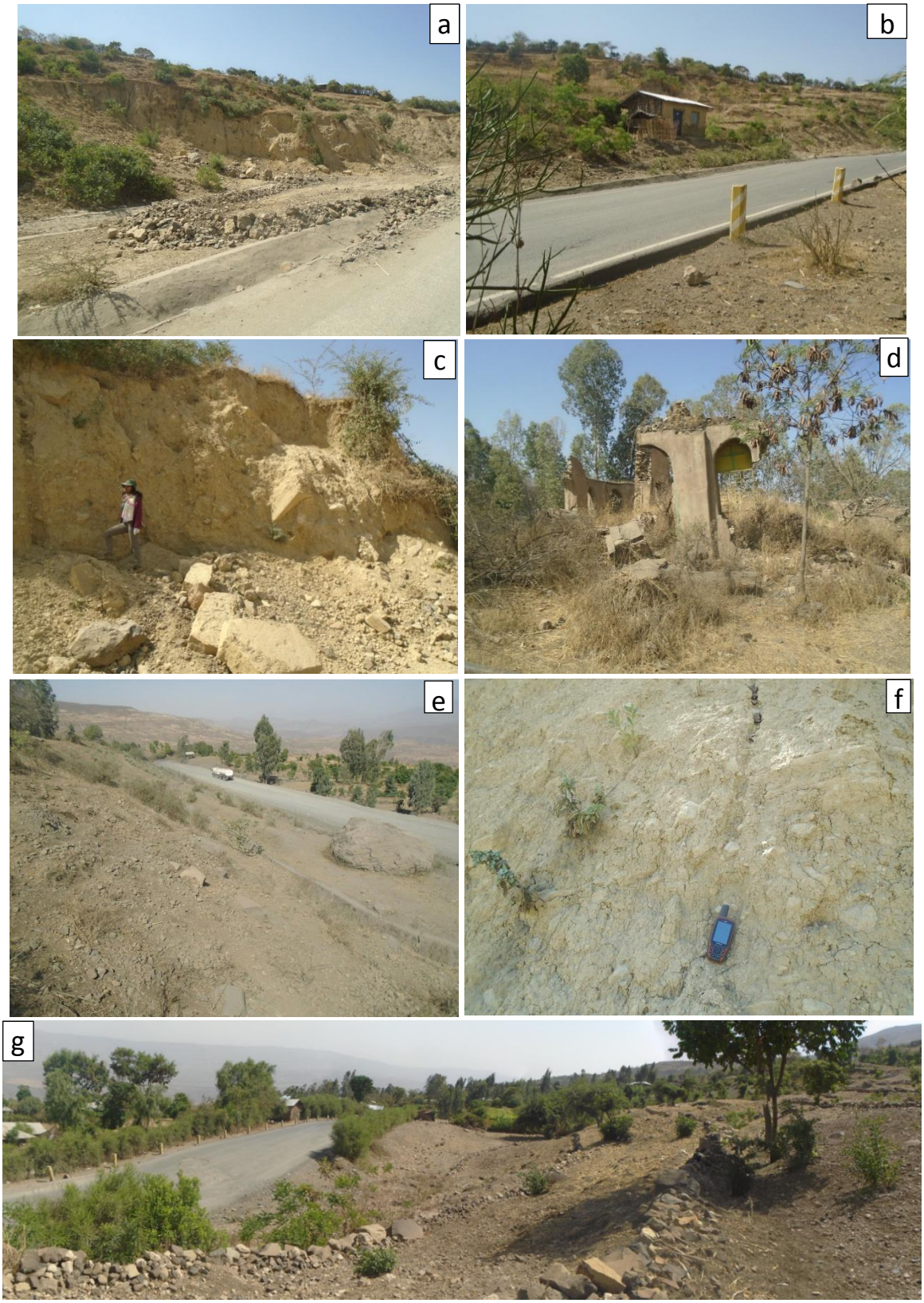

Figure 3-8 Current state of the landslide in the area (Kurar Village along main Asphalt road from Gohatsion to Dejen, at 28 Km from Gohatsion. (a)head scarp of the landslide (b)head of landslide (c) minor scarp (d)completely destroyed Church wall (e)compounded landslide picture at toe of the upper slide and head of next lower landslides (f)close up view of sliding material on minor scarp (g) Middle part of the upper most landslide block.

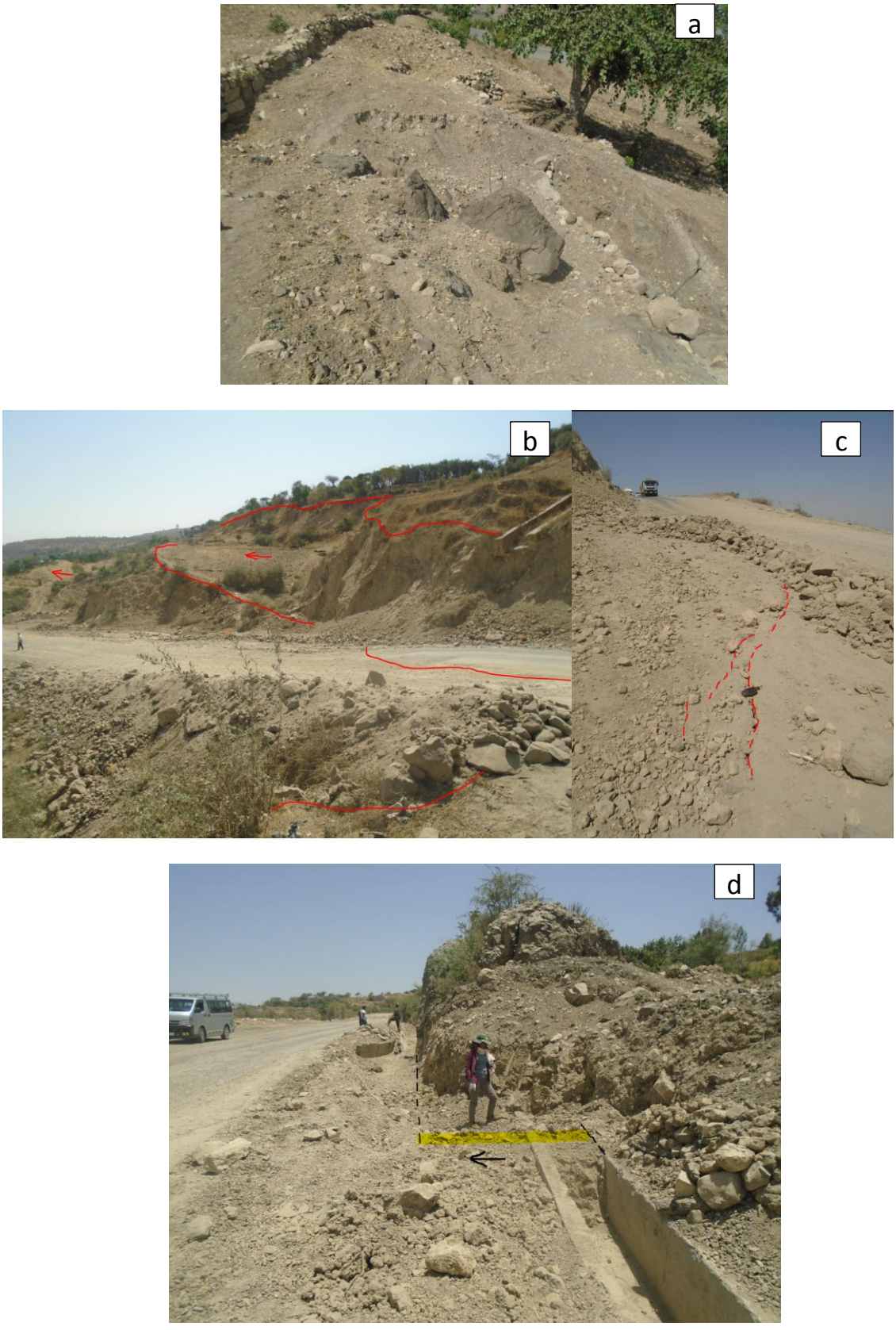

Figure 3-9 Current state of the landslide in the area (Kurar Village along main Asphalt road from Gohatsion to Dejen, at 28 Km from Gohatsion. (a) boulders of basaltic rock in the colluvium (b) and (c) head esarpments ad cracks observed on site (d)recent slide at around 11 Km from Gohastion in the Gorge along the same highway.

Extent of the landslide site

The landslide spans in extent with about 800m width and 1.2 Km length from head to toe in the central part (*Figure 3-10*). Considering the selected profiles of analysis and the resulting interpreted slip surface of deeper position and considering the spacing of the profiles, a tentative extent of about one million metric cubes of volume is estimated for the landslide at the site. Resting on rather low topographic slope the landslide generally forms series of very high and long main escarpments which have a northeast-southwest trend. To the northeast and southwest it is bound major torrents which are intermittent channels of running water with high discharge during rainy season as seen from debris in the channel.

Distribution of landslides

The landslide in the Abay Gorge is extensively distributed on both northern and southern slopes of the gorge. Gentle slopes spread out widely mid-way between on the gorge which are mostly limestone and shale. The selected site is on the northern side of the gorge facing south. The landslide site is located on a gentle topographic slope 8^0-10^0. There are many landslides in this area. Amongst the larger landslides there are overlapping secondary-landslides, many of which continue to be active. The various landslides that are noted in the area usually have distinct boundary marked by minor scarps and indicating various parts of the landslide activated at different times. They generally have translational slip surface as no significant rotation can be seen on the moved mass but are in most cases intact owing to the deeper slip surfaces in most cases. Depth to slip surface is variable along various sections of the slope profile and from profile to profile. The most active and shallower slip surfaces range in depth on average from as low as 3 to 30 meters as seen from inclinometer data (JICA and GSE, 2012).

In the study area, 10 landslide blocks were identified by the study of GSE (JICA and GSE, 2012). Only some of these conspicuous blocks are noted from the field reconnaissance during this study conducted in January, 2018. Continued modification of the morphology from repair work and leveling by inhabitants in the area for farming greatly modified the landslides morphology. Nevertheless, the major scarps are still evident and prominent in the area such as on the north eastern head area and the main escarp in the northwest (*Figure 3-10*). The area where a collapsed Church is found shows active deformation which is still apparent from the recently replaced and repaired gravel road in place of the damaged asphalt pavement. In the area close to the north eastern head area cracks are observed which also cross the main road

(*Figure 3-9* b and c). A number of installations were introduced following the investigation of GSE (JICA and GSE, 2012) which have been note in the field work. One of these is the horizontal wells installed into the slopes to drain out the water from the area and lower the water level. Nevertheless, the fact that the slide continues as seen in several locations along the main road, including sites which are not the target of this study, puts a question to the effectiveness of the counter measures.

Material properties

The materials on the locality of the landslide are uniform in composition with heterogeneous mixture of fine and coarse material supporting blocks and boulders of variable rocks. These are mostly indurated, yellowish white, silty and clayey dominated in some layers and significant proportion of rock fragments with a range of sizes. Although the majority of the rock fragments in the colluvium are of limestone, quite significant proportion of basaltic boulders and blocks are also found mixed in the material. The scarps in the head area are high enough to observe the material characteristics and show that near the ground surface, the colluvium is composed of heterogeneous mixture of clays and silts grading down to more gravel and cobble sized clast rich deposits of gravels and cobbles. Buried in the colluvium are also large blocks of limestone and basalt reaching up to 2 meter in diameter (*Figure 3-8* and *Figure 3-9*).

Plasticity in range of 20 – 45 % and wet unit weight range of 12.5 – 19KN/m^3 are reported from some studies (Lulseged Ayalew et al., 2009). An X-Ray fluorescence analysis of samples from the soil in the area revealed that the mineralogical compositions are Quartz, Albite, Muscovite and tridymite in the siltstone and shale derived soils while in the soil derived from limestone calcite and minor kaolinite and Muscovite are identified (JICA and GSE, 2012). Also the physical properties from few samples in the area indicate the unit weights to range from 2.11 to 2.8 gm/cm^3.

It is generally poorly sorted and shows moderate induration indicating quite old age of the deposit. The underlying materials are according to the geological map of the area, silt and shale with significant carbonaceous influx. In area where the presence of limestone is dominant the fine matrix and boulders attain more yellowish color.

Mechanism of failure and activity of the landslides

Most important geological structures that control occurrence of landslide in the area are the extensional joints well developed in the upper reaches of the valley in the basaltic layers. These are sub-vertical and have wider opening. The extensional structures do not penetrate into the underlying incompetent softer pyroclasts (tuff). The capping of these layers is one reason why instabilities are concentrated mostly in the contact between such incompetent interfaces where also thick colluvium is developed. In such cases the percolating water has greater chance to soak the base of most colluvium deposit facilitating and triggering recurrent instability. Field reconnaissance to the area was conducted in January where the expected rainfall is very low and activity of the landslide has ceased. Nevertheless, it was possible to observe the last landslide activity on the drainage ditched south of the studied area with offset of about 1.5 m between that passing through the landslide zone and the limit of the landslide (*Figure 3-9*d).

The activity of the landslides is also not uniform but shows marked difference from place to place where few blocks are more frequent than others while some blocks appear to be only mildly discernible. The inclinometer data shows moderate displacement of 10 $x10^{-3}$ mm/Year according to classification of Hungr et al. (2013). The surface extensometers installed across the cracks show 2.6 x 10^{-5} mm/sec displacement (*Figure 4-3*). The principal direction apparent from the scarps distribution and outline of landslide morphology is to the south east. The inclinometer data from the area when combined and analyzed for the resolved direction indicate azimuth of 135^{0} (southeast).On the other hand Inclinometer data from boreholes which register orthogonal sets of movement, one along the perceived direction of the landslide is to the southeast direction and the other in the northeast-southwest direction a slight deflection from southeast to east-southeast direction of movement is apparent. The landslide is translational with more or less long planar slip surface. A deeper slip surface is apparent according to the investigation of the JICA and GSE (2012) study report which compounds all shallower slips surfaces in all the slope profiles.

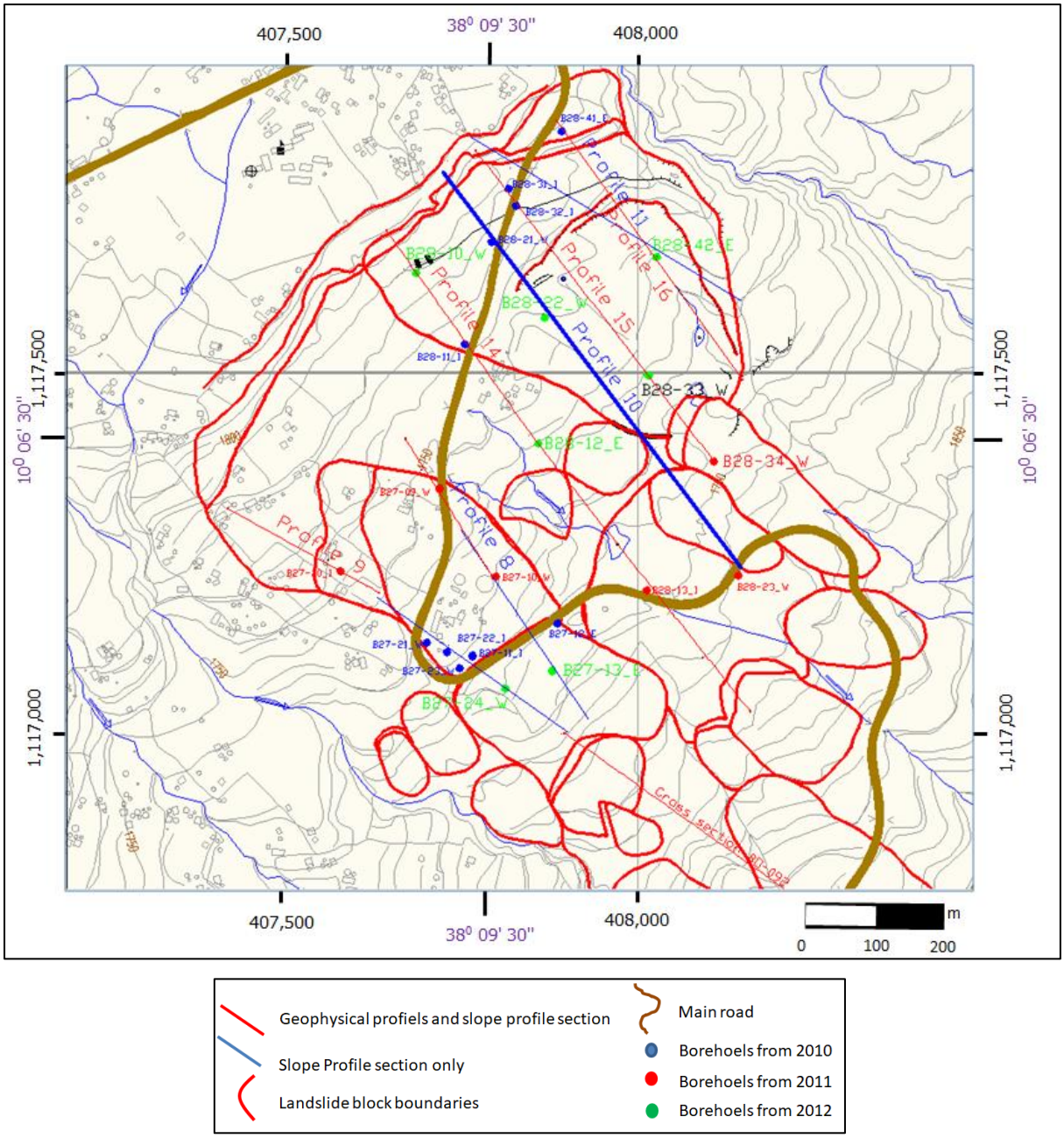

Figure 3-10 Location of profiles and boreholes in the studied landslide site (modified from JICA AND GSE (2012)

4. Methodology

In this chapter the methodology employed for the overall preparation of field and monitoring data for analysis of stability in 2D classical model and then application to a basic simple semi- 3D model is described. Most of the outputs are presented and discussed in the next chapters while typical outputs obtained are only shown in the sub-sections of the methodological chapter with emphasis on the steps and procedures used to derive the results which are presented and discussed in detail in the subsequent chapters.

4.1 Existing data interpretation and profile construction

There have been 6 profiles along a major landslide zone selected located between the chainages 27 Km and 28 Km along the main road from Gohatsion Town towards Dejen Town (*Figure 3-10*). This area is selected for the 2D based semi- 3D modelling and sensitivity analysis. The overall methodology followed in the study is summarized in the following sub-sections. Reference was made on the investigation data and published works from the study site in the past (Lulseged Ayalew and Yamagishi, 2004; Leulseged Ayalew et al., 2009; JICA and GSE, 2012; Masao et al., 2013).

Based on preliminary inquiry substantial monitoring data was found at the Geological Survey of Ethiopia which is being continually acquired from the monitored landslides in the Abay Gorge. Although some of the information has become less continuous with time the initial years of monitoring have yielded valuable information of year round data which can give a unique opportunity to utilize such information which rarely exists in the landslide affected terrain in the country.

Existing data includes borehole loggings and photos, topographic survey data, boundaries of landslide blocks, few physical laboratory tests of soil, geophysical survey using seismic refraction. Also in the boreholes drilled for the investigation of subsurface exploration monitoring devices were installed which have been gathering data for several years since the project started (JICA and GSE, 2012). The monitoring was especially instrumental to derive the most valuable information such as displacement depth corresponding to the slip surface position and groundwater level. These data were all integrated to develop overall slope model and material distribution in the topographic model.

Most important is the presence of detected slip surfaces in most of the test boreholes monitored, giving exact extent of landslide and even rate of displacement. The slip surface is

detected by using a special installed aluminium tubes in borehole which bend along with the sliding mass underneath. On the other hand overall displacement of the sliding mass is monitored by a special wire installed (borehole extension meter) in a borehole that digitally records instantaneous displacement by a winding coil. Another instrument called surface extensometer measures displacement across cracks on the surface in similar mechanism and by storing the data digitally in a data logger. Further, groundwater fluctuation is continuously monitored by digital transducer that converts the weight of water column in the perforated borehole above the depth of installation. As the instruments are automatic with high temporal resolution they generally give a detailed and large data set when used for year round analysis. Apart from this archives of the core samples and geophysical survey results of the area from the investigation of the joint JICA and GSE (2012) study are available in published and raw format that can further aid in constraining the characteristics and extent of the landslides in the study area.

The topographic data were used to generate the profiles following the series of parallel lines running from head of the landslide to the toe of the landslide. These profiles are selected so that they cross as many boreholes as possible. Also these profiles coincide with the location where geophysical profiles using seismic refraction and electrical resistivity were made (*Figure 3-10*) (JICA and GSE, 2012).

4.2 Monitoring data review

The Geological Survey of Ethiopia carried out an extensive landslide survey (JICA and GSE, 2012) together with Japanese counterpart. The study focused on long term monitoring and investigation of several sections in the Abay Gorge along the Main trunk road between Gohatsion and Dejen. Over the course of the investigation monitoring of groundwater level, displacements in boreholes, and rainfall intensity were made. These have been found to correlate quite well with the borehole core samples photo, which is also archived in the project (JICA and GSE, 2012). The figures *Figure 4-1* to *Figure 4-11* show some of the correlations such as the location of slip surface, water level fluctuations, and relation between displacement and precipitation.

The monitoring of borehole inclination also in some of the boreholes was not effective as it either was collapsed before any measurement or lacked repeat measurements due to extreme instability rendering it out of use. But still most of the boreholes had given valuable information necessary to derive the depth to slip surface. In addition strain gauges were also

installed in some new lately added boreholes which further gave information on slip surface position. Strain gauge data from Borehole 28-32 in, *Figure 4-1*, clearly shows the sharp strain recorded in a narrow zone which relates to about 33 meters depth and compares well with the material seen in the core photograph to the right. Inclinometer data from Boreholes 28-31 and 27-21 both show occurrence of clear and sharp displacement at about 13 and 14 meters depth respectively and indicate the slip surface to occur in the middle of the colluvium (*Figure 4-2*).

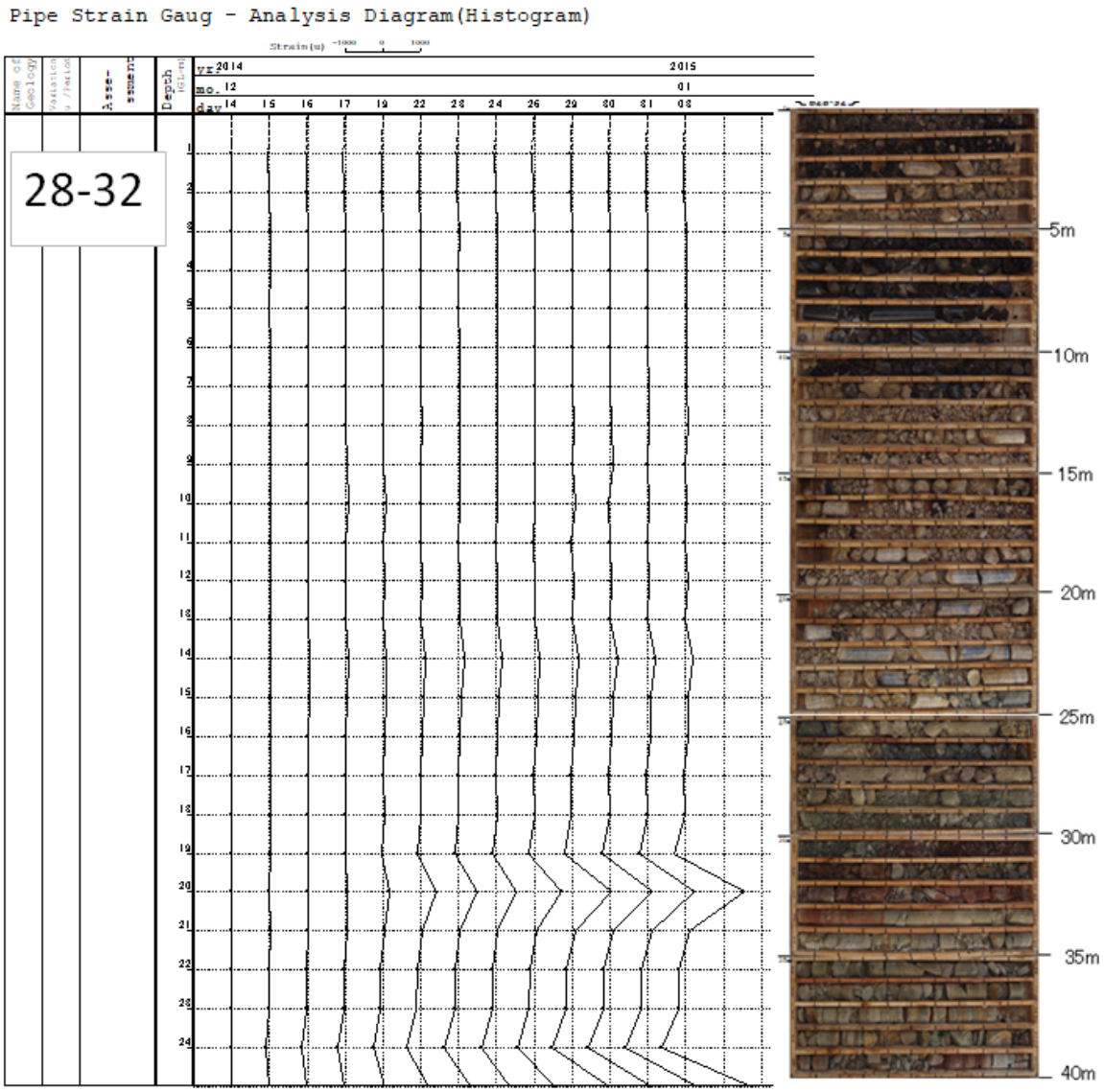

Figure 4-1 Borehole strain gauge data from a case of Borehole 28-32 close to Profile 15. To the right is corresponding core photograph showing geological materials (JICA and GSE, 2012).

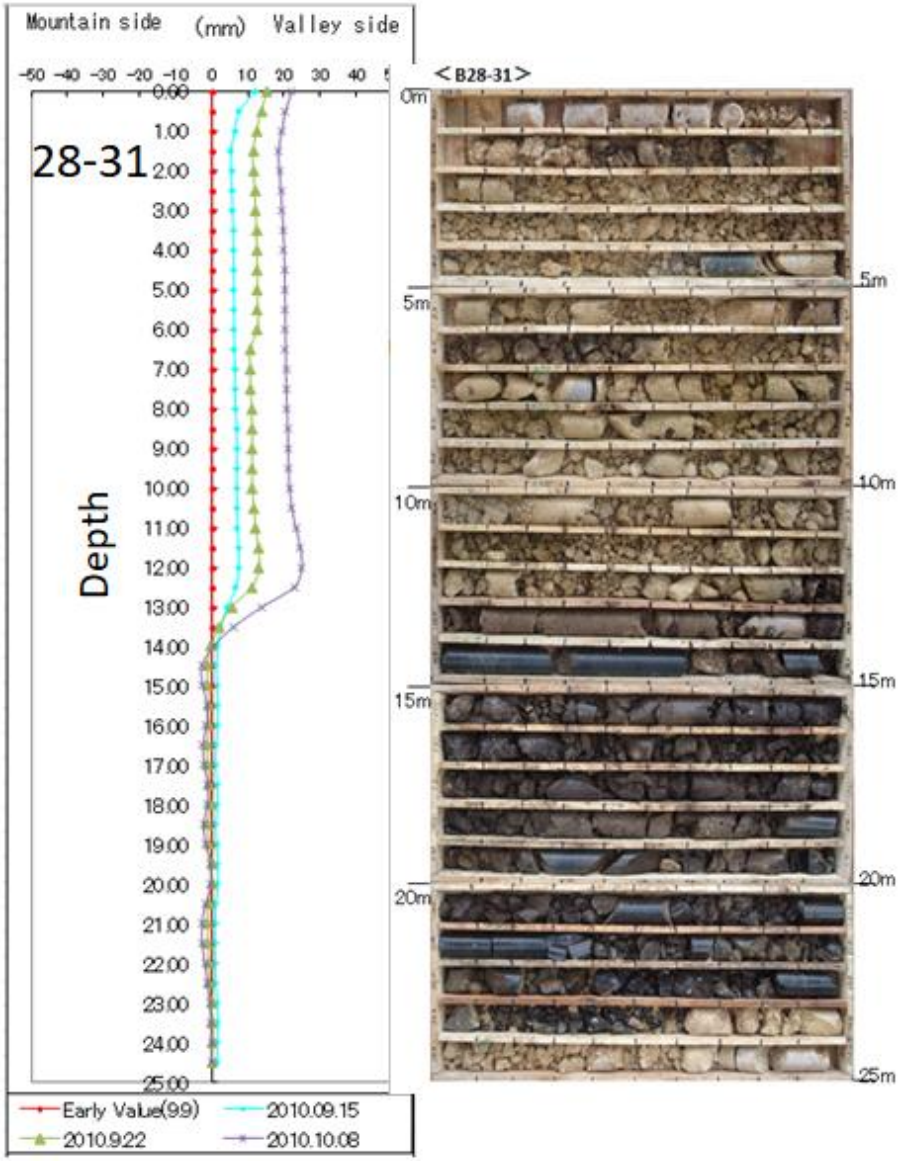
Mountain side (mm) Valley side
28-31
Depth
Early Value(99)
2010.09.15
2010.9.22
2010.10.08
<B28-31>
0m
5m
10m
15m
20m
25m

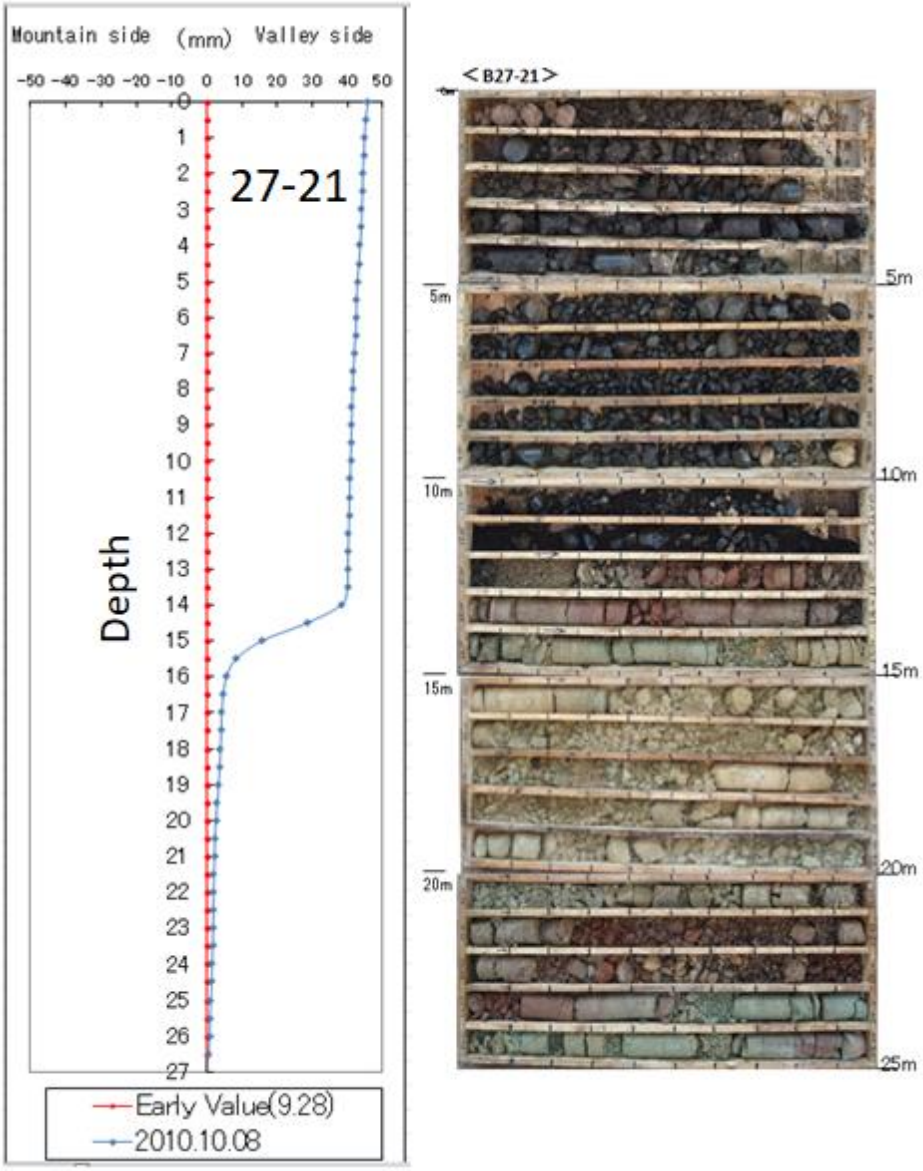
Mountain side (mm) Valley side
27-21
Depth
Early Value(9.28)
2010.10.08
<B27-21>
5m
10m
15m
20m
25m

Figure 4-2 Borehole Inclinometer data from a case of Borehole 28-31(left) and BH 27-21 (right) close to Profile 11 and profile 9 respectively. Each line of different color is measurement on specified data at the bottom. Apparent sharp displacement contrast corresponding to contrast in geological material in both figures (JICA and GSE, 2012)

The surface displacement from extensometers installed across major cracks showed strong correlation between time of movement (Figure 4-3) and precipitation (Figure 4-5). On the same date of maximum daily rainfall recorded in the station located in the middle of the landslide (JICA and GSE, 2012) a large displacement across the crack of more than 225 mm, was recorded (Figure 4-4). This shows impact of the precipitation as a triggering factor. The same record is noted in the borehole extensometer (Figure 4-4) where 44 mm of displacement is recorded associated with the same precipitation.

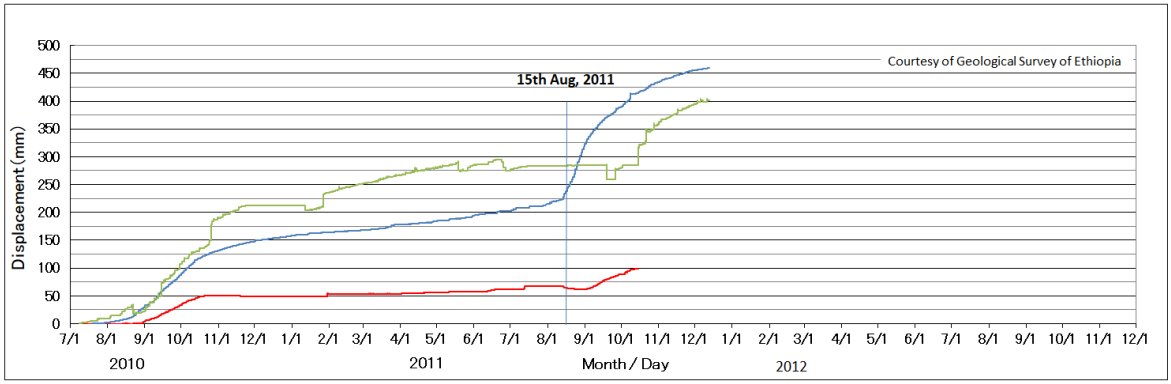

Figure 4-3Surface extensometer displacement measurement data from three locations in the landslide zone having a significant displacement as a result of strong effect of anomalous intense rain. Shown by red line are displacements corresponding to peak rainfall intensity (based on JICA and GSE, 2012).

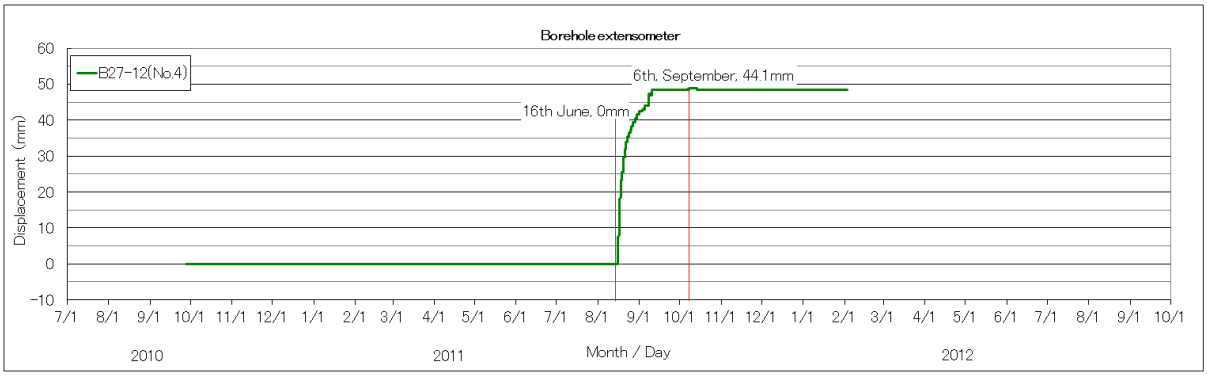

Figure 4-4 Borehole extensometer displacement measurement data from a case of Borehole 27-12 close to Profile 8 with strong effect of rainfall intensity resulting in significant displacement. Shown by red line are displacements corresponding to peak rainfall intensity (based on JICA and GSE, 2012).

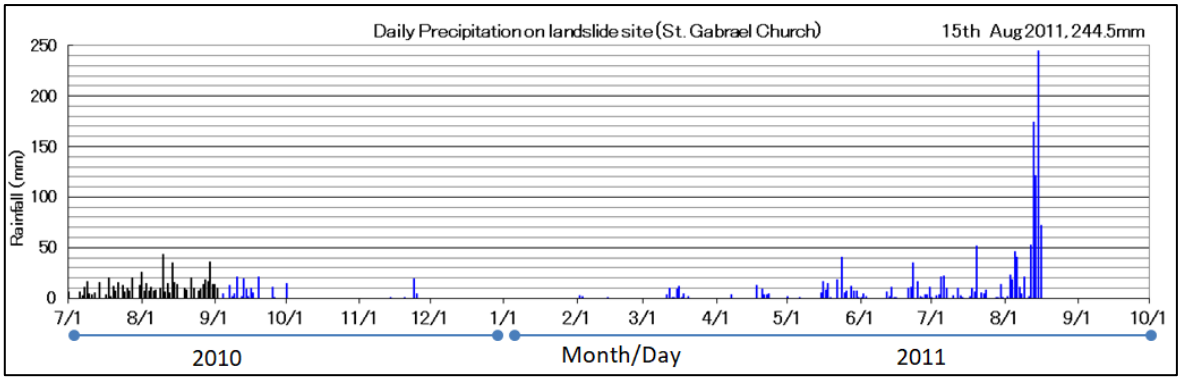

Figure 4-5 Precipitation data record from monitoring station located in the landslide site (JICA and GSE, 2012)

The water levels in the chosen profiles have been either interpolated from boreholes along the profile or from those located outside the line but closer. Some of the intended boreholes did not give credible information or were lost due to theft (JICA and GSE, 2012). But the available and more reliable ones (for example BH 27-12, BH 27-10, BH 28-33, BH 28-22, BH 28-10 and BH 28-23) have been valuable to derive the water level and its fluctuation.

Borehole 27-21 showed slight peak between October and November while remaining stable at 25m depth (*Figure 4-6*). A closer Borehole also showed constant phreatic water level at 25m depth (*Figure 4-7*). Other boreholes slightly further to the north east showed more fluctuation but were installed in the later stage of the investigation and hence had little coverage of time history. In this area the boreholes 28-10, 28-33, 28-23 showed large contrast in water levels between immediate post rainy season and the rest of the year. Fluctuations of about 10-15 m to water levels were recorded (Figure 4-8, Figure 4-10, Figure 4-11). Borehole 28-22 in the same locality, on the other hand only showed minor fluctuation of about 2-3 meter variation in water level (*Figure 4-9*). In the case of water level data from Borehole B28-33, two separate measurement series resulted in the apparent sharp discordance between the time series data. Inspection of the data reveal that also for consecutive 4 hours around the observed anomaly, no data, "0" was recorded, and that it was followed by continuation of normal measurement. Although no witness account has been confirmed it might be speculated as being related to onset of instantaneous landslide. The readings afterwards appear to be normal except perhaps changing of the sensor's depth position (lowered) due to the displacement. Also, in the case of water level data from B28-10, an anomalous peak appears on the date of 28th January 2012, starting from 03:36 AM to 13:12 AM (Figure 4-10).

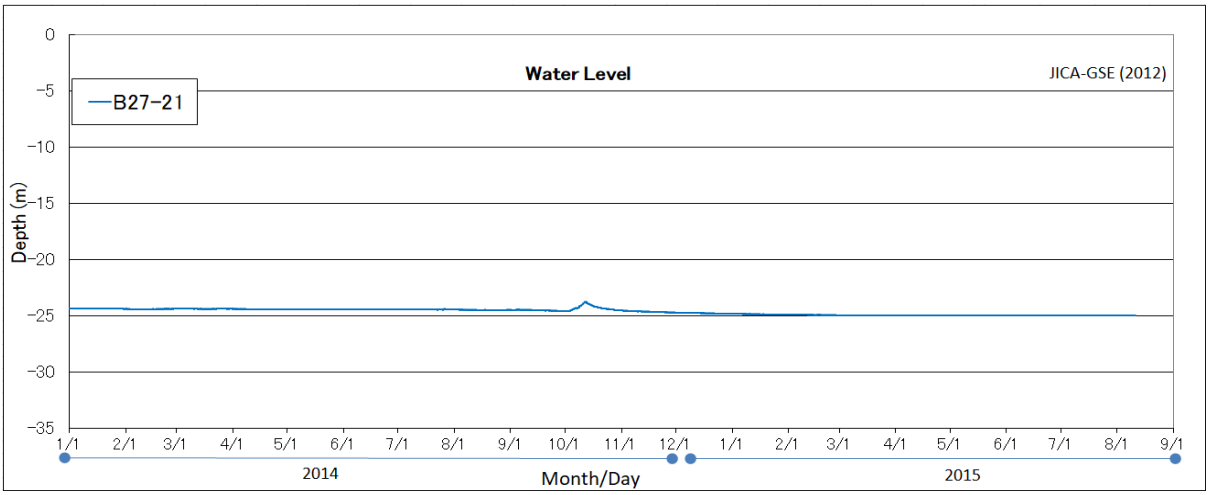

Figure 4-6 Water level fluctuation measurement data at BH27-21 close to Profile 9 (based on JICA and GSE, 2012).

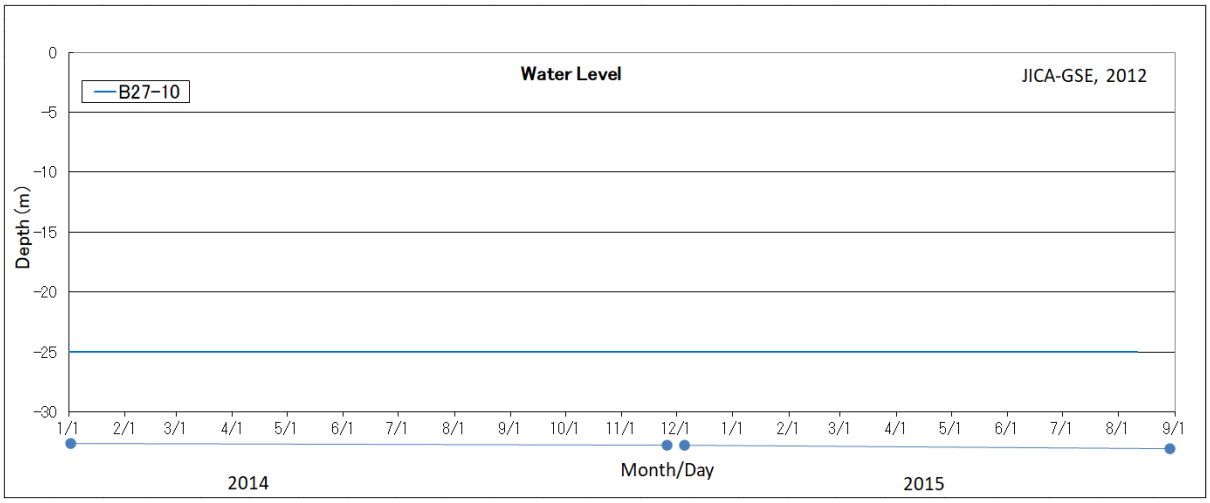

Figure 4-7 Water level fluctuation measurement data at BH27-10 close to Profile 8 (based on JICA and GSE, 2012).

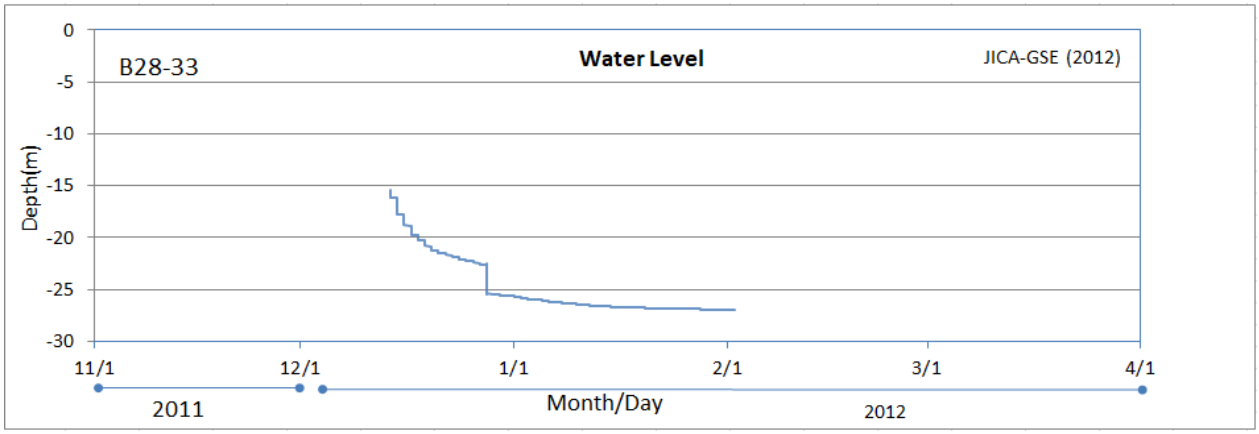

Figure 4-8 Water level fluctuation measurement data at BH28-33 close to Profile 11 and Profile 15 (based on JICA and GSE, 2012).

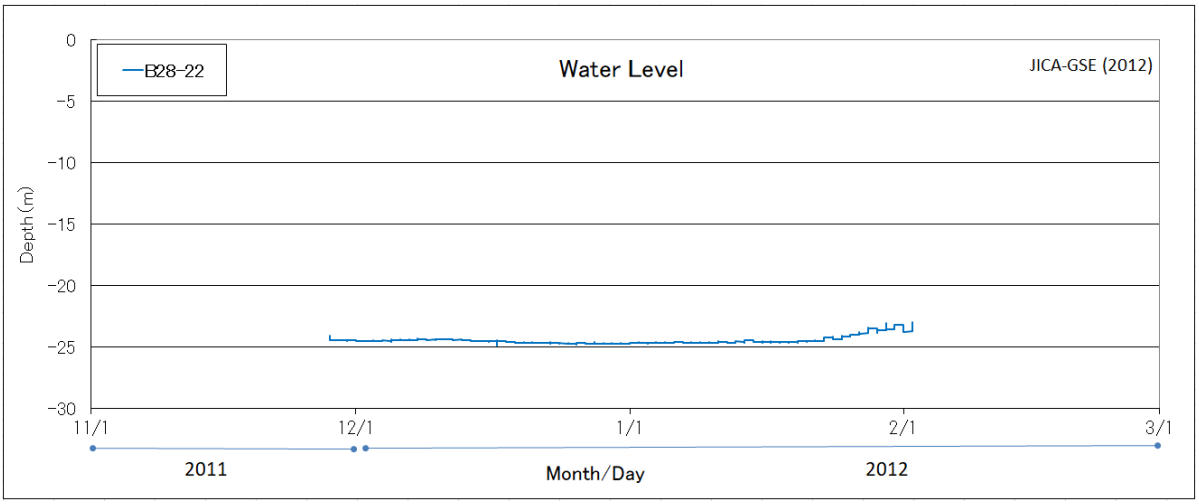

Figure 4-9 Water level fluctuation measurement data along BH28-22 close to Profile 15 and Profile 16 (based on JICA and GSE, 2012)

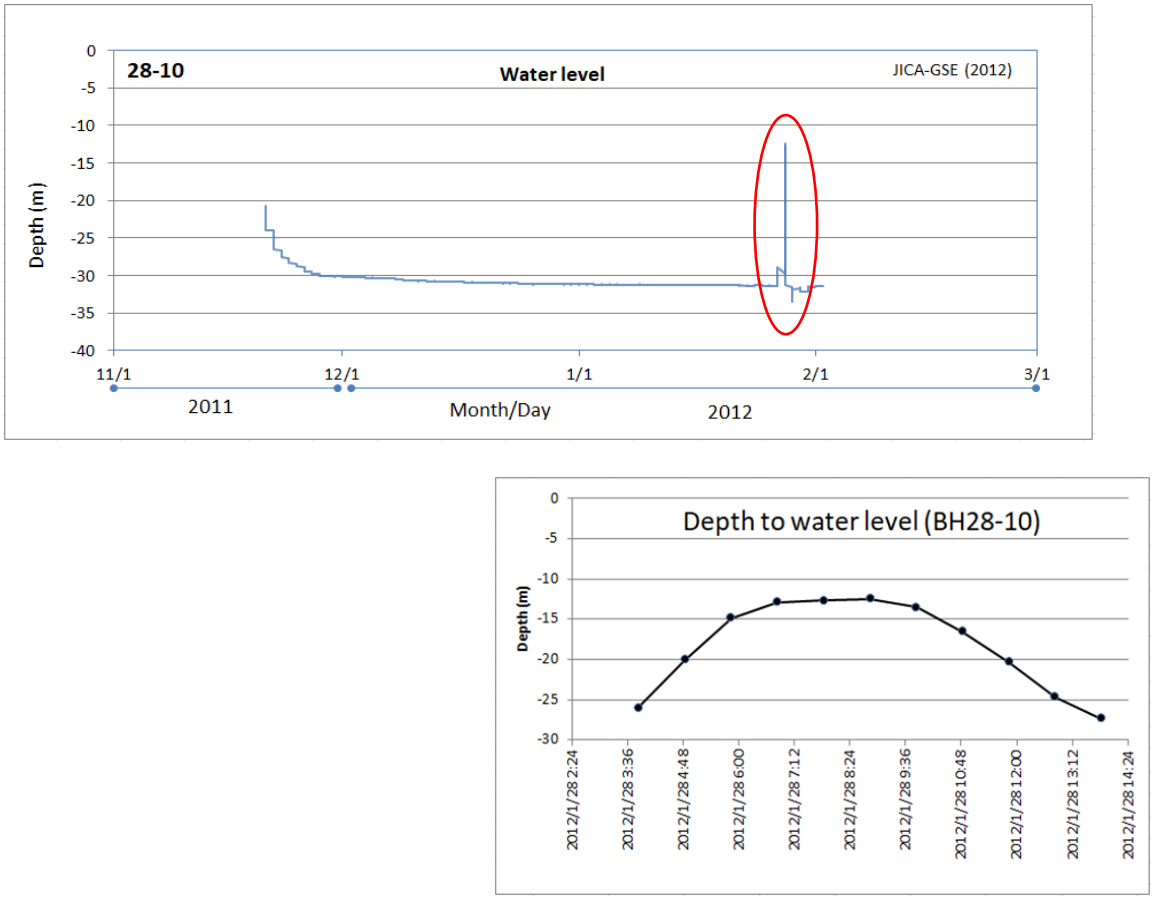

Figure 4-10 Water level fluctuation recorded data at BH28-10 close to Profile 14. Lower figure corresponds to the record at the time highlighted by red circle in the upper figure (based on JICA and GSE, 2012).

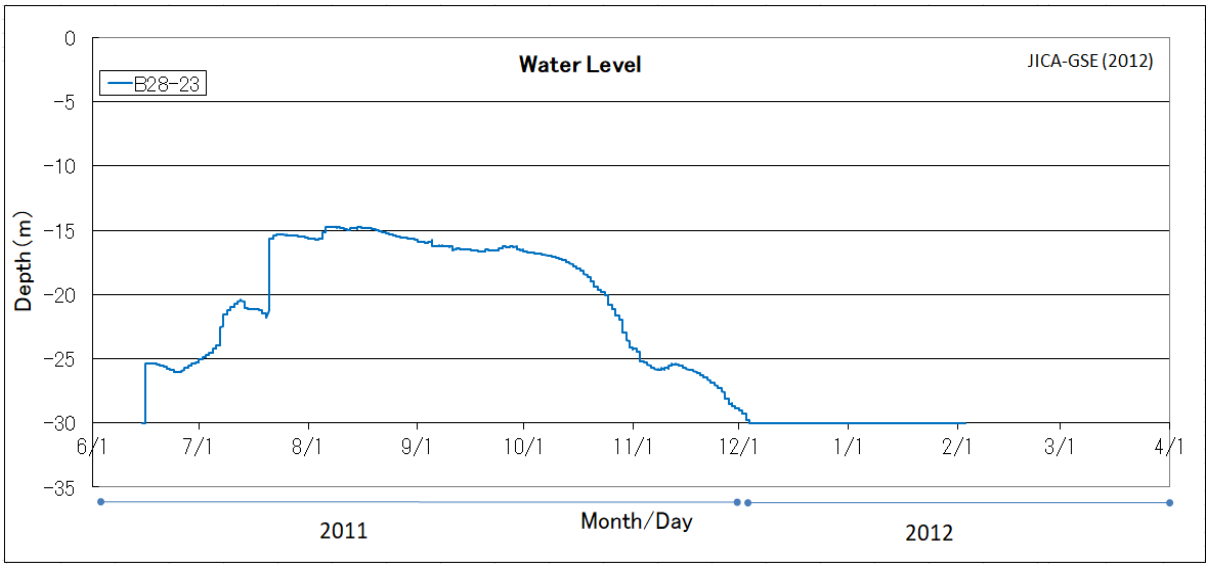

Figure 4-11 Water level fluctuation recorded data at BH28-23 close to Profile 16 (based on JICA and GSE, 2012).

Selection of slip surface

In view of the monitoring data and topographic map with landslide blocks and landslide movement direction consideration to model the deeper slip surface was chosen. This is chosen in view of two main reasons, the first is that the deeper slip surface has good number of transects to provide spatial information on the profile of the slope to model it with sufficient depth of boreholes in most cases. The second reason is that, the deeper slip surface is thought to extend throughout the whole area of instability acting as coherent body making it logical to model as single 3D model while encompassing a wider range of lateral inhomogeneity in terms of geometry and material property. The later hence is creates opportunity to test the role of such variability on the factor of safety derived in individual 2D factor of safety and the weighted 3D factor of safety.

The selection of the profiles is dictated mostly by the availability of the geophysical and monitoring data available which indeed conveniently also follow the general profile of the landslide from head to toe, in the northwest – southeast trend.

4.3 Geometric construction

Geometric construction and organization of the landslide based on the available data and field observation were all adjusted and implemented first in AutoCAD® software where geophysical profiles were plotted under the chosen slope profile along with location of boreholes. Most of the interpretations are based on the interpreted slope models by the JICA and GSE (2012) study with modification along additional profiles and simplification for

stability analysis. The boundary between the various subsurface materials (lithology and superficial deposits) were then derived from the contrast in geophysical profiles as compared to the information seen in the borehole logs plotted together under the slope profile. These were extrapolated to all of the slope profile section. Whenever there was shortage of boreholes along some of the profiles, nearest boreholes (usually few tens of meters away) were projected into the profile to estimate the boundary on the geophysical profile (Figure 4-12).

Further, monitoring data of groundwater level and slip surface position were also projected on to the slope profile section from the boreholes along the profile line. Wherever borehole information were not encountered along some part of the profile, information was projected from closest boreholes to the profile by taking the inherent geometric offset into account. The plotted information along the profiles at the point of boreholes was then extended likewise to all of the slope profile section through logical extrapolation such as: (1) relative positions in subsequent boreholes (2) dip or continuity of the connecting lines (3) following the topography (4) the contact between the unconsolidated colluvium and bed rock. The bed rocks were mostly also delineated across the profile section following the geophysical profile aided by observed contacts in boreholes.

The final product of this process was the overall slope model which is ready for running stability analysis and sensitivity analysis (Figure 4-13). The most important aspects were to define the slip surface outline in each profile section, the water table line, the topographic profile and the material properties involved in the slide, in this case the colluvium.

The subsequent tasks were implemented by importing the dataset in AutoCAD® drawing exchange format file (*.DXF) to ArcGIS® Shape file (*.SHP). This is chosen as the capability of editing objects with attribute was more efficiently manageable in ArcGIS®.

The first task in ArcGIS® was to divide the slope model into slices of variable width and extract pertinent information for individual slices. This was repeated for all slope profiles being considered to integrate into the semi-3D model.

The selection of slicing width was based upon (1) significant breaks in topographic profile (2) the break along interpolated lines representing the estimated groundwater level and (3) slip surface gradient change. Several authors advocate such an approach rather than having uniform spacing or interval of slices as the logical and computational implications will be

much clearer (Duncan 1996; Cornforth, 2005). After deciding and drawing of the slices in ArcGIS®, the geometric attributes of the slope model were extracted using various spatial manipulation tools.

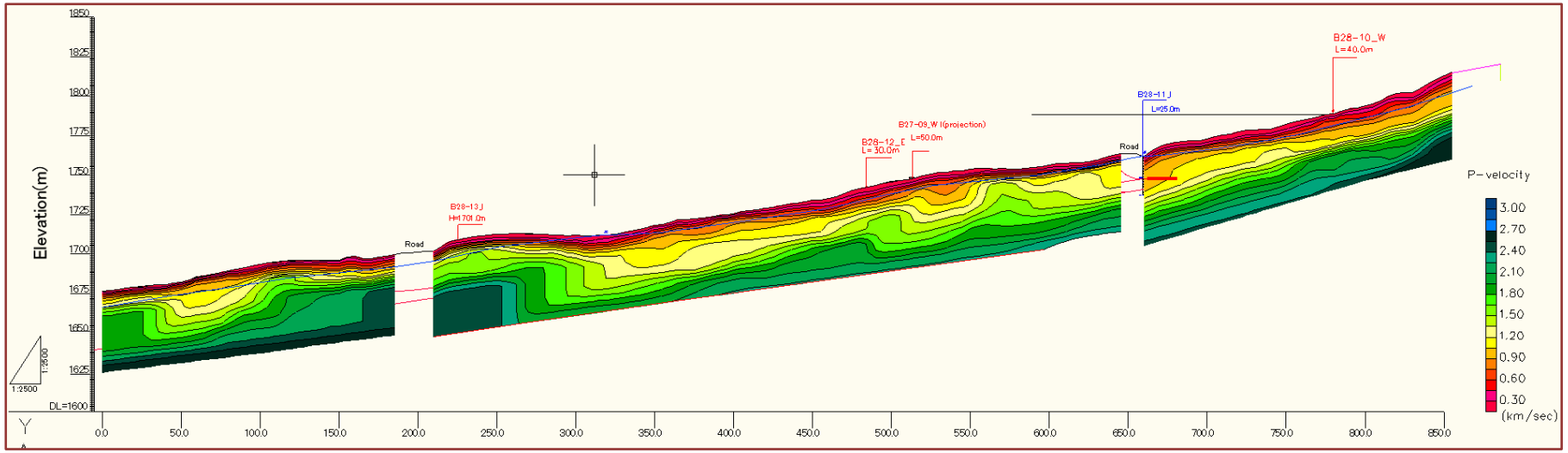

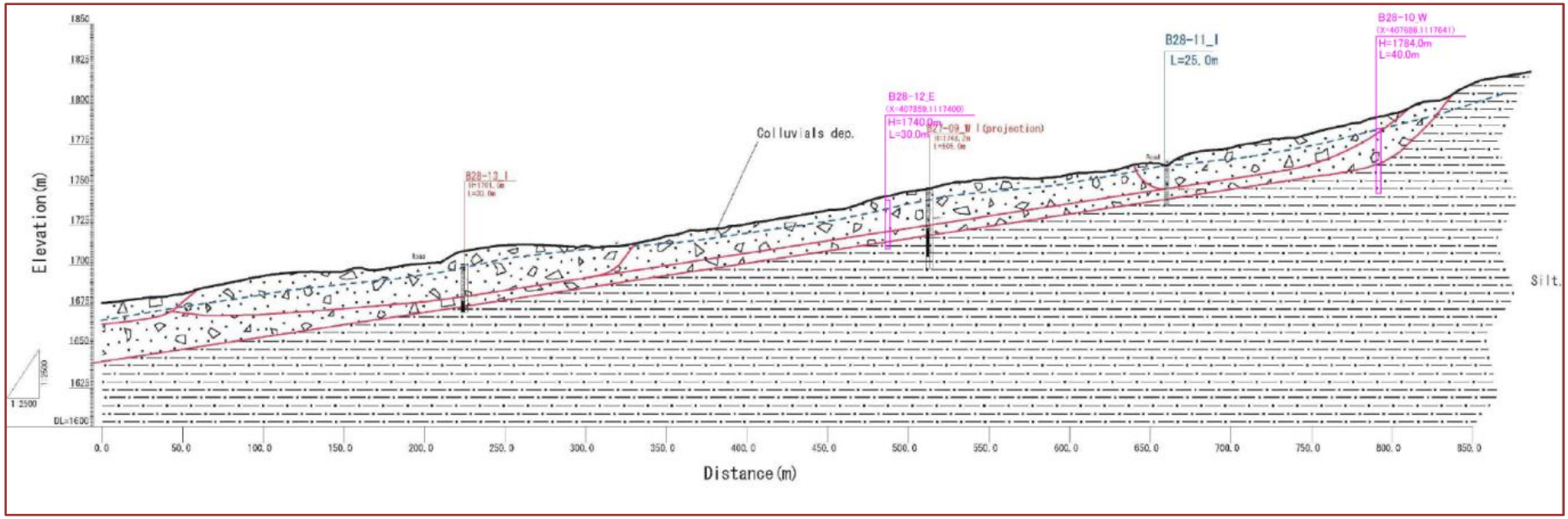

(!! Figure 4-12 next page)

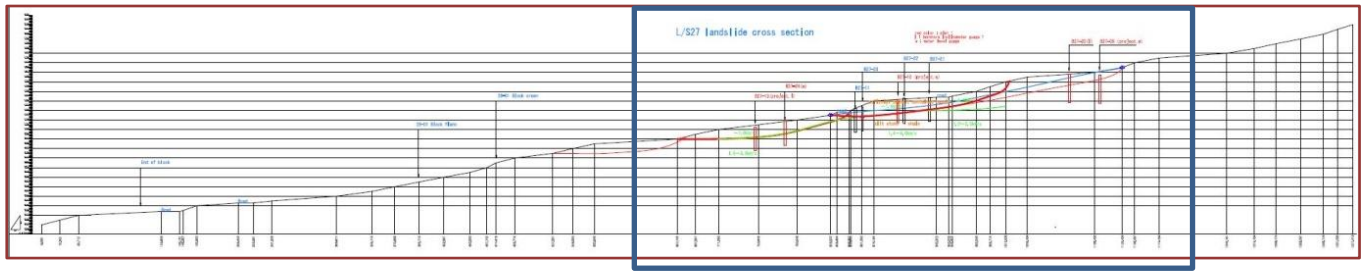

Figure 4-12 Schematics of an example (profile 14) show casing the typical process involved in AutoCAD to generate the overall slope model from Geophysical data and borehole logs and monitoring data overlay (upper) to generate the slope model (middle) and eventually giving the needed information (lower) modified from JICA and GSE (2012) (close up view in Figure 4-13).

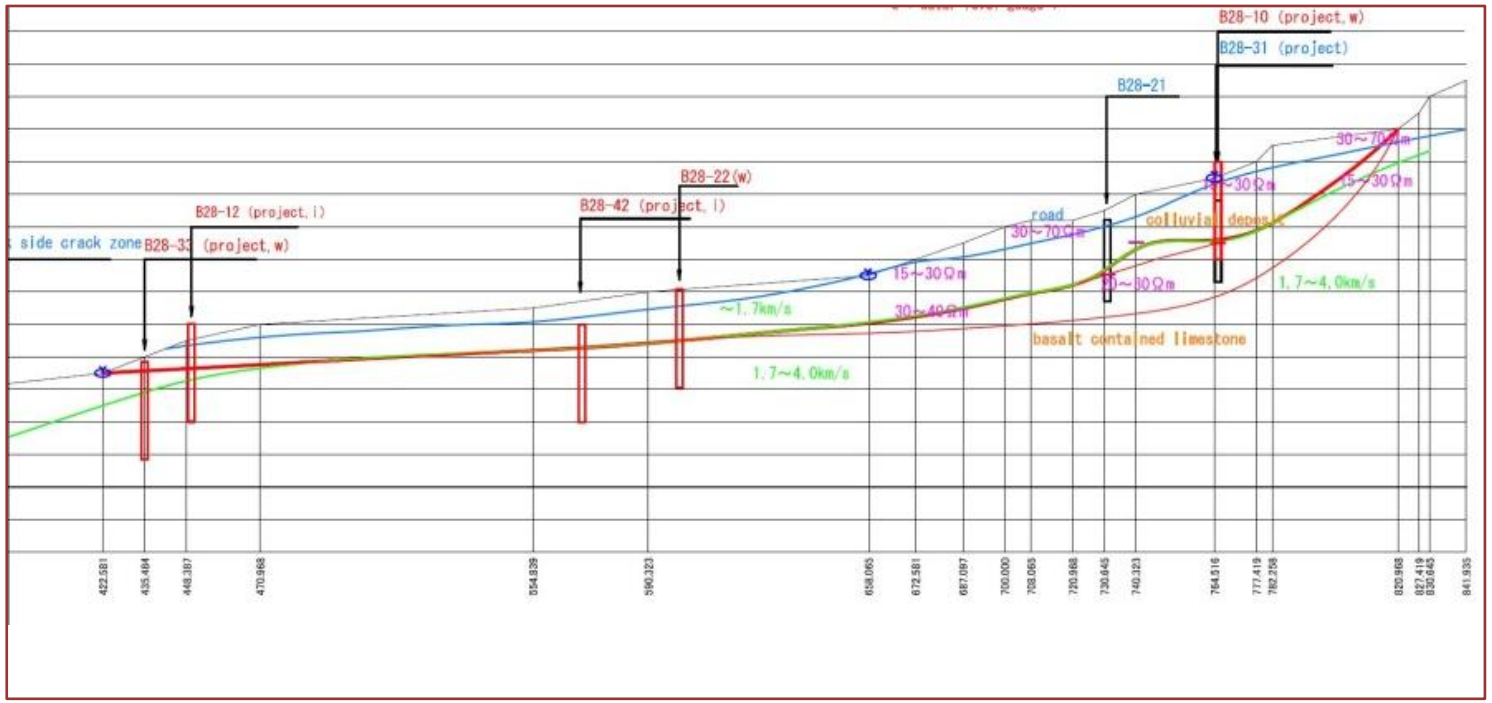

Figure 4-13 slope model example from Figure 4-12 zoomed to show the parameters used for the stability analysis

4.4 Derivation of numerical input values

Slice width is the individual width of the slices that is considered in the calculation of the stability factor of safety as shown in Figure 4-14 represented by the term 'b'. It was extracted by using the COGO function in advanced editing tools of ArcMap in ArcGIS 10.4® applied on the imported line objects drawn in AutoCAD® software. The COGO tools are able to measure the orthogonal distance between line and another point located out of the line. Hence on every selected side of the slice a point from the next side is used to find orthogonal distance in between to find the width of the slice. This was repeated for the number of slices at a time and the results stored in text file and later on stored in a database (spread sheet). The width of the water table is in most cases equal to the width of the slice unless it dies out in some cases which were in those cases reduced to the width of slice the water crosses, manually.

Slice heights which are the other important definitions of the slices involved in stability analysis are as shown in Figure 4-14 represented by two pairs on upslope and down slope side. These were obtained by individually calculating the heights of the slice sides in the attributes of the objects in ArcMap® using the 'Calculate Geometry' option. This was also stored in a spread sheet database with identification of the slice along with the respective width. The length of the upslope slicing line normally becomes the length of the slicing line on the down slope side for the next slice upslope.

Water level heights measures in each slice as height of phreatic water level above the slip surface are also shown in Figure 4-14. It is also obtained after clipping the slice height by groundwater table line and performing similar operation as was done for the extraction of slice height and stored in the data base.

Inclination Angle of slice base which in other words is the inclination of the slip surface under the slice being considered (α in Figure 4-14) was calculated by using the COGO function in advanced editing tools of ArcMap in ArcGIS 10.4®. The particular tool utilizes individual measurement of the feature from each slice where the upslope side of the slice is chosen to assign base inclination for each slice. Hence in COGO tool a function which measures angle between any two angles was chosen and applied between the upper side of the slice and a straight segment of the slip surface it intersects with for each slice. These were then subtracted from 90^0 to arrive at the inclination from horizontal for each slice's base and stored in the database.

All the constructed profiles from the previous study by JICA and GSE (2012) and from this work are given in the following subsequent figures along with the input parameters generated for each profile in the tables associated with the slope diagrams.

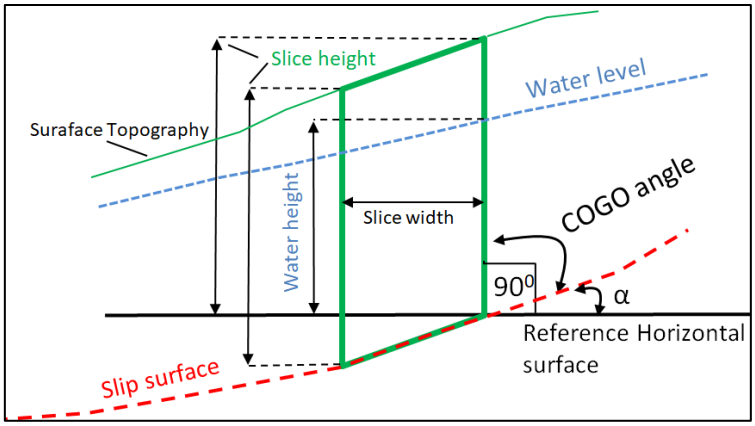

Figure 4-14 Schematics showing the various geometric values extracted in ArcGIS for individual slices

Slope profile 8

Inputs generated for Profile 8 are given in *Table 4-1*. The diagrammatic configuration is as shown in *Figure 4-14*. The profile slope model constructed for the stability analysis is given in *Figure 4-15*.

Table 4-1 List of parameters generated from the available data for the slope profile 8

Slice Number	Lower slice height (h_1)	Upper slice height (h_2)	Slice Width (b)	Inclination of Slice Base (α)	Height of water table (u_2)	Width of water table (b)
sl8-1	0.0	6.2	25.6	6.8	2.1	25.6
sl8-2	6.2	8.8	50.1	4.7	4.3	50.1
sl8-3	8.8	10.4	49.8	4.8	5.9	49.8
sl8-4	10.4	8.9	16.0	4.5	8.9	16.0
sl8-5	8.9	12.5	7.9	35.3	9.1	7.9
sl8-6	12.5	3.5	4.6	-5.7	0.0	4.6
sl8-7	3.5	8.8	7.4	3.4	2.6	7.4
sl8-8	8.8	12.9	16.1	3.6	5.7	16.1
sl8-9	12.9	14.0	47.1	3.3	8.8	47.1
sl8-10	14.0	13.1	35.6	3.4	7.6	35.6
sl8-11	13.1	12.9	14.2	4.6	6.0	14.2
sl8-12	12.9	18.5	35.8	4.4	12.5	35.8
sl8-13	18.5	18.9	37.5	4.5	18.9	37.5
sl8-14	18.9	19.0	42.5	5.0	16.0	42.5
sl8-15	19.0	0.0	25.0	9.3	0.0	25.0

Slope Profile 9

Inputs generated for Profile 9 are given in Table 4-2. The diagrammatic configuration is as shown in *Figure 4-14*. The profile slope model constructed for the stability analysis is given in Figure 4-16.

Table 4-2 List of parameters generated from the available data for the slope profile 9

Slice Number	Lower slice height (h_1)	Upper slice height (h_2)	Slice Width (b)	Inclination of Slice Base (α)	Height of water table (u_2)	Width of water table (b)
sl9-1	0.0	6.0	12.6	-10.7	1.4	12.6
sl9-2	6.0	10.2	22.6	-6.3	8.1	22.6
sl9-3	10.2	12.3	27.5	1.9	10.4	27.5
sl9-4	12.3	12.4	15.9	5.5	12.4	15.9
sl9-5	12.4	8.5	36.9	7.5	7.1	36.9
sl9-6	8.5	12.2	12.2	10.8	8.1	12.2
sl9-7	12.2	9.9	11.0	14.6	8.1	11.0
sl9-8	9.9	8.1	15.5	18.0	5.3	15.5
sl9-9	8.1	13.6	11.2	20.2	7.3	11.2
sl9-10	13.6	15.1	11.2	4.6	8.6	11.2
sl9-11	15.1	14.4	35.0	4.5	6.9	35.0
sl9-12	14.4	11.2	32.8	4.3	4.5	32.8
sl9-13	11.2	14.3	21.1	4.4	7.4	21.1
sl9-14	14.3	16.0	19.2	4.6	9.4	19.2
sl9-15	16.0	23.2	21.1	4.6	15.9	21.1
sl9-16	23.2	23.0	22.8	4.4	15.1	22.8
sl9-17	23.0	20.4	12.2	4.5	13.9	12.2
sl9-18	20.4	20.3	20.0	4.5	12.9	20.0
sl9-19	20.3	19.4	17.4	4.7	12.9	17.4
sl9-20	19.4	20.1	17.7	6.6	12.0	17.7
sl9-21	20.1	18.7	20.0	6.8	14.1	20.0
sl9-22	18.7	25.7	30.0	7.0	18.8	30.0
sl9-23	25.7	23.9	40.1	8.4	17.1	40.1
sl9-24	23.9	17.8	40.0	8.2	11.4	40.0
sl9-25	17.8	0.0	25.0	14.9	0.0	25.0

Slope profile 10

Inputs generated for Profile 10 are given in Table 4-3. The diagrammatic configuration is as shown in *Figure 4-14*. The profile slope model constructed for the stability analysis is given in Figure 4-17.

Table 4-3 List of parameters generated from the available data for the slope profile 10

Slice Number	Lower slice height (h l)	Upper slice height (h 2)	Slice Width (b)	Inclination of Slice Base (α)	Height of water table (u 2)	Width of water table (b)
sl10-1	24.6	21.2	39.7	8.7	18.8	39.7
sl10-2	21.2	20.5	50.0	8.7	15.1	50.0
sl10-3	20.5	19.9	25.4	8.7	14.2	25.4
sl10-4	19.9	20.7	24.3	8.7	18.6	24.3
sl10-5	20.7	22.8	23.5	8.5	22.8	23.5
sl10-6	22.8	23.1	26.9	8.6	21.1	26.9
sl10-7	23.1	19.9	50.0	8.7	17.4	50.0
sl10-8	19.9	18.0	49.7	8.8	11.9	49.7
sl10-9	18.0	25.5	50.2	6.5	20.6	50.2
sl10-10	25.5	25.6	49.6	6.6	20.0	49.6
sl10-11	25.6	22.8	51.4	6.4	18.7	51.4
sl10-12	22.8	23.1	48.7	7.0	18.8	48.7
sl10-13	23.1	22.1	24.2	6.5	16.9	24.2
sl10-14	22.1	20.9	30.4	6.5	16.2	30.4
sl10-15	20.9	31.5	45.3	6.5	25.9	45.3
sl10-16	31.5	30.7	17.6	6.4	27.2	17.6
sl10-17	30.7	33.7	12.4	6.7	31.1	12.4
sl10-18	33.7	37.1	20.0	2.8	36.0	20.0
sl10-19	37.1	40.3	29.0	11.1	33.0	29.0
sl10-20	40.3	31.6	21.6	23.9	23.3	21.6
sl10-21	31.6	0.0	28.6	33.9	0.0	28.6

Slope profile 11

Inputs generated for Profile 11 are given in Table 4-4. The diagrammatic configuration is as shown in *Figure 4-14*. The profile slope model constructed for the stability analysis is given in Figure 4-18

Table 4-4 List of parameters generated from the available data for the slope profile 11

Slice Number	Lower slice height (h l)	Upper slice height (h 2)	Slice Width (b)	Inclination of Slice Base (α)	Height of water table (u 2)	Width of water table (b)
sl11-1	0.0	23.7	29.3	5.6	14.1	29.3
sl11-2	23.7	20.9	23.9	5.6	11.0	23.9
sl11-3	20.9	17.1	26.4	5.7	8.9	26.4
sl11-4	17.1	18.9	28.0	5.8	11.4	28.0
sl11-5	18.9	19.3	21.4	5.5	10.9	21.4
sl11-6	19.3	15.2	27.5	5.5	5.3	27.5
sl11-7	15.2	12.1	22.8	5.8	4.0	22.8
sl11-8	12.1	21.3	16.2	5.7	10.0	16.2
sl11-9	21.3	29.2	33.8	5.8	18.7	33.8

Slice Number	Lower slice height (h l)	Upper slice height (h 2)	Slice Width (b)	Inclination of Slice Base (α)	Height of water table (u 2)	Width of water table (b)
sl11-10	29.2	30.0	18.7	5.4	19.3	18.7
sl11-11	30.0	27.9	31.3	5.8	18.4	31.3
sl11-12	27.9	31.8	10.3	5.5	19.8	10.3
sl11-13	31.8	29.2	21.1	5.5	22.3	21.1
sl11-14	29.2	27.5	7.6	10.9	23.2	7.6
sl11-15	27.5	36.3	20.0	11.2	30.6	20.0
sl11-16	36.3	5.6	41.4	19.2	5.6	41.4
sl11-17	5.6	0.0	14.5	46.8	0.0	14.5

Slope Profile 14

Inputs generated for Profile 14 are given in *Figure 4-5*. The diagrammatic configuration is as shown in *Figure 4-14*. The profile slope model constructed for the stability analysis is given in *Figure 4-19*.

Table 4-5 List of parameters generated from the available data for the slope profile 14

Slice Number	Lower slice height (h l)	Upper slice height (h 2)	Slice Width (b)	Inclination of Slice Base (α)	Height of water table (u 2)	Width of water table (b)
sl14-1	0.0	34.4	50.0	8.7	26.4	50.0
sl14-2	34.4	37.8	50.0	8.7	26.4	50.0
sl14-3	37.8	32.9	50.0	8.7	25.1	50.0
sl14-4	32.9	30.9	35.0	8.7	23.5	35.0
sl14-5	30.9	29.0	25.0	8.7	22.7	25.0
sl14-6	29.0	34.0	40.0	8.7	25.6	40.0
sl14-7	34.0	25.9	50.0	8.7	23.9	50.0
sl14-8	25.9	24.6	50.0	8.7	19.7	50.0
sl14-9	24.6	24.2	50.0	8.7	18.6	50.0
sl14-10	24.2	25.2	50.0	8.7	18.4	50.0
sl14-11	25.2	29.2	50.0	8.7	21.5	50.0
sl14-12	29.2	29.5	50.0	8.7	21.3	50.0
sl14-13	29.5	24.5	50.0	8.7	19.2	50.0
sl14-14	24.5	23.8	50.0	8.7	20.6	50.0
sl14-15	23.8	18.9	20.0	41.0	13.5	20.0
sl14-16	18.9	19.3	30.0	8.8	12.3	30.0
sl14-17	19.3	20.8	25.0	8.7	12.3	25.0
sl14-18	20.8	19.3	25.0	8.8	11.6	25.0
sl14-19	19.3	15.4	25.2	16.3	7.6	25.2
sl14-20	15.4	5.5	21.5	26.4	0.0	21.5
sl14-21	5.5	0.0	10.5	39.0	0.0	10.5

Slope Profile 15

Inputs generated for Profile 15 are given in Table 4-6. The diagrammatic configuration is as shown in *Figure 4-14*. The profile slope model constructed for the stability analysis is given in *Figure 4-20*.

Table 4-6 List of parameters generated from the available data for the slope profile 15

Slice Number	Lower slice height (h l)	Upper slice height (h 2)	Slice Width (b)	Inclination of Slice Base (α)	Height of water table (u 2)	Width of water table (b)
sl15-1	0.0	19.4	50.0	8.5	16.0	50.0
sl15-2	19.4	13.2	30.0	8.5	13.2	30.0
sl15-3	13.2	8.5	20.0	12.1	6.8	20.0
sl15-4	8.5	3.6	8.3	32.8	2.3	8.3
sl15-5	3.6	7.8	16.7	6.2	3.4	16.7
sl15-6	7.8	14.6	25.4	6.3	7.6	25.4
sl15-7	14.6	25.4	50.0	6.2	16.1	50.0
sl15-8	25.4	25.0	50.0	6.2	17.2	50.0
sl15-9	25.0	21.3	50.0	6.2	14.5	50.0
sl15-10	21.3	18.1	50.0	6.2	13.3	50.0
sl15-11	18.1	24.7	50.0	6.3	20.5	50.0
sl15-12	24.7	24.8	25.0	6.3	24.2	25.0
sl15-13	24.8	30.3	25.0	6.3	26.7	25.0
sl15-14	30.3	28.2	35.0	7.3	26.2	35.0
sl15-15	28.2	35.8	15.0	6.2	31.2	15.0
sl15-16	35.8	8.5	40.0	8.8	8.5	40.0
sl15-17	8.5	0.0	8.1	52.3	0.0	8.1

Slope Profile 16

Inputs generated for Profile 16 are given in Table 4-7. The diagrammatic configuration is as shown in *Figure 4-14*. The profile slope model constructed for the stability analysis is given in *Figure 4-21*.

Table 4-7 List of parameters generated from the available data for the slope profile 16

Slice Number	Lower slice height (h l)	Upper slice height (h 2)	Slice Width (b)	Inclination of Slice Base (α)	Height of water table (u 2)	Width of water table (b)
sl16-1	0.0	13.3	45.9	6.2	4.5	45.9
sl16-2	13.3	11.7	50.0	6.2	4.8	50.0
sl16-3	11.7	4.6	50.0	6.2	3.7	50.0
sl16-4	4.6	6.8	50.1	6.2	3.4	50.1
sl16-5	6.8	8.3	50.0	6.2	3.9	50.0
sl16-6	8.3	14.0	50.2	6.2	5.3	50.2
sl16-7	14.0	8.9	50.0	6.3	7.1	50.0

Slice Number	Lower slice height (h l)	Upper slice height (h 2)	Slice Width (b)	Inclination of Slice Base (α)	Height of water table (u 2)	Width of water table (b)
sl16-8	8.9	8.5	15.0	6.3	8.2	15.0
sl16-9	8.5	18.1	35.0	6.0	13.8	35.0
sl16-10	18.1	19.0	20.0	6.3	15.8	20.0
sl16-11	19.0	19.8	30.0	6.3	18.5	30.0
sl16-12	19.8	34.9	35.1	6.3	29.4	35.1
sl16-13	34.9	33.1	14.9	8.6	28.0	14.9
sl16-14	33.1	0.0	40.8	16.0	0.0	40.8

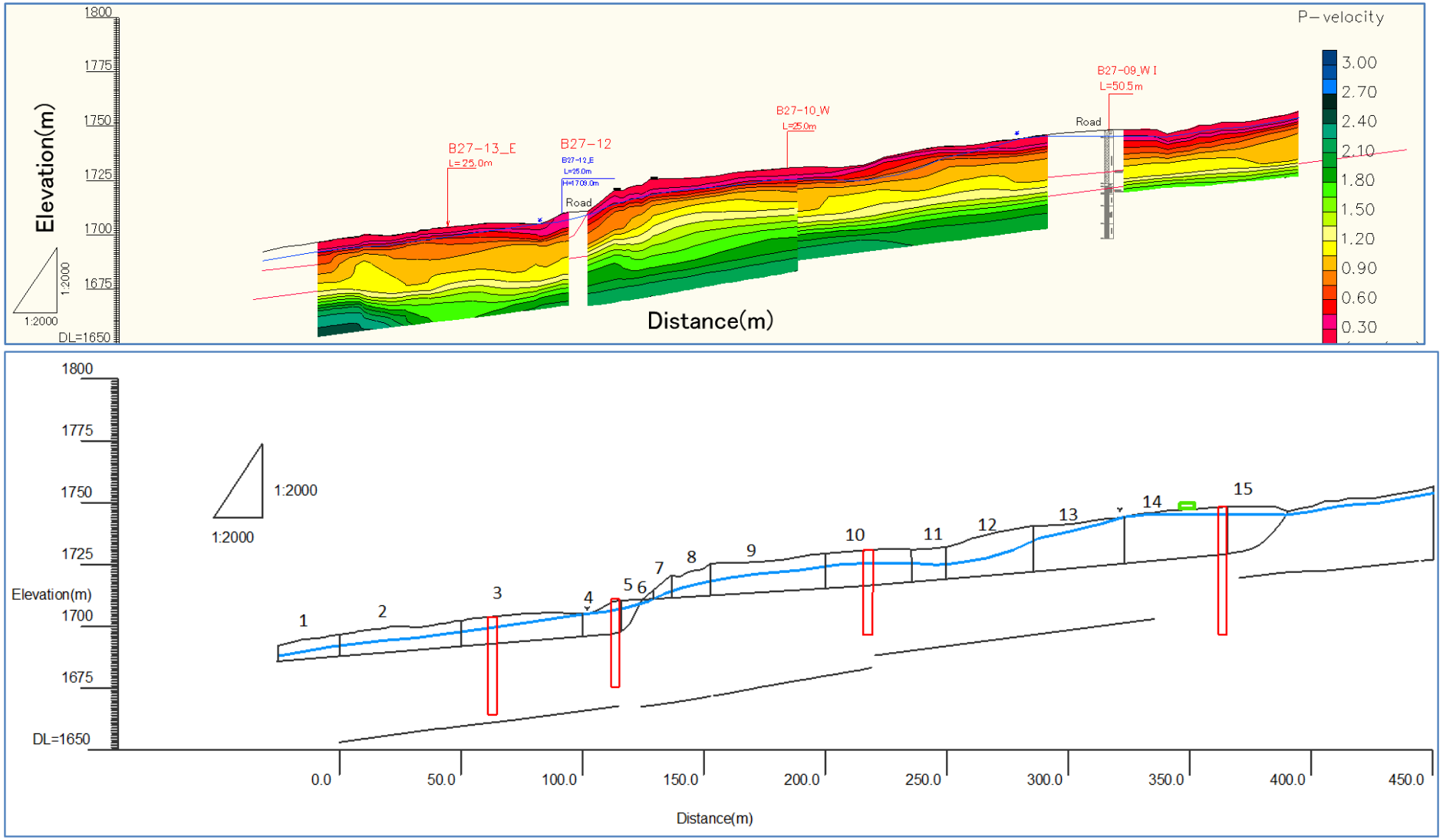

Figure 4-15 slope profile No 8 from geophysical profiling (seismic refraction) and available and projected boreholes (monitoring and core log) (JICA and GSE, 2012) in the upper diagram and the extracted geometric input for stability analysis in lower diagram.

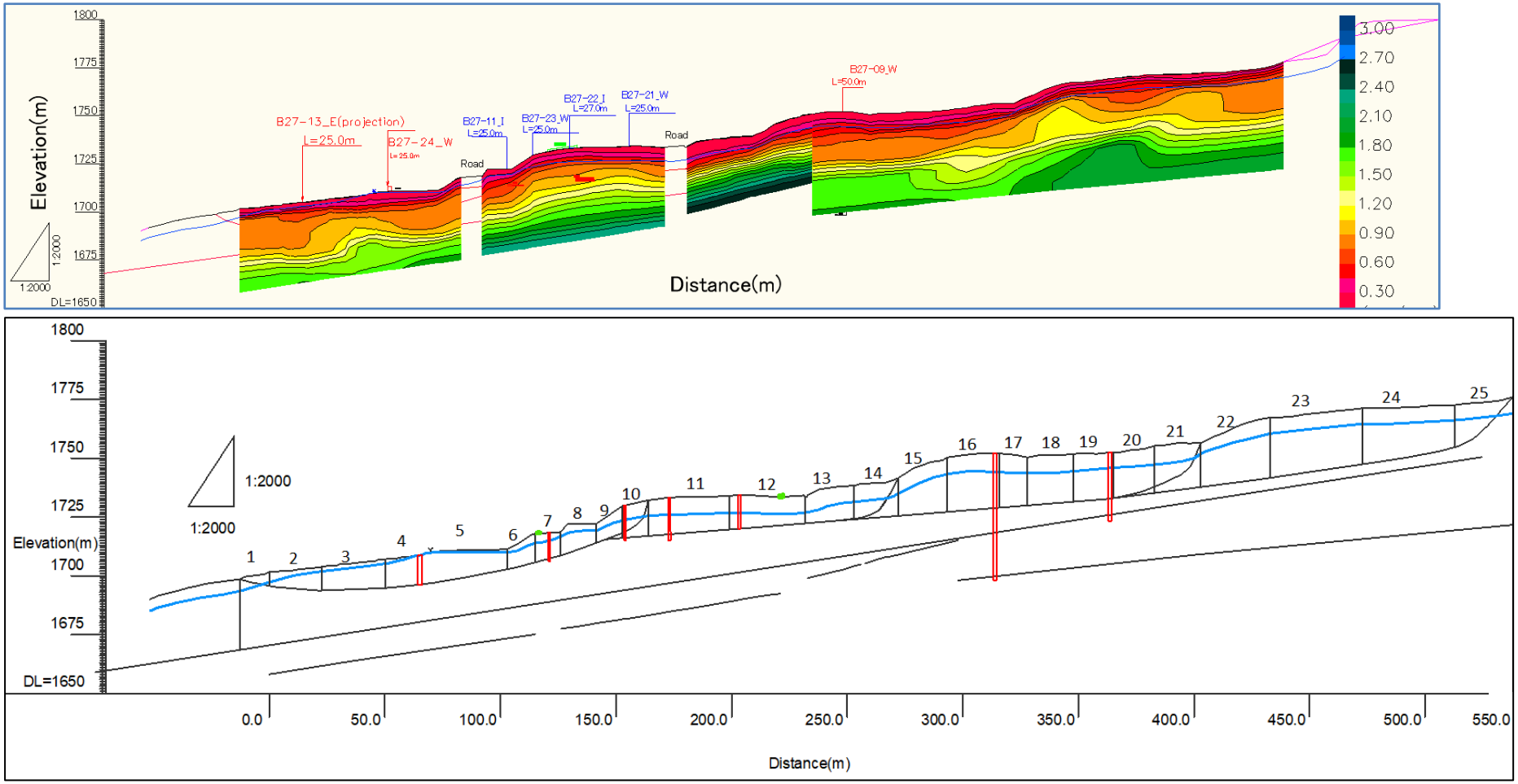

Figure 4-16 Slope profile No 9 from geophysical profiling (seismic refraction) and available and projected boreholes (monitoring and core log) (JICA and GSE, 2012) in the upper diagram and the extracted geometric input for stability analysis in lower diagram.

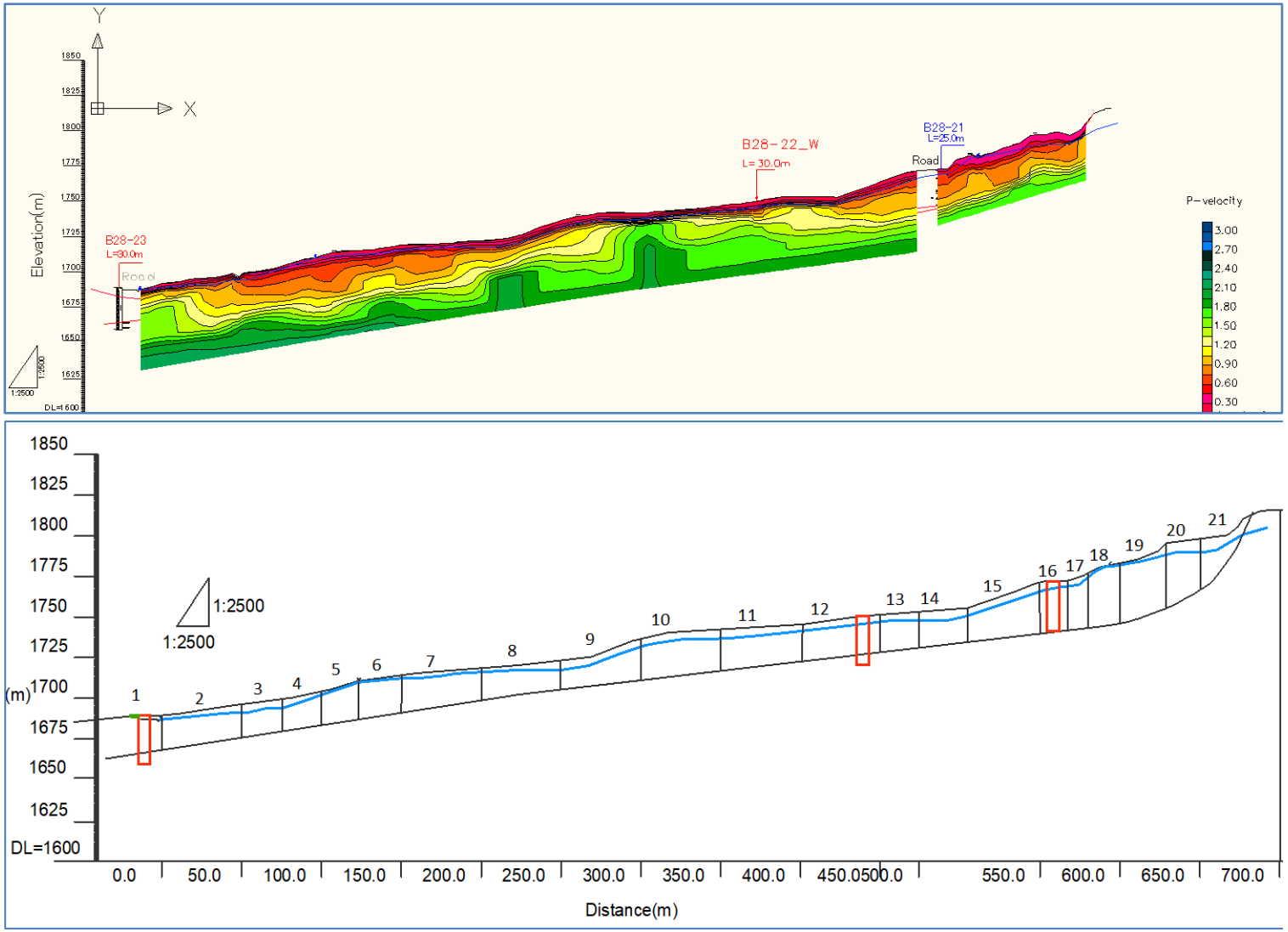

Figure 4-17 Slope profile No 10 from geophysical profiling (seismic refraction) and available and projected boreholes (monitoring and core log) (JICA and GSE, 2012) in the upper diagram and the extracted geometric input for stability analysis in lower diagram.

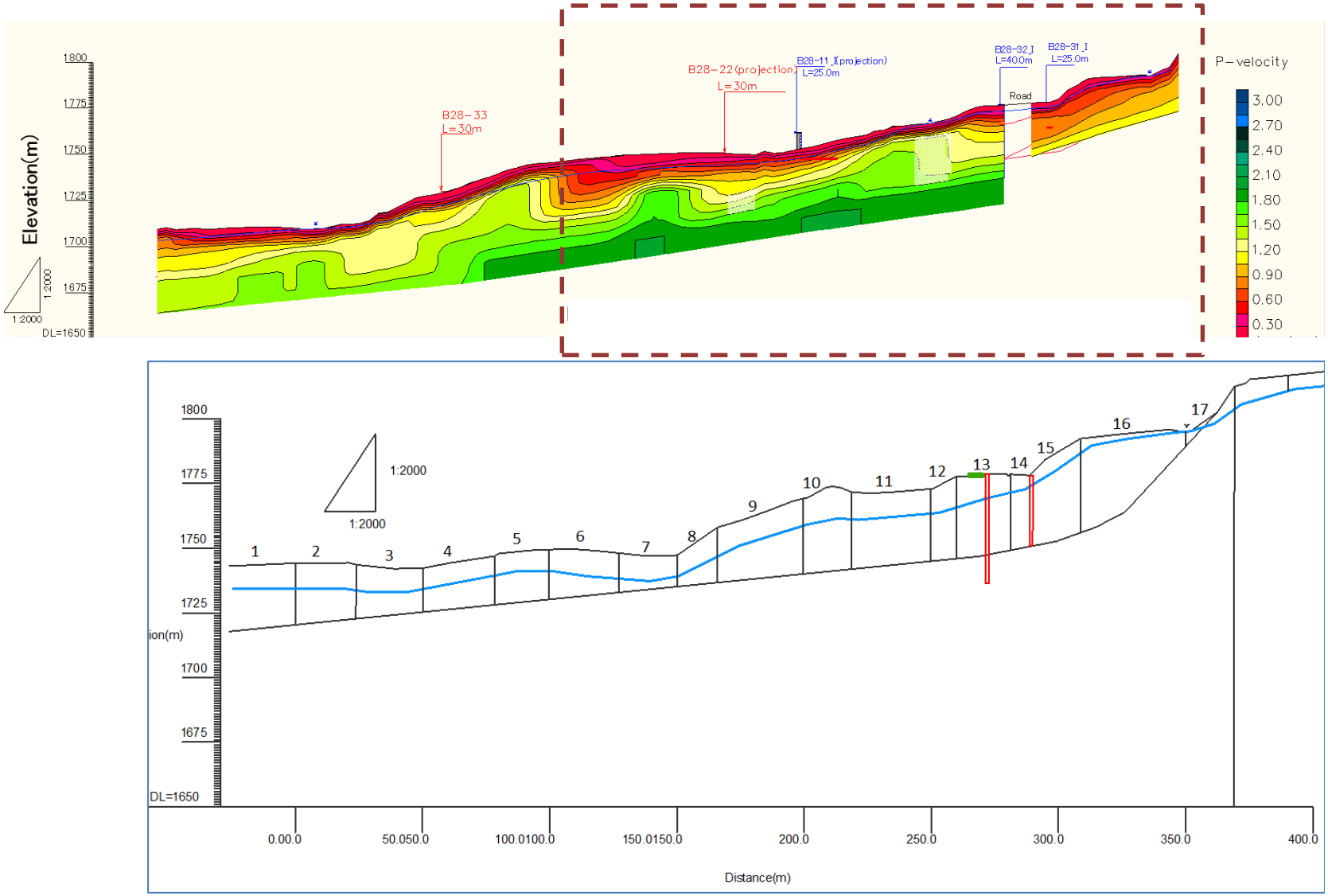

Figure 4-18 Slope profile No 11 from geophysical profiling (seismic refraction) and available and projected boreholes (monitoring and core log) (JICA and GSE, 2012) in the upper diagram and the extracted geometric input for stability analysis in lower diagram.

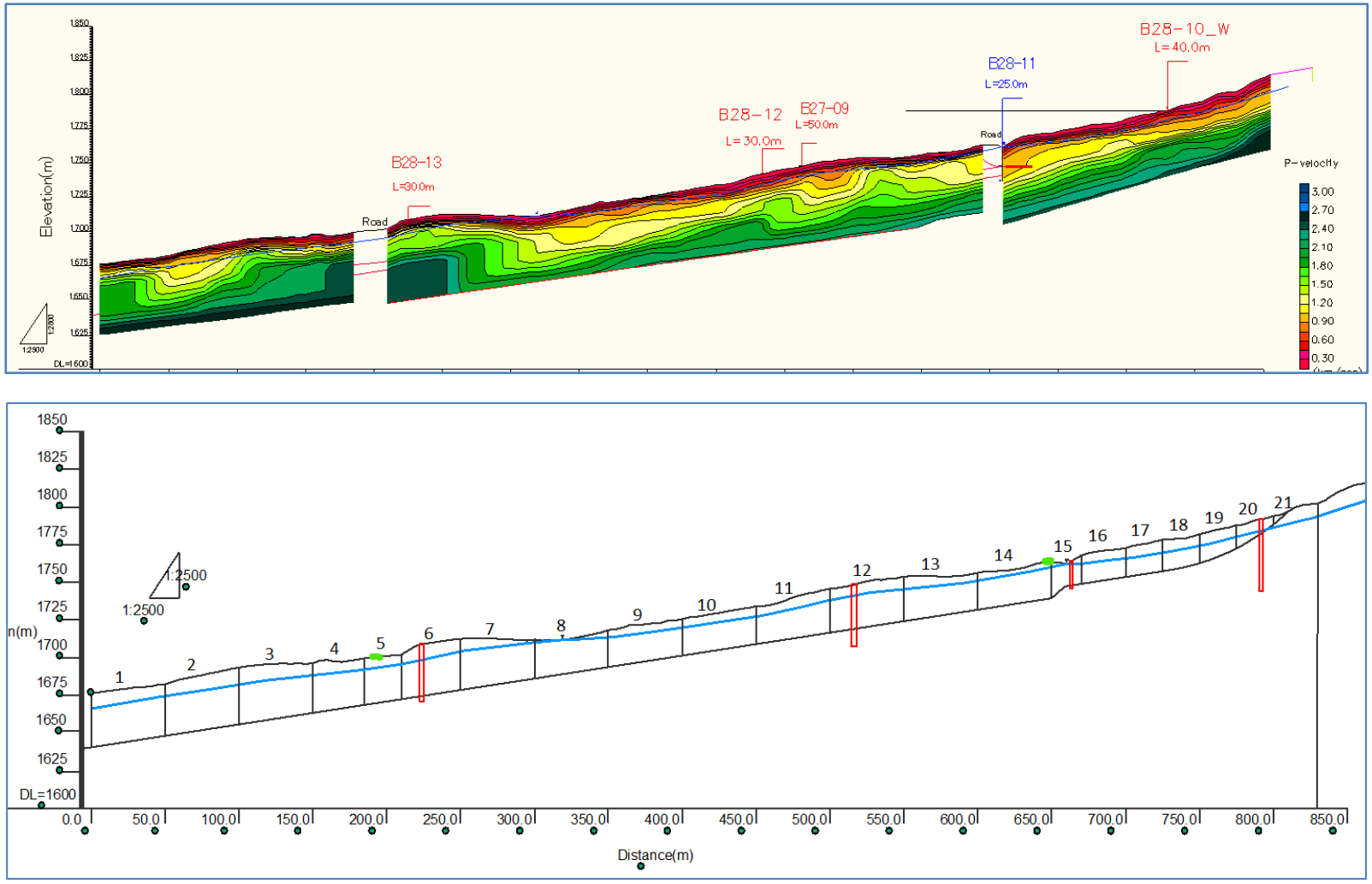

Figure 4-19 Slope profile No 14 from geophysical profiling (seismic refraction) and available and projected boreholes (monitoring and core log) (JICA and GSE, 2012) in the upper diagram and the extracted geometric input for stability analysis in lower diagram.

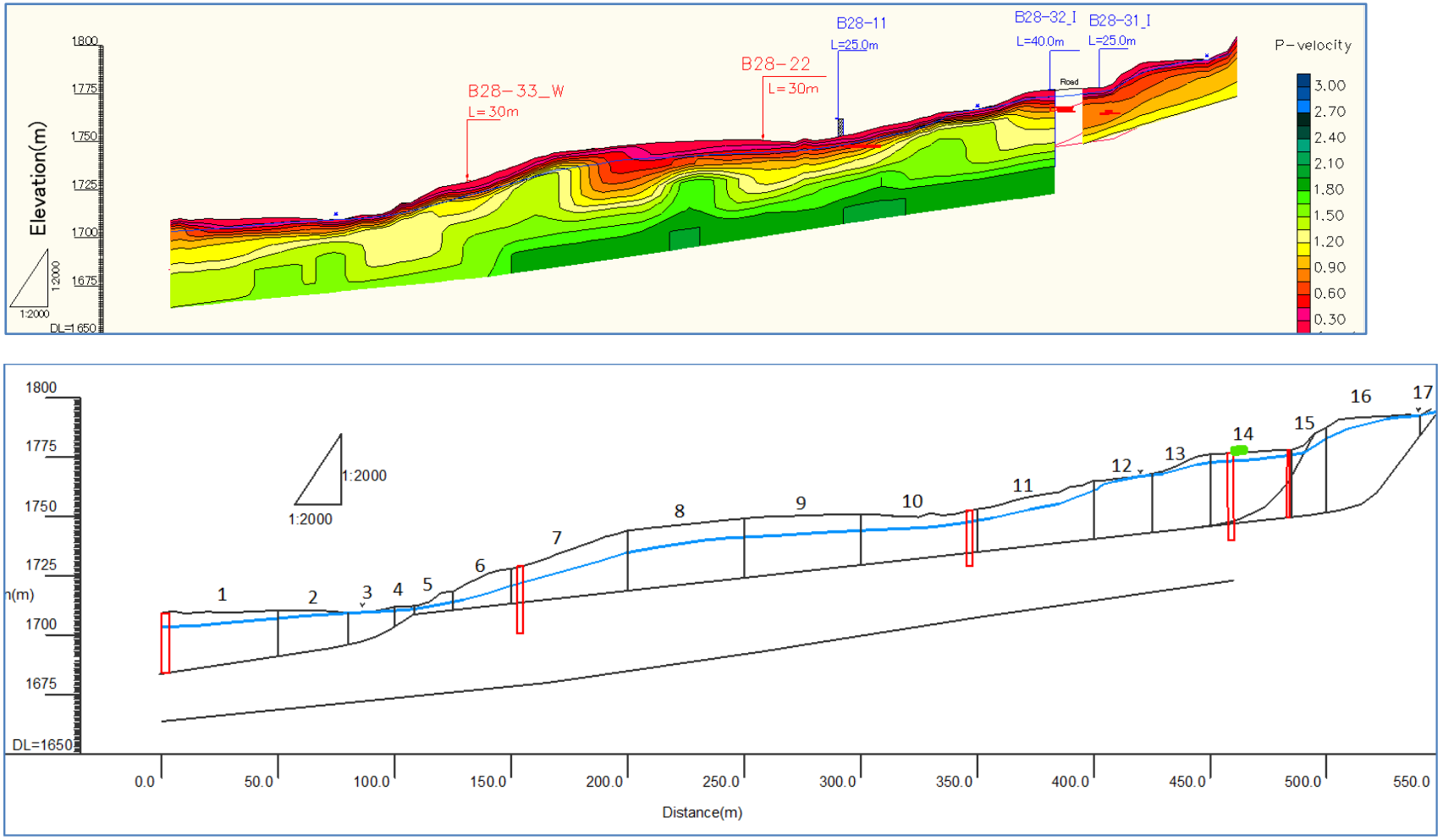

Figure 4-20 Slope profile No 15 from geophysical profiling (seismic refraction) and available and projected boreholes (monitoring and core log) (JICA and GSE, 2012) in the upper diagram and the extracted geometric input for stability analysis in lower diagram.

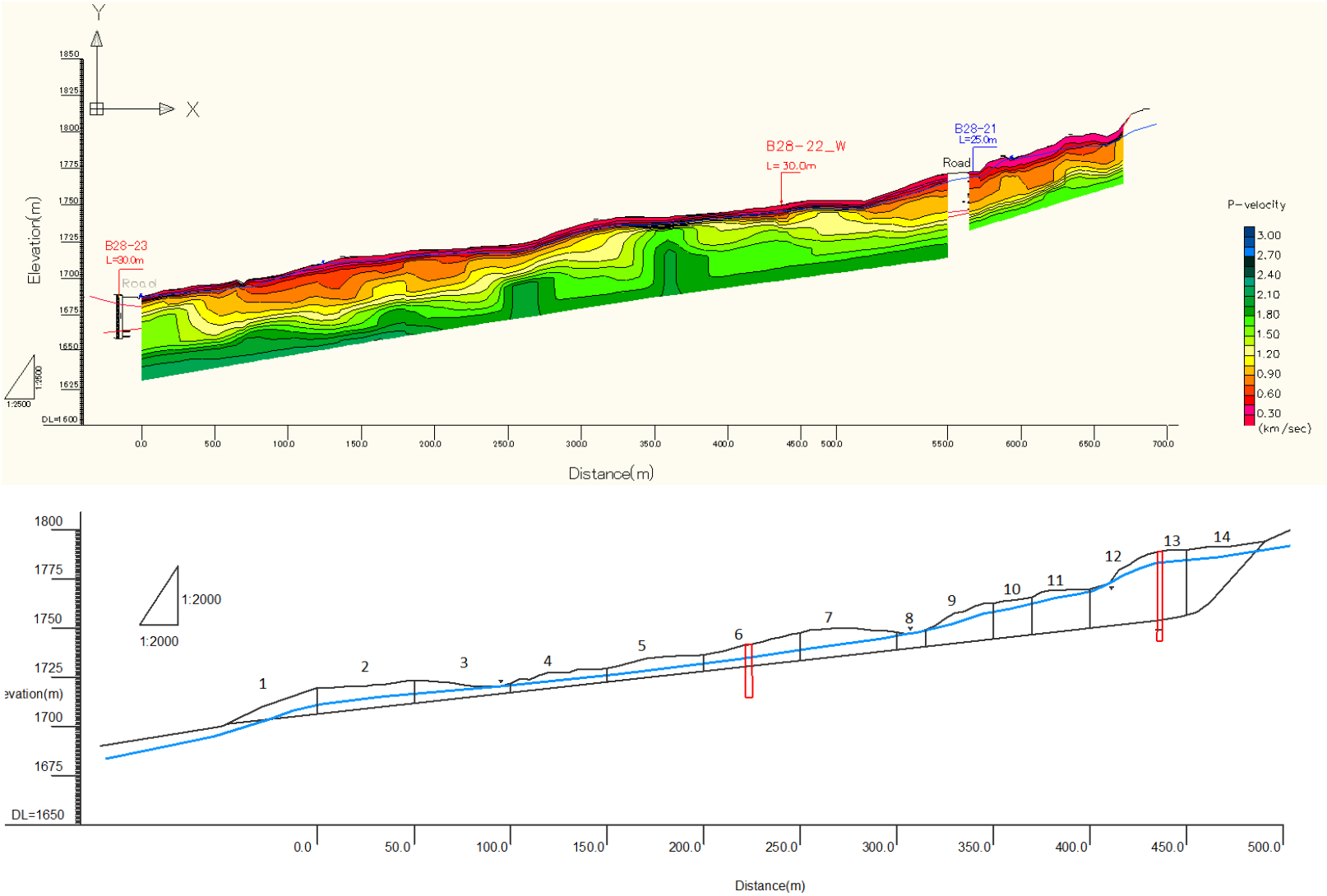

Figure 4-21 Slope profile No 16 from geophysical profiling (seismic refraction) and available and projected boreholes (monitoring and core log) (JICA and GSE, 2012) in the upper diagram and the extracted geometric input for stability analysis in lower diagram.

4.5 Back analysis

Back analysis was carried out to determine the mobilized shear strength parameters of the sliding mass which corresponds to the colluvium in general. The values of shear strength parameters are usually difficult to determine in laboratory test such as standard direct shear test. However, for cases of already failed slope with sufficient constrain on the various aspects of the landslide, back analysis can help to fix either of the shear parameters, cohesion (c) or internal friction angle (φ), while solving for the other. Such constrains include depth to slip surface which are obtained from monitoring data and the unit weight of the soil. Hence, by back calculating the unknown parameters in the known states of the landslide (failed) and making credible assumptions based on monitoring data and easy to measure properties, reliable estimates can be obtained for using in the 2D and 3D model to obtain factor of safety and also to carry out sensitivity assessment.

For the unit weight variable data for colluvium in the Abay Gorge has been reported ranging from 12.5 to 19 KN/m3 (Lulseged Ayalew et al., 2009). The maximum of the range has been considered in this study for the stability analysis.

In this study back analysis approach proposed by (Duncan et al. 2014) has been adopted with satisfactory result among several approaches. In the approach a parameter $\lambda_{c\varphi}$ representing apparent depth of slip surface is derived based on assumed range of c and φ values in the simple relation as shown in Eq. 4 (Duncan et al. 2014).

$$\lambda_{c\varphi} = \frac{\gamma_{soil} * \mathrm{H} * \mathrm{Tan}\,(\varphi)}{c} \qquad \text{(Eq. 4)}$$

$$\varphi_{\mathrm{d}} = \frac{\varphi}{\mathrm{FoS}} \qquad \text{(Eq. 5)}$$

$$\mathrm{c_d} = \frac{\mathrm{c}}{\mathrm{FoS}} \qquad \text{(Eq. 6)}$$

The factor of safety is derived using the slope stability charts (Janbu, 1968). Range of pair of c and φ values which do not have to necessarily give factor of safety 1, are used to generate range of dimensional parameters, $\lambda_{c\varphi.}$ Combination of the $\lambda_{c\varphi}$values and slope angle (β), are used in combination to read out the Stability number, N_{cf}, from the stability chart of Janbu (1968). These values are then used to calculate the corresponding factor of safety using Eq.

10. The values of the parameters P_e and P_d are derived according to the equations given in Eq. 7 and Eq. 8 respectively. As no external water above the slope toe exists and since the slope angels are close to 10^0 in the analysed slopes with low depth of the tension cracks with respect to the height of the slope, adjustment factor of 1 is used for both the tension crack and submergence. No adjustments are used in the analysis as the slopes are without significant construction on the crest.

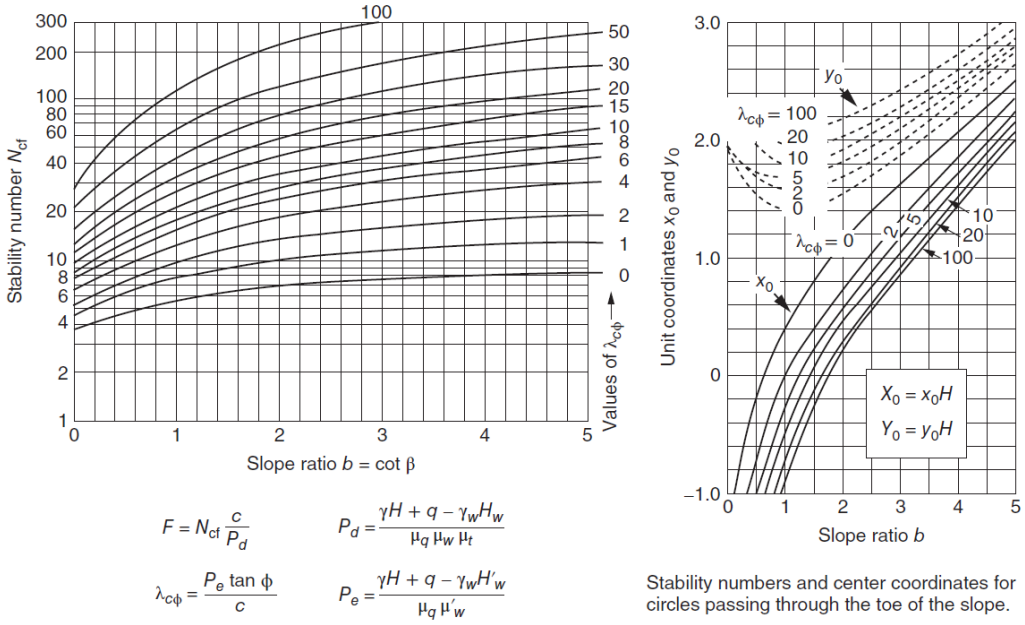

Figure 4-22 Slope stability charts for c–ϕ type of soils (Janbu, 1968 as cited in Duncan et al., 2014) used in the derivation of stability number, N_{cf} and hence the corresponding factor of safety, F, for back calculating the shear parameters.

In Eq. 4, φ and c are assumed values used to generate range of $\lambda_{c\varphi}$ values. The initially assumed φ and c values were then converted to φ'd and cd respectively by dividing with factor of safety derived using the stability charts (Eq. 10). This procedure was carried out for each profile where an example is given in Table 4-8 for the case of profile 8. It is intended to incorporate lateral inhomogeneity of the material involved in the landslide in terms of shear parameters where each profile gave slightly different shear parameters. The target slip surface considered for the semi- 3D stability analysis is the deepest one along the six slope profiles. The deeper landslide at the contact between the colluvium and the bed rock is considered for the semi- 3D analysis. The shallow landslides are localized and do not extend much further and have little chance to generate variable properties to use in 3D modelling (at least in the current study area) as these often have only not more than profile established across them.

The shear parameters were back analysed first by drawing the slope geometry together with the estimated critical slip surface in the reference simplified model. After obtaining the shear parameters and corresponding factors of safety the dimensionless parameter, $\lambda_{c\varphi}$, is calculated with the obtained shear strength parameters and another parameter, P_e (Eq. 8). The value of, $\lambda_{c\varphi}$ and the slope angle are then used to plot and determine the stability number, N_{cf}. This is then used in the final computation for the factor of safety (Eq. 10) incorporating another correction factor, P_d computed with the formula in equation (Eq. 7). The shear strength estimated is then divided by the factor of safety to back calculate the residual shear strength parameters. This is repeated for range of shear parameters in the present study. When each shear parameter is plotted against the dimensionless parameter, a correlation curve was obtained from which the shear parameter corresponding to the depth observed in the real case (depth to slip surface as observed from the inclinometer data) are obtained.

$$P_d = \frac{\gamma H + q - \gamma_w H_w}{\mu_q \mu_w \mu_t} \quad \text{(Eq. 7)}$$

$$P_e = \frac{\gamma H + q - \gamma_w H'_w}{\mu_q \mu'_w} \quad \text{(Eq. 8)}$$

$$\lambda_{c\phi} = \frac{P_e \tan \phi}{c} \quad \text{(Eq. 9)}$$

$$F = N_{cf} \frac{c}{P_d} \quad \text{(Eq. 10)}$$

Where,
Pd : adjustment factor
Pe : adjustment factor
$\lambda_{c\phi}$: dimensionless parameter of Janbu (1968)
: average unit weight of soil (N/m^3)
H : slope height above toe (m)
q : surcharge (N)
γw : unit weight of water (N/m^3)
Hw : height of external water level above toe (m)
H′w : the height of water within the slope (m)
μq : surcharge reduction factor (chart in Janbu, 1968 cited in Duncan et al., 2014, Figure A.2)
μw : submergence reduction factor (chart in Janbu, 1968 cited in Duncan et al., 2014, Figure A.3)
μt : tension crack reduction factor (chart in Janbu, 1968 cited in Duncan et al., 2014, Figure A.4)
μ'w : the seepage correction factor (chart in Janbu, 1968 cited in Duncan et al., 2014, Figure A.3).

*Table 4-8 An example from Profile 8, demonstration of parameters used for counting back relative shear parameters (*c'd and φ'd*) from their plots against apparent depth (*λcφ*).*

ϕ	c	Unit weight, (KN/m^3)	Height (m)	$\lambda_{c\varphi}$	FoS (Janbu, 1968)	$c'_d = c' / FoS$ (KPa)	$\varphi'_d = \varphi' / FoS$ (^{o})
2	33	19	52	0.52	0.50	66.4	4.0
5	30	19	52	1.44	0.81	36.9	6.2
8	27	19	52	2.56	1.02	26.6	7.9
11	24	19	52	3.96	1.05	22.9	10.5
14	21	19	52	5.77	1.20	17.5	11.7
17	18	19	52	8.20	1.63	11.1	10.5
20	15	19	52	11.61	1.69	8.9	11.8
23	12	19	52	16.74	1.81	6.6	12.7
26	9	19	52	25.33	2.03	4.4	12.8
29	6	19	52	42.56	2.08	2.9	14.0

Figure 4-23 shows an example for the plots of $\lambda_{c\varphi}$ versus c'd and φ'd from the above table and likewise for the rest of the profiles not shown here as well. The scatter plots have logarithmic relation and these are used to back determine the corresponding mobilized shear parameters in the particular depth as indicated by red dashed line (*Figure 4-23*) in each case which are those observed slip surfaces from the boreholes monitoring data along the profile.

The $\lambda_{c\varphi}$ represents the reference depth and its estimated shear parameters (φ'd or c'd) for the particular case at all depths. In this case the depth to the slip surface is referred from the values of $\lambda_{\varphi c}$ (on the x-axis) and the shear parameters are read from the corresponding vertical axes as shown in the example (Figure 4-23).

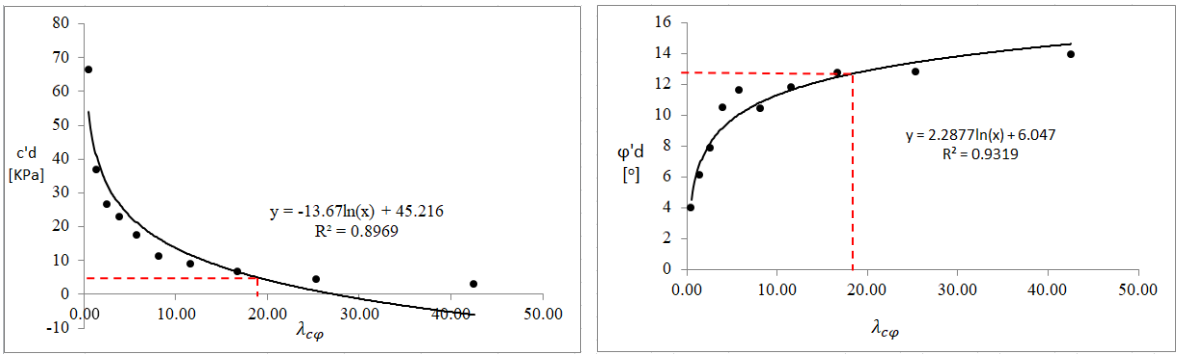

Figure 4-23 Plots from Table 4-8 used to retrieve the representative c' and ϕ' using the fitted logarithmic function as shown by red dotted line at the known depth of slip surface from borehole monitoring data along the profile (an example from Profile 8).

These were implemented in a Spread Sheet Program (Microsoft Excel®). The value obtained are tabulated as in *Table 4-8* and plotted graphically. The trend is then obtained to estimate values corresponding to known depth of slip surface from monitoring data (inclinometer displacement depth) in the borehole crossing the profile under investigation. The extracted values for both c and φ are then treated as strength parameters and used in the main stability calculations using simplified Janbu's method. Similar methods were implemented for each profile at the available inclinometer data.

4.6 2D Slope stability analysis

In the study a spread sheet program (Microsoft Excel®) is used to carry out the 2D Factors of safety (Figure 4-25) computation. Sets of multiple, parallel profiles, are chosen along the landslide body to generate the slope stability analysis model. In the program simplified Janbu's method is implemented with 15 iterations for convergence of value of factor of Safety (FoS). These were then integrated into semi– 3D factor of safety using Lambe-Whiteman (Lambe and Whiteman, 1969) example in Microsoft Excel®. Structured and automated formats were created following the formulae of the limit equilibrium methods in simplified Janbu's method for the 2D analysis part as well as the compilation to semi– 3D safety factor. Demonstration of the configuration evaluated is given in *Figure 4-24*. In Table 4-9 are given the summary of the inputs required in the stability analysis. The steps of computation are also shown in the following equations (Eq. 11 to Eq. 19).

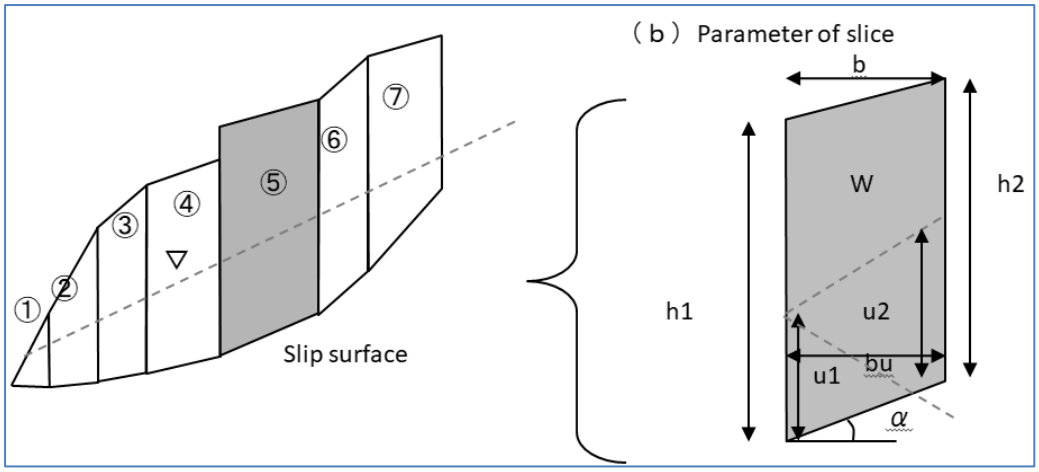

Figure 4-24. Demonstration of slices developed and used in the 2D slope stability models (Modified from drawing in JICA AND GSE, 2012).

Key

h1, h2：height of downslope and upslope side of slice respectively

u1, u2：height of water level used to compute pore water pressure on down-slope and up-slope sides, respectively.

b：width of the slice

bu: width of water level considered (pore water pressure). b_u = b, however, it can also attain conditions where b_u < b, in the case shown by dotted red line.

α：inclination of base of slice (i.e. angle of slip surface) in degrees.

Value requested from slice parameter at once (Common item to all stability analysis types）

Table 4-9 Input parameters for slope stability analysis

Inputs for stability analysis	Source
'wet unit weight of body	Published data
' cohesion of slip surface	Back analysed
internal friction angle	Back analysed
'distance between the toe and crack at the scarp	From landslide profile
'distance between L and a line of parallel to L tangential line on the slip surface	From landslide profile
'Height of valley side of a slice	From constructed slope model
'Height of mountain side of a slice	From constructed slope model
width of slice	From constructed slope model
' inclination angle of slip surface	From constructed slope model
'Height of hydraulic pressure of mountain side	From constructed slope model
'width of height of hydraulic pressure	From constructed slope model

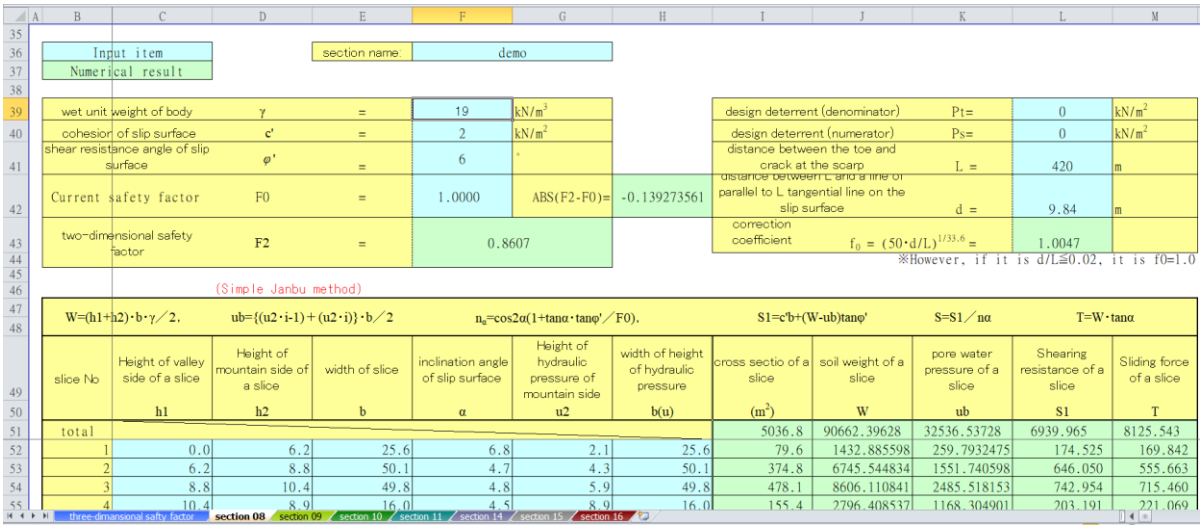

Input item / Numerical result				section name:	demo							
wet unit weight of body	γ	=	19	kN/m³			design deterrent (denominator)	Pt=	0	kN/m²		
cohesion of slip surface	c'	=	2	kN/m²			design deterrent (numerator)	Ps=	0	kN/m²		
shear resistance angle of slip surface	φ'	=	6	°			distance between the toe and crack at the scarp	L =	420	m		
Current safety factor	F0	=	1.0000	ABS(F2-F0)=	-0.139273561		distance between L and a line of parallel to L tangential line on the slip surface	d =	9.84	m		
two-dimensional safety factor	F2	=	0.8607				correction coefficient $f_0 = (50 \cdot d/L)^{1/33.6}$ =		1.0047			

※However, if it is d/L≦0.02, it is f0=1.0

(Simple Janbu method)

$W=(h1+h2)\cdot b\cdot\gamma/2$, $ub=\{(u2\cdot i-1)+(u2\cdot i)\}\cdot b/2$, $n_\alpha=\cos2\alpha(1+\tan\alpha\cdot\tan\varphi'/F0)$, $S1=c'b+(W-ub)\tan\varphi'$, $S=S1/n\alpha$, $T=W\cdot\tan\alpha$

slice No	Height of valley side of a slice h1	Height of mountain side of a slice h2	width of slice b	inclination angle of slip surface α	Height of hydraulic pressure of mountain side u2	width of height of hydraulic pressure b(u)	cross sectio of a slice (m^2)	soil weight of a slice W	pore water pressure of a slice ub	Shearing resistance of a slice S1	Sliding force of a slice T
total							5036.8	90662.39628	32536.53728	6939.965	8125.543
1	0.0	6.2	25.6	6.8	2.1	25.6	79.6	1432.885598	259.7932475	174.525	169.842
2	6.2	8.8	50.1	4.7	4.3	50.1	374.8	6745.544834	1551.740598	646.050	555.663
3	8.8	10.4	49.8	4.8	5.9	49.8	478.1	8606.110841	2485.518153	742.954	715.460
4	10.4	8.9	16.0	4.5	8.9	16.0	155.4	2796.408537	1168.304901	203.191	221.069

three-dimensional safty factor | section 08 | section 09 | section 10 | section 11 | section 14 | section 15 | section 16

Figure 4-25 Snap shot from screen of excel program prepared for carrying out the 2D stability and sensitivity analysis

The procedure of the calculation based on the stability analysis following that of Janbu's simplified method is explained below. The shear strength parameters of the sliding colluvium are obtained from the back analysis while the wet unit weight is set at 19 KN/m^3 based on published study (Lulseged Ayalew et al., 2009). The role of seismic forces has not been considered in this analysis to keep the simple Spread Sheet program based computations manageable for the scope of this study.

The Simplified Janbu's method of slope stability model is an analytical approach which does not take lateral forces between slices in the vertical direction into account. In the analysis the input parameters are used to generate the slice weight (Eq. 11), pore water pressure is calculated (Eq. 12) based on the phreatic water table obtained from the monitoring data. Shearing resistance developed on the base of the slice is then computed with (Eq. 13) while the overall driving force is computed (Eq. 14). Subsequently the factor of safety is solved for by iteration as in the equation it appears on both sides of the equation the factor of safety term appears on both sides of the equation (Eq. 16). In this case 15 iterations were enough to give convergent results.

An arbitrary value of 1 is taken as starting factor of safety (F_0 = 1) and temporary factor of safety, F, is computed. This process is iterated (repeated) 15 times where on every iteration F is replaced by computed temporary factor of safety until the difference between subsequent values of F are negligible. This final value is taken as the representative final factor of safety for the slope being analysed.

Slice weight

$$W = \frac{(h_1+h_2)*b*\gamma_s}{2} \quad \text{(Eq. 11)}$$

Pore-water pressure

$$U_b = \frac{u_2*b*9.807}{2} \quad \text{(Eq. 12)}$$

Shearing resistance at the base of slices

$$S = \frac{c*b+(W-U_b)*\tan(\varphi)}{\frac{\cos\alpha_i{}^2*\ 1+\tan\alpha_i*\tan\varphi}{F_0}} \quad \text{(Eq. 13)}$$

Sliding force of each slice

$$T = W*\tan(\alpha) \quad \text{(Eq. 14)}$$

Factor of safety

$$F = \frac{S}{T} \quad \text{(Eq. 15)}$$

$$F_0 = \frac{c*b_i+(W_i-U_{bi})*\tan\varphi}{\frac{\cos\alpha_i{}^2*\ 1+\tan\alpha_i*\tan\varphi}{F_0}} * \frac{1}{W_i*\tan\alpha_i} \quad \text{(Eq. 16)}$$

Once the factor o sfadety is obtained a correction factor is applied as shown in Eq. 17correction is applied. *Figure 4-27* shows the relation between d and L.

$$F = f_0 * F_0 \quad \text{(Eq. 17)}$$

Where,

$$\boldsymbol{f_0} = \mathbf{50} * \boldsymbol{\frac{d}{L}}^{\frac{1}{33.6}} \quad \text{(Eq. 18)}$$

Key: W = weight of slice, [Kg] h_1, h_2 = height of slice on both sides (lower and upper respectively), [m] b = width of slice (and water level in slice), [m] u_2 = Height of water on upslope side, [m] γ_s = Wet unit weight of soil, [KN/m^3] u_b = = Pore water pressure, [KN] α = inclination angle of slip surface, [^{o}] S1 = shearing resistance of each slice, [KN]	S = total shearing force, [KN] φ = Internal friction angle, [^{o}] c = Cohesion [KN/m^2] T = sliding force, [KN] f_0= correction factor

Correction factor takes into account the ratio of length of landslide from toe to the tension crack on the crown of the landslide (L) to the depth of the line tangent to the slip surface but parallel to the toe-tension crack line (d). This situation is depicted in Figure 4-26. This was introduced to account for the usually lower factor of safety obtained for Janbu's method in comparison to other methods.

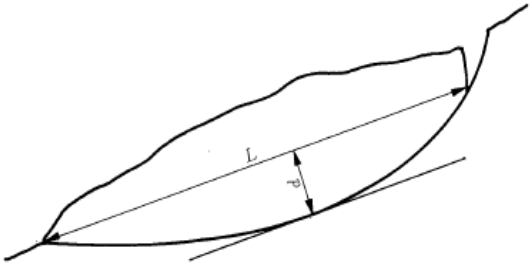

Figure 4-26 Correction factors introduced in Janbu's simplified method

4.7 Semi– 3D stability Analysis

Review of various approaches to 3D stability assessment of slopes is made from pool of published literature pertinent to the terrain and geological condition of the study area. An example of one of the model, Lambe and Whitman (1969), is used for the type of stability model employed in this study (*Figure 4-27*). The 3D stability model is introduced once sufficient numbers of slices are considered to pull together and derive combined semi- 3D factor of safety following an example from Lambe-Whitman (1969). Lambe-Whitman (1969) proposed to use the expression of the form in Eq. 19 to compute the approximate 3D factor of safety based on conventional 2D safety factor on multiple profiles along the landslide weighted by cross section area of each considered respective profiles used as shown in Figure 2. Formula for the calculation of the proposed semi- 3D model is shown in (Eq. 19), based on *Figure 4-27*. The implementation in Microsoft Excel is shown in *Figure 4-28*.

$$F_{3D} = \frac{A_1 \cdot F_1 + A_2 \cdot F_2 + A_3 \cdot F_3}{A_1 + A_2 + A_3} \qquad \text{(Eq. 19)}$$

Where, F_{3D} : Approximate value of three-dimensional safety factor
F_1, F2, F3: Safety factor by two-dimensional analyses
A_1, A2, A3: Sectional area of each section

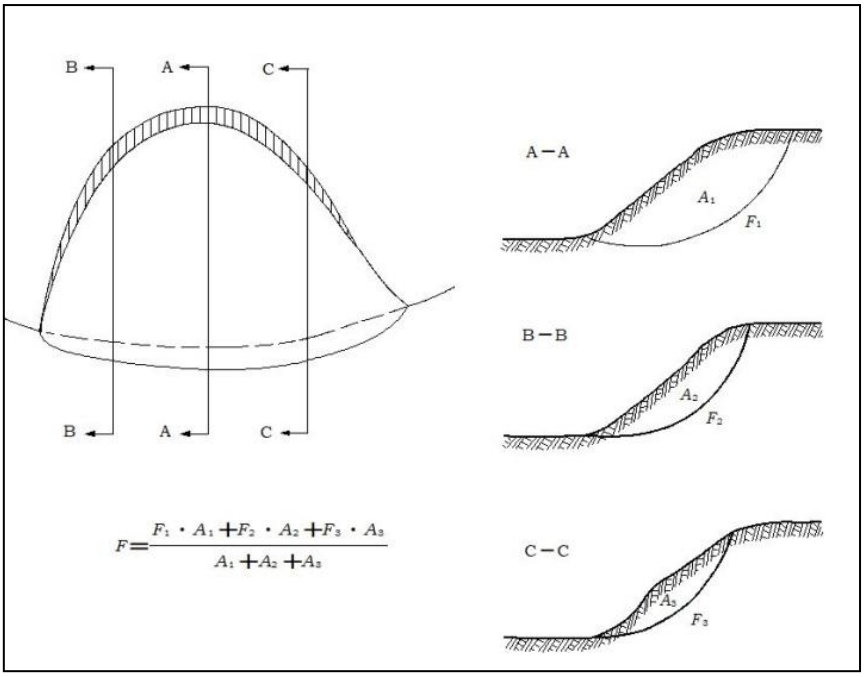

Figure 4-27 Sketch of semi- 3D Modeling approach from Lambe and White man (1969)

Approximate three-dimensional stability analysis

(Lambe-Whitman method)

section №	8	9	10	11	14	15	16
name of section	demo	demo	demo	demo	demo	demo	demo
two-dimensionalsafty factor F_2	2.783	1.995	1.401	1.530	1.173	1.750	1.647
cross section A (m^2)	5036.80	8687.61	17208.98	8380.15	20855.14	10823.60	6828.80

approximate three-dimensional safty factor F_3	=	$\frac{A_8 \cdot F_8 + A_9 \cdot F_9 + A_{10} \cdot F_{10} + A_{11} \cdot F_{11} + A_{14} \cdot F_{14} + A_{15} \cdot F_{15} + A_{16} \cdot F_{16}}{A_8+A_9+A_{10}+A_{11}+A_{14}+A_{15}+A_{16}}$

approximate three-dimensional safty factor F_3	=	1.580

three-dimansional safty factor | section 08 | section 09 | section 10 | section 11 | section 14 | section 15 | section 16 | Sheet1 | Sheet3

Figure 4-28 Snap shot from screen of excel program prepared for carrying out the semi- 3D stability and sensitivity analysis

The 2D stability analysis was carried out by a tool developed in Microsoft Excel based on simplified Janbu's method and which was linked to also do semi- 3D stability analysis (Figure 4-28). The results of series of factors of safety (FoS) and also the cross section area in each considered slope profile were then extracted. The factors of safety are weighted by the cross sectional area and averaged as shown in Eq. 19 (Lamb and Whiteman, 1969) to compute the semi- 3D factors of safety.

4.8 Sensitivity analysis

Effects of changes in the dynamic parameters influence on stability condition are tested by sensitivity analysis. Effect of groundwater level, internal friction angle, and cohesion are tested to assess the degree of influence of each parameter on the stability of the slope. In the current study five scenarios were used for sensitivity evaluation on the developed slope stability model. These are three cases of single parameter variation at a time to see overall impact on the change of the factor of safety in both the 2D and semi- 3D models. Then back-analysis of either of the shear parameters to solve for other shear parameter at constant water level while keeping the factor of safety at 1 were carried out for the 2D model.

All the scenarios were implemented in simplified Janbu's method by varying the variables in the model by 30%, 50% and 100%, giving a total of four cases including the starting with the back analysed shear parameters. The percentage variation was used to avoid issue of scaling between different parameters involved in the sensitivity analysis and to make comparisons of sensitivity across changes in variables of different nature possible. The parameters involved in sensitivity analysis are cohesion (c), internal friction angle (φ) and water level. For the sensitivity analysis three slope profiles were chosen from the landslide which run in the central part (profile 14), in the left part (profile 8) and the right part (profile 16) of the landslide body from head to toe, sub parallel to each other.

In all instants to see the effect of each considered parameter independently, the remaining parameters were kept constant at initial reference conditions as summarized by *Table 4-10*. The water level was varied between initial starting level as estimated from primary field investigation data of JICA and GSE (2012) and step wise varied by reduction to 100% of initial reference level and then increasing by 50% and 100% of the initial reference level (*Table 4-11*). On the other hand, the shear parameters were varied by decreasing from initial back analysed values to 30%, 50% and 100% of the values (Table 4-12 and Table 4-13)

Furthermore, the stability at FoS of unity, was also used to test sensitivity of shear strength parameters by comparing how either of the two parameters (c and φ) are varied with incremental assigned value of the other to keep the slopes at fixed stable condition with FoS of 1. In similar manner, sensitivity of the semi- 3D factor of safety for the particular landslide has been assessed. All the 7 profiles have been varied for their water level; internal friction

angle and cohesion one at a time while keeping the others constant Table 4-11, 4-12 and 4-13)

Table 4-10 Change in both 2D and semi- 3D FoS, as a function of change in internal friction angle increment uniformly across all the considered slope profiles at initial water level condition.

Cases	Fixed conditions	Variable inputs to Semi- 3D Factors of Safety derivation			
Case 1	- c'_d (KPa) - original water level	φ, (^{0}) (0%)	φ, (^{0}) (-30%)	φ, (^{0}) (-50%)	φ, (^{0}) (-100%)
Case 2	- φ'_d (^{0}) - original water level	c, (^{0}) (0%)	c, (^{0}) (-30%)	c, (^{0}) (-50%)	c, (^{0}) (-100%)
Case 3	- c'_d (KPa) - φ'_d (^{0})	Water level (original)	Water level (-100%)	Water level (+50%)	Water level (+100%)

Table 4-11 Change in both 2D and semi- 3D FoS, as a function of change in water level change in all the considered slope profiles at constant shear parameters back analysed for each profile.

Profile	c' (KPa)	φ' (^{0})	Change in water level (m)			
8	5.7	12.6	Water level (m) (+0%)	Water level (m) (+10%)	Water level (m) (+30%)	Water level (m) (+50%)
9	5.2	11.6				
10	3.3	11.9				
11	0	11.6				
14	3.6	11				
15	1.7	12.2				
16	0.3	11.8				

Table 4-12 Scenarios tested for sensitivity of the slope stability at constant water level (referenced to observation of the investigation result)

Profile	c' (KPa)	Change in φ' (^{0})			
		φ (+0%)	φ(-30%)	φ (-50)	φ (-100)
8	5.7	12.6	8.82	6.3	0
9	5.2	11.6	8.12	5.8	0

Profile	c' (KPa)	Change in φ' (^{0})			
		φ (+0%)	φ(-30%)	φ (-50)	φ (-100)
10	3.3	11.9	8.33	5.95	0
11	0	11.6	8.12	5.8	0
14	3.6	11	7.7	5.5	0
15	1.7	12.2	8.54	6.1	0
16	0.3	11.8	8.26	5.9	0
Water level increment (m)					

Table 4-13 Change in both 2D and semi- 3D FoS, as a function of change in internal friction angle at constant water level (referenced to observation of the investigation result).

Profile	φ' (^{0})	Change in c' (KPa)			
		c (+0%)	c (-30%)	c (-50%)	c (-100%)
8	12.6	3.99	2.85	2.85	0
9	11.6	3.64	2.6	2.6	0
10	11.9	2.31	1.65	1.65	0
11	11.6	0	0	0	0
14	11	2.52	1.8	1.8	0
15	12.2	1.19	0.85	0.85	0
16	11.8	0.21	0.15	0.15	0

5 Results and interpretation

In this section the results of the series of analysis carried out along each selected profiles of the landslide as well as the resulted semi- 3D approximation of factor of safety are given. The next chapter discusses the implications and relations between the analyses carried out based on the results presented in this chapter.

5.1 Back analysis

According to apparent depth to slip surface (Eq. 4) gave the following results for a combination of c and φ values. The assumed range of shear parameters used to compute the dimensionless $\lambda_{c\varphi}$ were divided by the respective factors of safety from the stability chart of Janbu (1968) to obtain the representative residual shear strength parameter values at various depths of the slope surface as c'd and φ'd (Duncan et al. 2014). The plot of each parameter against factors of safety is shown in Figure 5-1 for each profile based on the values in *Table 4-8*, similarly constructed for each profile.

Profile 8

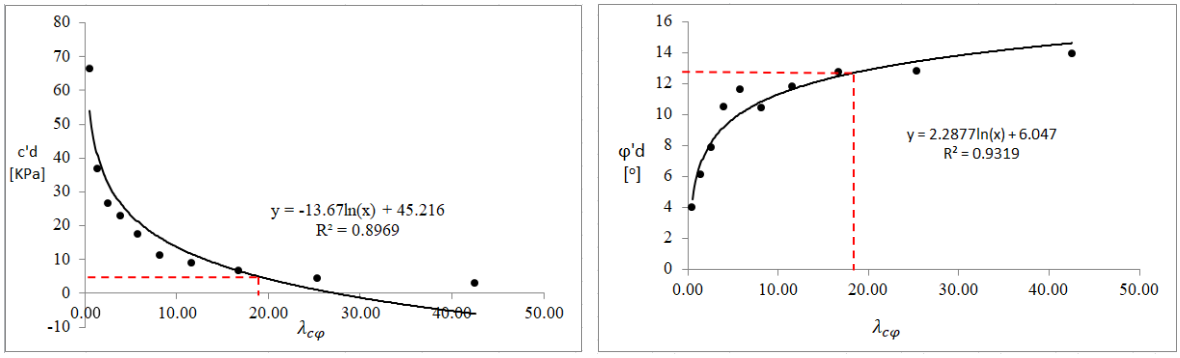

Profile 9

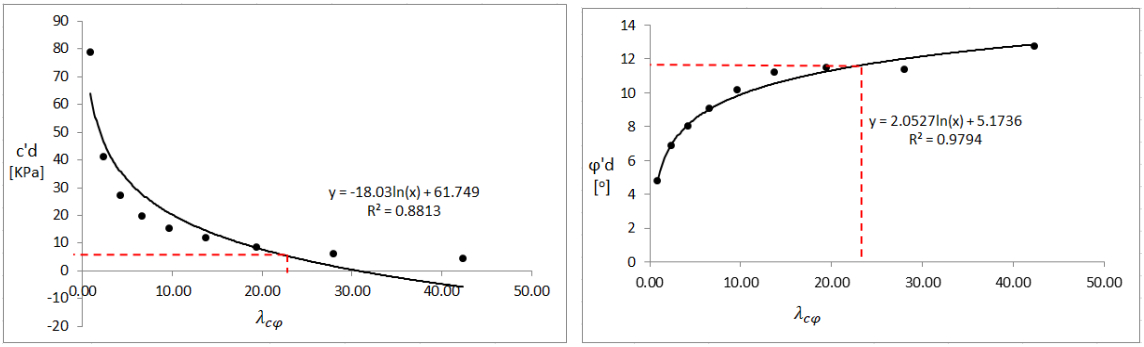

Profile 10

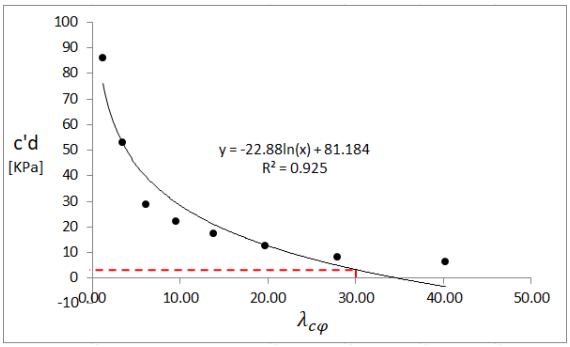

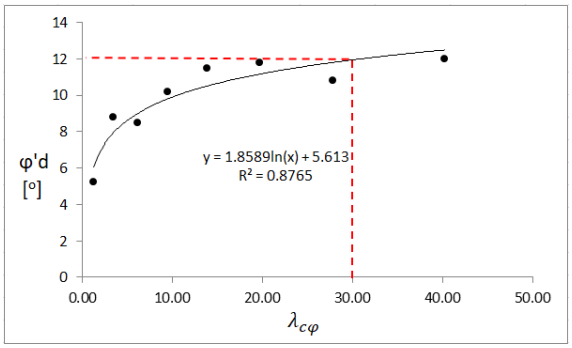

Profile 11

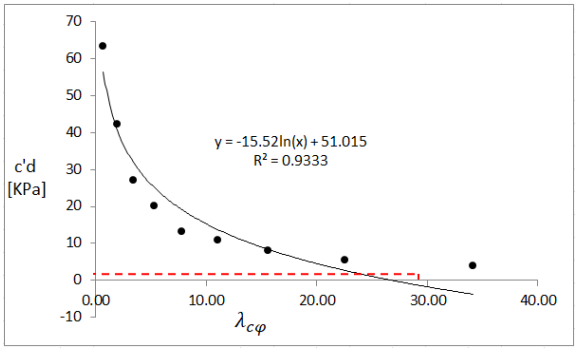

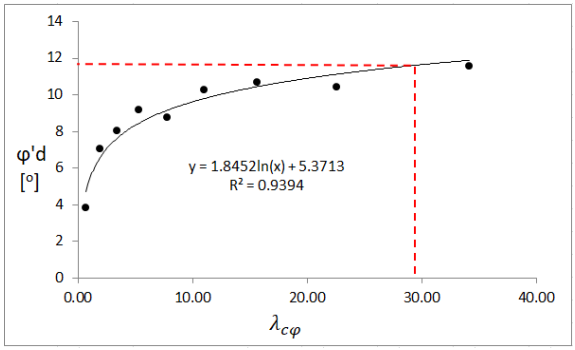

Profile 14

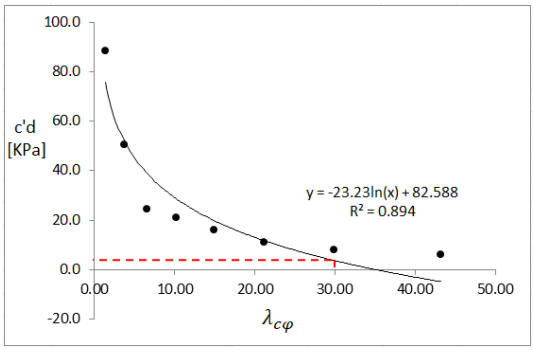

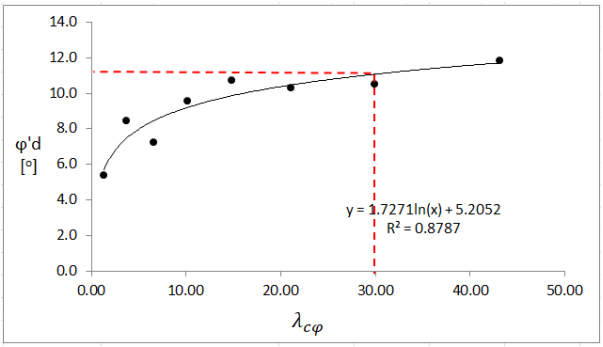

Profile 15

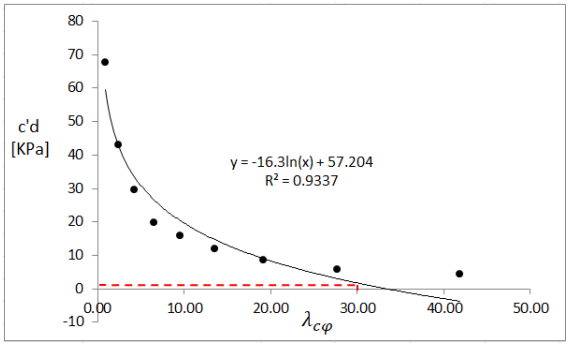

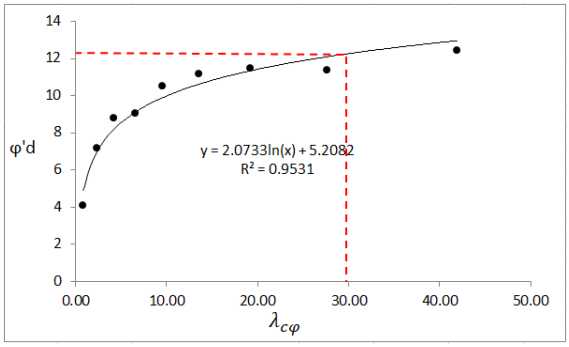

Profile 16

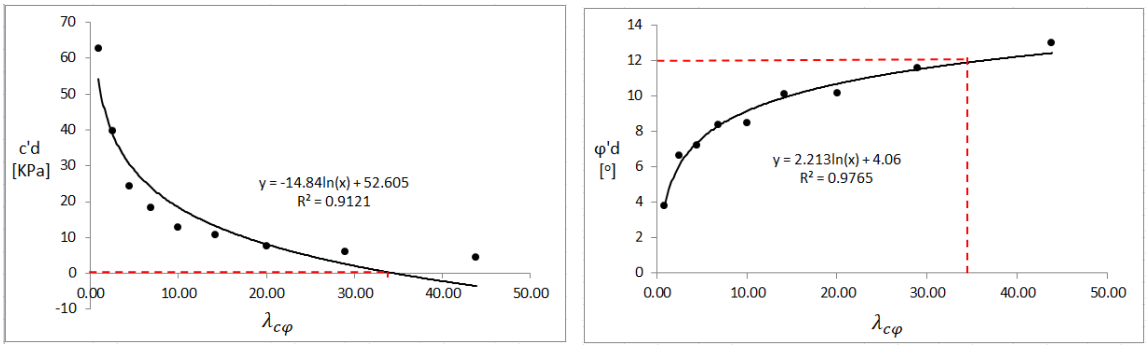

Figure 5-1 Back analyzed shear parameters (diagrams on the left for cohesion and diagrams on the right for internal friction angle) is using dimensionless parameter related to slip surface depth and range of assumed c' and φ' values (Red dashed line).

The results of the individual slope profile analysis by considering the above plots (Figure 5-1) to determine the shear parameters corresponding to the respective depth of the slip surface are given in Table 5-1.

Table 5-1 Back analyzed shear parameters for each slip surface in the individual slope profiles. Bold values are considered in this analysis representing the target deeper slip surface in all considered profiles (Bold texts).

Profile	Average slip surface depth	Cohesion (KPa)	Int. fric. Ang. (^{o})
Profile 8	18m	5.7	12.6
Profile 9	23m	5.2	11.6
Profile 10	30m	3.3	11.9
Profile 11	29m	0	11.6
Profile 14	30m	3.6	11
Profile 15	30m	1.7	12.2
Profile 16	34m	0.3	11.8

5.2 2D stability analysis

Slope profile 8

The slope stability analysis carried out along the profile No. 8 is shown in Annex 1. The overall profile has 9^0 average topographic slope and multiple slip surfaces adjacent to each other which were modelled as continuous. Shallower slip surfaces are also identified in the reviewed previous studies data (around 13m depth) but the deeper slip surfaces (around 18m for example in the case of profile 8) were used for further analysis as this were sought to constitute the larger and extensive slide which is intended to be modelled in the semi- 3D approach, rather than the localized slides with only single substantiated profile passing

through. The same analogy was adopted across all the other profiles considering the deeper identifiable slip surface from the monitoring data, borehole well logs and geophysical constrained boundaries. Overall the 2D factor of safety using simplified Janbu's method for the slope gave 1.94 for normal assumed initial water level condition according to the investigation data and back analysed shear parameters in this study. The factor of safety calculation iteration using simplified Janbu's method are shown in Annex 1 and the cross sectional area as calculated based on the input geometric extents of the profile are also shown in Annex 2.

Slope Profile 9

The slope stability analysis carried out along the profile No. 9 is shown in Annex 3. The overall profile has ca. 10^0 average topographic slope and multiple slip surfaces where deeper slip surface has been considered in this analysis. The shallower slip surface occurs at ca. 12 m depth while the deeper one rests at about 23 m depth. Overall the 2D factor of safety using simplified Janbu's method for the slope is 1.37 for normal assumed initial water level condition according to the investigation data and back analysed shear parameters in this study. The factor of safety calculation iteration using simplified Janbu's method are shown in Annex 3 and the cross sectional area as calculated based on the input geometric extents of the profile are also shown in Annex 4.

Slope profile 10

The slope stability analysis carried out along the profile No. 10 is shown in Annex 5. The overall profile has 12^0 average topographic gradient and multiple slip surfaces where deeper slip surface 30m depth has been considered in this analysis. Overall the 2D factor of safety using simplified Janbu's method for the slope is 0.84 for normal assumed initial water level condition according to the investigation data and back analysed shear parameters in this study. The factor of safety calculation iteration using simplified Janbu's method are shown in Annex 5 and the cross sectional area as calculated based on the input geometric extents of the profile are also shown in Annex 6.

Slope profile 11

The slope stability analysis carried out along the profile No. 11 is shown in Annex 7. The overall profile has 12^0 average topographic gradients a slip surface located about 29m deep has been considered in this analysis. Overall the 2D factor of safety using simplified Janbu's

method for the slope is 1.03 for normal assumed initial water level condition according to the investigation data and back analysed shear parameters in this study. The factor of safety calculation iteration using simplified Janbu's method are shown in Annex 7 and the cross sectional area as calculated based on the input geometric extents of the profile are also shown in Annex 8.

Slope Profile 14

The slope stability analysis carried out along the profile No. 14 is shown in Annex 9. The overall profile has 12^0 average topographic gradient and multiple slip surfaces. The shallow slip surface is located at ca 20 m depth while the deeper and one considered for further analysis in this study is located at 30m depth. Overall the 2D factor of safety using simplified Janbu's method for the slope is 0.73 for normal assumed initial water level condition according to the investigation data and back analysed shear parameters in this study. The factor of safety calculation iteration using simplified Janbu's method are shown in Annex 9 and the cross sectional area as calculated based on the input geometric extents of the profile are also shown in Annex 10

Slope Profile 15

The slope stability analysis carried out along the profile No. 15 is shown in Annex 11.The overall profile has 12^0 average topographic gradient and multiple slip surfaces. The shallower slip surface has average depth of 5.6 m while the deeper and one considered in this analysis is located ca 30 m depth. Overall factor of safety using simplified Janbu's method for the slope is 1.06 for normal assumed initial water level condition according to investigation data and back analysed shear parameters in this study. The factor of safety calculation iteration using simplified Janbu's method are shown in Annex 11 and the cross sectional area as calculated based on the input geometric extents of the profile are also shown in Annex 12.

Slope Profile 16

The slope stability analysis carried out along the profile No. 16 is shown in Annex 13. The overall profile has 10^0 average topographic gradients and the slip surface considered in this analysis has 34 m depth. Overall factor of safety using simplified Janbu's method for the slope is 1.08 for normal assumed initial water level condition according to investigation data and back analysed shear parameters in this study. The factor of safety calculation iteration

using simplified Janbu's method are shown in Annex 13 and the cross sectional area as calculated based on the input geometric extents of the profile are also shown in Annex 14.

The overall factors of safety computed for the 2D slope models along the 7 slope profiles are summarized in Table 5-2 including depth and shear parameters considered. The phreatic water level conditions are based on data from data of the investigation of JICA and GSE (2012).

Table 5-2 Summary of 2D stability analysis results and inputs for analysis ti initial water level (investigation result).

Profile	Slip surface depth (m)	c_d' (KPa)	φ'_d (^{o})	Wet unit weight ($K{\cdot}N/m^3$)	FoS (simplified Janbu)
Profile 8	18	5.7	12.6	19	1.94
Profile 9	23	5.2	11.6	19	1.37
Profile 10	30	3.3	11.9	19	0.84
Profile 11	29	0	11.6	19	1.03
Profile 14	30	3.6	11	19	0.73
Profile 15	30	1.7	12.2	19	1.06
Profile 16	34	0.3	11.8	19	1.08

5.3 Semi- 3D Factor of Safety

From the discussed methodology the factors of safety from each sub-parallel profile lines of stability analysis were integrated by area weighted averaging following the example of Lamb and Whiteman (1969). The associated factors of safety obtained in 2D stability analysis of simplified Janbu are combined by weighted averaging with respective cross sectional area and used in this study to generate the semi- 3D factor of safety (Eq. 19). The factors of safety are obtained with initial water conditions as per the investigation data. The water levels were later on varied and tested for impact on semi- 3D FoS. Comparison with the case of semi- 3D effect in the case of water level increased from initial position to 50% higher, slight improvement in terms of the expected response is observed (*Table 5-3* and Table 5-4). Profiles 8 and 9 always gave higher factor of safety in all cases. This can be related to the probable case that the landslides should not be included in the analysis.

Table 5-3 The individual profile 2D FoS weight averaged by the respective profile's landslide cross sectional area (A) to generate semi- 3D FoS at the initial reference water level condition (from investigation).

Slope Section		8	9	10	11	14	15	16
2D safety factor	F	1.94	1.37	0.84	1.03	0.73	1.06	1.08
cross section Area (m^2)	A	5037	8688	17209	8380	20855	10824	6829
Semi- 3D safety factor	1.01							

$$\text{Approximate 3D- safety factor} = \frac{(A8*F8) + (A9*F9) + (A10*F10) + (A11*F11) + (A14*F14) + (A15*F15)}{(A8+A9+A10+A11+A14+A15+A16)}$$

Table 5-4 The individual profile 2D FoS weight averaged by the respective profile's landslide cross sectional area (A) to generate semi- 3D FoS at elevated water level condition by 50% from the initial reference level across all profiles.

Slope Section		8	9	10	11	14	15	16
2D safety factor	F	1.72	1.46	0.93	0.88	0.86	0.96	0.94
cross section Area (m^2)	A	5037	8688	17209	8380	20855	10824	6829
Semi- 3D safety factor	1.02							

5.4 Sensitivity Analysis

5.4.1 Sensitivity of 2D slope model

For all sensitivity analysis comparison and changes were made with reference to the initial condition which is given in *Table 5-5*. Sensitivity analysis were carried for three slope profiles one on the central profile (Profile No. 14) from head to toe and two profiles on side, whereby to the left profile No. 16 and to right profile No 8, are selected. Results of the sensitivity analysis are collectively given case by case in tables *Table 5-6* to *Table 5-10* and in the plots therein.

Table 5-5 Reference initial condition definition

Parameters	Initial conditions	Variation for the 2D FoS (profile 8, 14 and 16)	Variation for the 3D FoS (all profiles)
Water level	As determined and defined in the investigation	Stepped increment and reduction by percentage for each profile	Stepped increment and reduction as percentage uniformly across all profiles
Cohesion	Back calculated values for each profile	Stepped reduction by percentage for each profile	Stepped reduction by percentage uniformly across all profiles
Friction angle	Back calculated values for each profile	Stepped reduction by percentage for each profile	Stepped reduction by percentage uniformly across all profiles

In scenario 1, the water table was varied from its initial position, which is the level as determined in the investigation of (JICA and GSE, 2012), is first reduced by 100%, and then increased by 50% and 100% steps. These were then plotted to assess sensitivity of the factor of safety to the change in water level. To that effect all other parameters were kept constant, at initial values. Table 5-6 shows the scenarios and obtained results for profiles 8, 14 and 16.

Table 5-6 Sensitivity analysis of 2D Factor of Safety (FoS) to changes in water level, also plotted in the diagram to the right (Hw: height of water level). Profile 8, Profile 14 and Profile 16.

Profile 8, Scenario 1	Changing levels of water table			
	Hw original	Hw –100%	Hw +50%	Hw +100%
c'$_d$	5.7	5.7	5.7	5.7
φ'$_d$	12.6	12.6	12.6	12.6
FoS	1.94	2.30	1.70	1.50
FoS (%change)	0	20	11	23

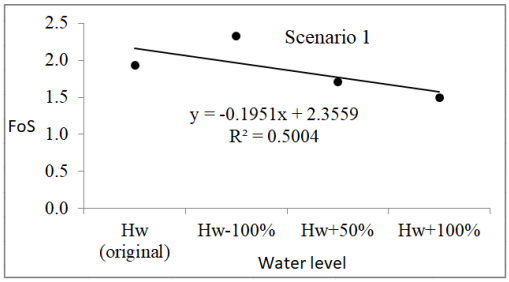

Profile 14, Scenario 1	Changing levels of water table			
	Hw original	Hw –100%	Hw +50%	Hw +100%
c'd	3.6	3.6	3.6	3.6
φ'd	11.0	11.0	11.0	11.0
FoS	0.73	0.95	0.86	0.58
FoS (%change)	0	30	18	21

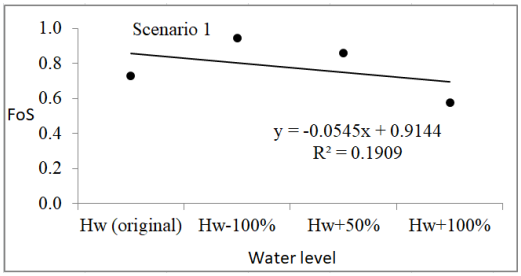

Profile 16, Scenario 1	Changing levels of water table			
	Hw original	Hw –100%	Hw +50%	Hw +100%
c'd	0.3	0.3	0.3	0.3
φ'd	11.8	11.8	11.8	11.8
FoS	1.08	1.30	0.94	0.80
FoS (%change)	0	20	-13	-26

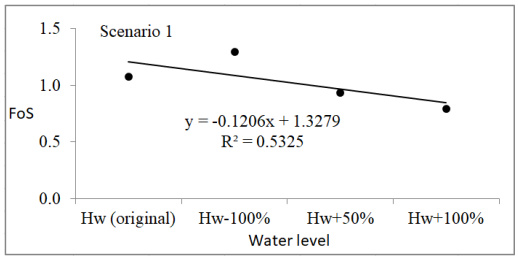

In scenario 2 the cohesion (c) was varied from its initial back calculated value decreasing by 30%, 50% and 100% from the initial value. Factor of safety is calculated in each instant to assess the sensitivity to change in cohesion in this case. The other parameters (water level and φ) were kept constant, at initial conditions. Table 5-7 shows the scenarios and obtained results.

Table 5-7 Sensitivity analysis of 2D Factor of Safety (FoS) to changes in cohesion, also plotted in the diagram to the righ (Profile 8, Profile 14 and Profile 16.

Profile 8, Scenario 2	Changing values of cohesion (KPa)			
	c' (0%)	c' (–30%)	c' (–50%)	c' (–100%)
c'd	5.7	4.0	2.9	0
φ'd	12.6	12.6	12.6	12.6
FoS	1.94	1.85	1.80	1.66
FoS (%change)	0	4.3	7.1	14.5

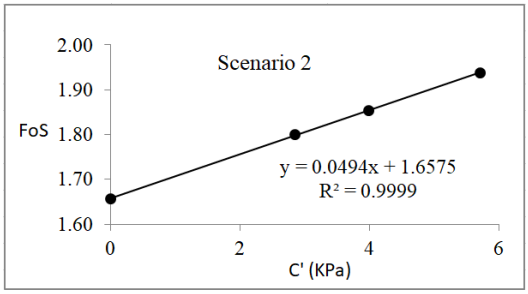

Profile 14, Scenario 2	Changing values of cohesion (KPa)			
	c' (0%)	c' (–30%)	c' (–50%)	c' (–100%)
c'd	3.6	2.5	1.8	0
φ'd	11	11	11	11
FoS	0.73	0.72	0.71	0.68
FoS (%change)	0.0	1.9	3.1	6.1

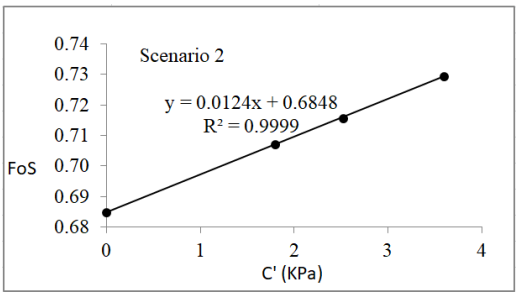

Profile 16, Scenario 2	Changing values of cohesion (KPa)			
	c’ (0%)	c’ (–30%)	c’ (–50%)	c’ (–100%)
c’d	0.30	0.21	0.15	0.00
φ’d	11.80	11.80	11.80	11.80
FoS	1.08	1.07	1.07	1.07
FoS (%change)	0.0	0.3	0.5	0.9

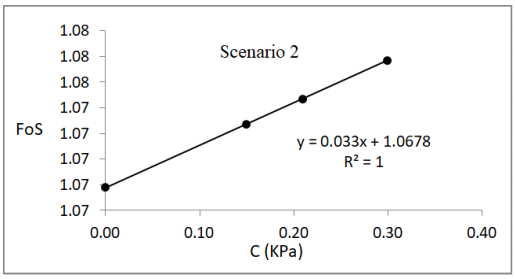

In scenario 3 the internal friction angle (φ) was varied by decreasing from its initial back calculated by 30%, 50% and 100% from the initial value. Factor of safety is calculated in each instant to assess the sensitivity to change in internal friction angle in this case. The other parameters (water level and c) were kept constant, at initial values. Table 5-8 shows the scenarios and obtained results.

Table 5-8 Sensitivity analysis of 2D Factor of Safety (FoS) to changes in internal friction angle, also plotted in the diagram to the right. (Profile 8, Profile 14 and Profile 16)

Profile 8, Scenario 3	Changing values of internal friction angle (^{0})			
	φ‘ (0%)	φ’ (–30%)	φ’ (–50%)	φ’ (–100%)
φ‘	12.6	8.8	6.3	0
c'_d	5.7	5.7	5.7	5.7
FoS	1.94	1.43	1.10	0.28
FoS (%change)	0	26	43	85

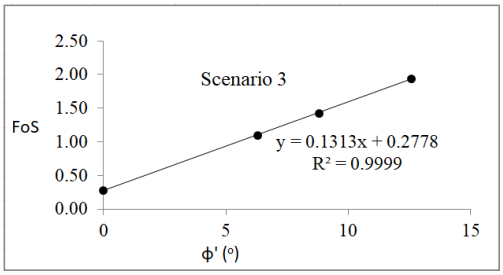

Profile 14, Scenario 3	Changing values of internal friction angle			
	φ‘ (0%)	φ’ (–30%)	φ’ (–50%)	φ’ (–100%)
φ‘	11	7.7	5.5	0
c'_d	3.6	3.6	3.6	3.6
FoS	0.73	0.52	0.38	0.04
FoS (%change)	0	28	47	94

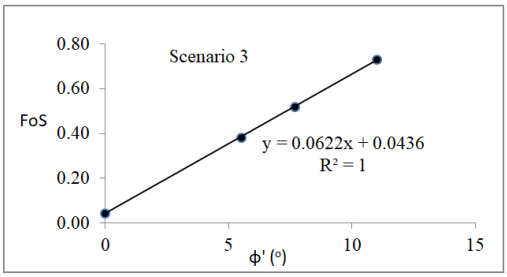

Profile 16, Scenario 3	Changing values of internal friction angle			
	φ‘ (0%)	φ’ (–30%)	φ’ (–50%)	φ’ (–100%)
φ‘	11.80	8.26	5.90	0.00
c'_d	0.30	0.30	0.30	0.30
FoS	1.08	0.75	0.54	0.01
FoS (%change)	0	30	50	99

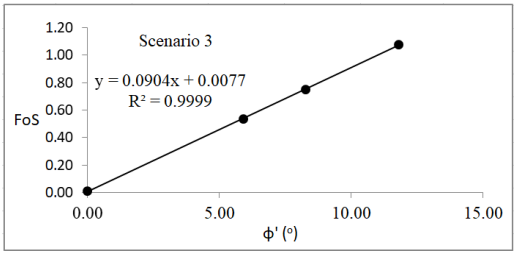

In scenario 4 the internal friction angle (φ) was varied from its initial back calculated value increased by 30%, 50% and 100% of the initial value. In this scenario the factor of safety is set to 1 (assuming the slope is on the verge of being stable) and the cohesion (c) was calculated in each instant at constant water level for various decreasing values of internal friction angle. In this case the needed internal friction angle to stabilize the material (FoS = 1) at various levels of cohesion. Table 5-9 shows the scenarios and obtained results.

Table 5-9 Back calculated cohesion for varied values of internal friction angle at 2D FoS of 1, also plotted in the diagram to the right. (Profile 8, Profile 14 and Profile 16)

Profile 8, Scenario 4	Back calculated c’ at constant FoS =1			
	φ’ (0%)	φ’ (–60%)	φ’ (–80%)	φ’ (–100%)
φ’	6	4.2	3.9	2.1
FoS	1	1	1	1
c’	4.7	9.0	9.8	14.1
c (%change)	0	28	47	94

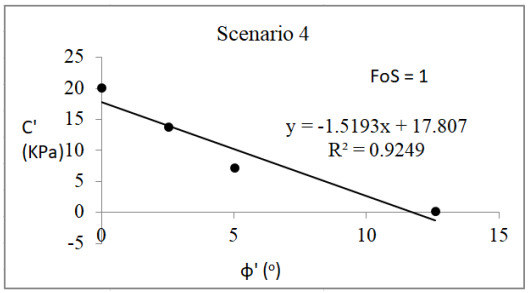

Profile 14, Scenario 4	Back calculated c’ at constant FoS =1			
	φ’ (0%)	φ’ (–60%)	φ’ (–80%)	φ’ (–100%)
φ’	11	7.7	5.5	0
FoS	1	1	1	1
c’	25.4	42	53	80
c (%change)	0	39	52	68

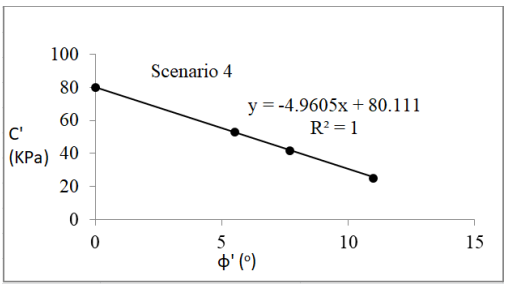

Profile 16, Scenario 4	Back calculated c’ at constant FoS =1			
	φ’ (0%)	φ’ (–60%)	φ’ (–80%)	φ’ (–100%)
φ’	11.8	7.1	5.9	0
FoS	1	1	1	1
c’	0	11	14.2	30
c (%change)	Increase!			

In scenario 5 the cohesion (c) was varied from its initial back calculated value increasing by 30%, 50% and 100% of the initial value. Factor of safety is set to 1 and the cohesion (c) was calculated in each instant at constant water level. In this case the achieved internal friction angle to stabilize the material (FoS = 1) is evaluated as cohesion is varied by certain increments. Table 5-10 shows the scenarios and obtained results.

Table 5-10 Back calculated friction angle for varied values of cohesion at 2D FoS of 1, also plotted in the diagram to the right. (Profile 8, Profile 14 and Profile 16)

Profile 8, Scenario 5	Back calculated φ’ at constant FoS =1			
	c’ (0%)	c’ (+30%)	c’ (+50%)	c’ (+100%)
c’	5.7	7.4	9.4	11.4
FoS	1	1	1	1
φ’	5.5	4.9	4.1	3.4
φ (%change)	0	12	34	62

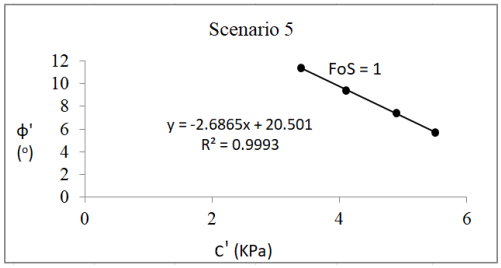

Profile 14, Scenario 5	Back calculated φ’ at constant FoS =1			
	c’ (0%)	c’ (+30%)	c’ (+50%)	c’ (+100%)
c’	3.6	4.68	5.4	7.2
FoS	1	1	1	1
φ’	15.2	15	14.8	14.5
φ (% change)	0	1	3	5

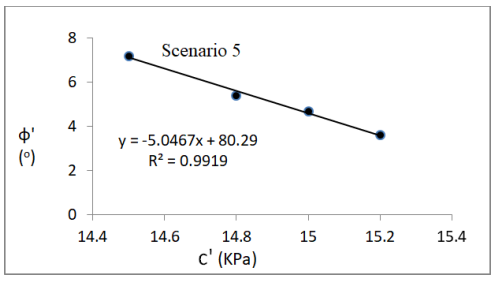

Profile 16, Scenario 5	Back calculated φ' at constant FoS =1			
	c' (0%)	c' (+30%)	c' (+50%)	c' (+100%)
c'	0.3	0.4	0.5	0.6
FoS	1	1	1	1
φ'	10.9	10.9	10.9	10.8
φ (%change)	0	0	0	1

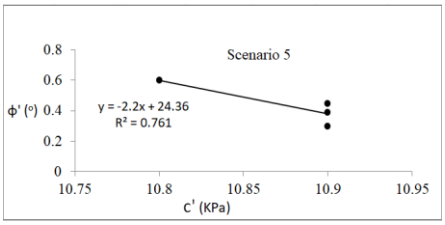

5.4.2 Sensitivity of Semi- 3D slope model

The changes in semi- 3D factor of safety in response to the variation of water level (reduction of level) by 10%, 30% and 50% is as shown in Table 5-11. The change in factor of safety in response to independent change in values of cohesion and friction angle by 30%, 50% and 100% reduction, one at a time, are shown in Table 5-12and *Table 5-13*, respectively. It can be seen that friction angle has the most influence on the variation of 3D FoS in similar manner to the 2D cases of the tested profiles (Figure 5-2). Further, water level fluctuation is note to be intermediate in influencing the semi- 3D FoS to lesser extent than the friction angle but significantly higher than the cohesion (shown in Figure 5-2). The semi- 3D FoS appears to have negligible sensitivity to changes in cohesion.

Table 5-11Sensitivity analysis of semi- 3D Factor of Safety (FoS) to uniform changes in water level across all profiles at constant initial shear strength c'_d and φ'_d value. *Hw: height of water level)*

Initial c'_d and φ'_d value of each profile	Hw original	Hw –100%	Hw +50%	Hw +100%
water level change by %	0	–100%	+50%	+100%
Semi- 3D FoS	1.01	1.26	1.02	0.79
Semi- 3D FoS change in %	91	89	91	93

Table 5-12 Sensitivity analysis of semi- 3D Factor of Safety (FoS) to uniform changes in cohesion and a fixed chosen water level and internal friction angle (i. e. as is during investigation of the area by JICA and GSE (2012) level across all profiles.

Change in c'_d at constant φ'_d					
Profile	φ'_d	c'_d	c' (–30%)	c' (–50)	c' (–100%)
Profile 8	12.6	5.7	3.99	2.85	0
Profile 9	11.6	5.2	3.6	2.6	0

Change in c'_d at constant φ'_d					
Profile	φ'_d	c'_d	c' (–30%)	c' (–50)	c' (–100%)
Profile 10	11.9	3.3	2.31	1.6	0
Profile 13	11.6	0	0	0	0
Profile 14	11	3.6	2.52	1.8	0
Profile 15	12.2	1.7	1.19	0.8	0
Profile 16	11.8	0.3	0.2	0.2	0
Semi- 3D FoS		1.01	0.99	0.98	0.95
Semi- 3D FoS change in %		0	2	3	6
Cohesion change %		0	30	50	100

Table 5-13 Sensitivity analysis of semi- 3D Factor of Safety (FoS) to uniform changes in internal friction angle and a fixed chosen water level and cohesion (i. e. as is during investigation of the area by JICA and GSE (2012) level across all profiles.

Change in φ' at constant c'_d					
Profile	c'_d	φ'_d	φ'_d (–30%)	φ'_d (– 50%)	φ'_d (–100%)
Profile 8	5.7	12.6	8.8	6.3	0
Profile 9	5.2	11.6	8.1	5.8	0
Profile 10	3.3	11.9	8.3	5.9	0
Profile 13	0	11.6	8.1	5.8	0
Profile 14	3.6	11	7.7	5.5	0
Profile 15	1.7	12.2	8.5	6.1	0
Profile 16	0.3	11.8	8.3	5.9	0
Semi- 3D FoS		**1.01**	**0.72**	**0.53**	**0.06**
Semi- 3D FoS change in %		0	28	47	93
Internal friction angle change %		0	30	50	100

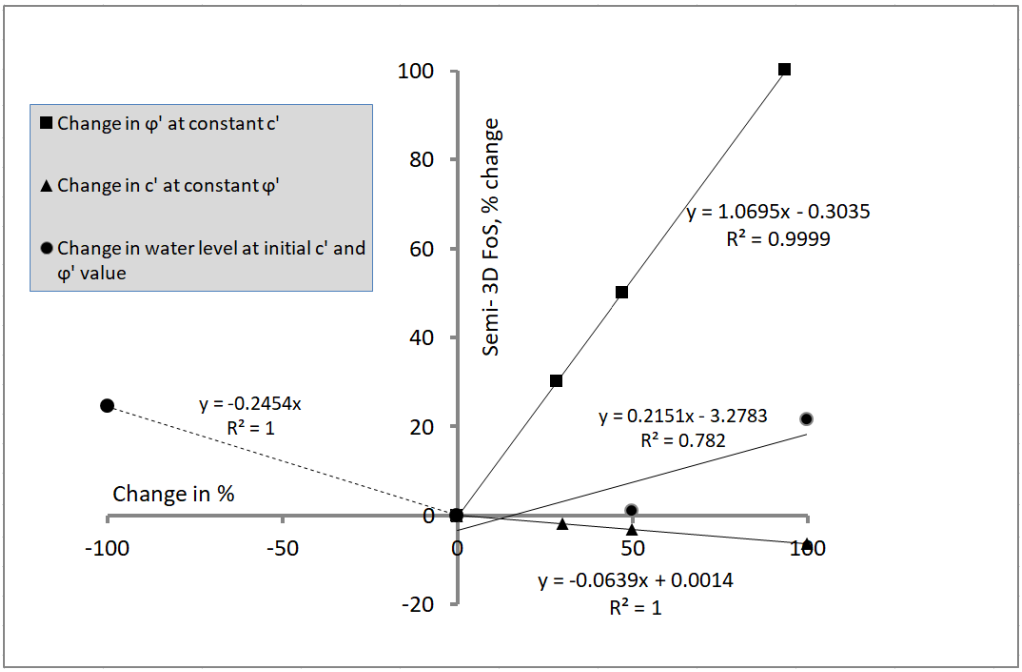

Figure 5-2 Comparison of the sensitivity of the semi- 3D factor of safety to individual changes in shear strength parameters and water level unifrmly across all profiles, based on Table 5-11, Table 5-12 and Table 5-13.

6 Discussion

6.1 Back Analysis

The back calculation of c and φ using the location of the slip surface has had mixed success and does not seen to work where there is significant progressive failure or distinct layering and inhomogeneity in the slope. In general while the determined cohesion is very low, it is not entirely zero except in one case (prolife 13 and 16) as expected in progressive failure condition.

More than one slip surface has been interpreted in the various slope profiles although the main focus and scope of this study is on the deeper detected slip surface. The deeper slip surface is selected in view of two main reasons, the first is that the deeper slip surface has good number of transects to provide spatial information on the profile of the slope to model it with sufficient depth of boreholes in most cases. The second reason is that, the deeper slip surface is thought to extend throughout the whole area of instability acting as coherent body making it logical to model as single 3D model while encompassing a wider range of lateral inhomogeneity in terms of geometry and material property. The later hence is creates opportunity to test the role of such variability on the factor of safety derived in individual 2D factor of safety and the weighted 3D factor of safety. Most cohesion values obtained are low and zero for cases of profile 13 and 16 (0.3 KPa). All other profiles gave cohesion values which are low but quite different from zero ranging from 3.3 to 5.7 KPa, which are still pertaining to the residual nature of the materials involved in the slide but with certain over estimation. On the other hand the friction angles cluster to 11^0 to 12.6^0 which is in good agreement with other back analysis results from the area (Samuel Molla, 2010).

The back calculated shear parameters for the landslides using critical slip surface in the colluvium were back calculated to 0.3 KPa for cohesion and 11^0 for friction angle (Samuel Molla, 2011). While the back calculated friction angle is quite similar (11^0 to 12.6^0) in this study) there appears significant disparity from the cohesions values back calculated in the current study (which range from 0 to 5.7 KPa). This difference might also be partly due to the differences in approaches adopted for the back analysis.

On the other hand the values obtained from Laboratory test of samples from similar area gave higher values for both parameters, where a cohesion of 30–75 KPa and a friction angle between 23^0 and 28^0 (Lulseged Ayalew et al., 2009) are reported. Apparently the results indicate the peak shear strength parameters as such values cannot be expected in the colluvium soil undergoing multiple slip. Similarly, an unpublished data from the Geological Survey of Ethiopia for further investigation in the area from borehole soil samples gave cohesion and friction angle values of 53 KPa and 15^0 respectively, based on direct shear test (Unpublished report, Geological Survey of Ethiopia) also a peak shear strength value.

6.2 2D Stability Analysis

Results of the stability analysis of considered slopes (profiles) showed variable FoS ranging from stable to unstable at the water level as determined from the investigation data. The values, as can be seen range from 0.84 to 1.94, shown in Table 5-2. This suggests in fact the variable proneness to instability and the need to assess over all condition of instability.

The most important parameter which affects instability in the area is the rainfall. Although as can be seen in sensitivity analysis that the friction angle changes has the highest influence on the derived FoS. The role of seismic forces has not been considered in this analysis to keep the simple Spread Sheet program based computations manageable for the scope of this study. It also has less significance in terms of recurrent occurrence as historical data show less seismicity influence in the area. Rather the major triggering factor has been considered to be the seasonal rainfall through the rapid increase of water tables in perched aquifers and unconsolidated colluvium.

In Profile 8, the factor of safety is remained greater than 1 even under complete saturation and under very low cohesion. But an extreme drop in FoS resulted from reduction very low friction angle considered in the sensitivity analysis. In Profile 14, the factor of safety is improved but remains unstable even under very low water level condition and all shear strength parameter changes imposed. It is one of the most unstable profiles in the area. Profile 16 showed marginal stability where changing of water level and friction angle brought about shifting of the FoS above and below unity. Nevertheless, the cohesion had little impact to alter the stability condition.

Looking at the distribution of the denominator and numerators in the employed Janbu's equation, the following plots emerge with regard to force balance across the profile (*Figure*

6-1, *Figure 6-2* and *Figure 6-3*). For example in *Figure 6-1*, the resisting force is exceeded along entire slope (Profile 10) but the lower (left end) is well balanced. Also the last upper slope side (right end) show sharp rise in resisting force is related with the dimension of the slices leading to localized over estimation of the resisting force which eventually is worked out for the global case when summed together keeping the equilibrium pursuant to the assumptions in Janbu's method.

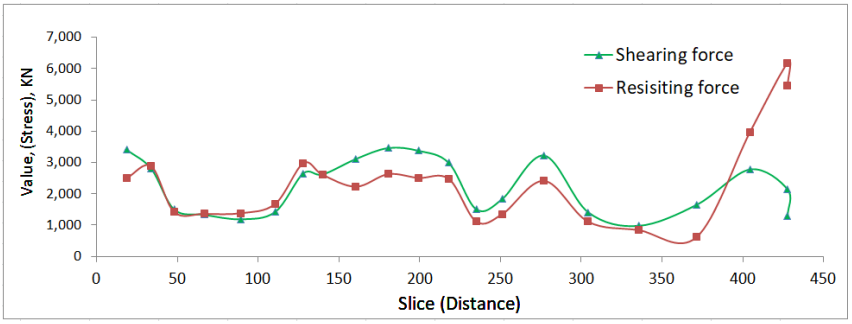

Figure 6-1 Profile of resisting and driving force of slope instability along Profile 10.

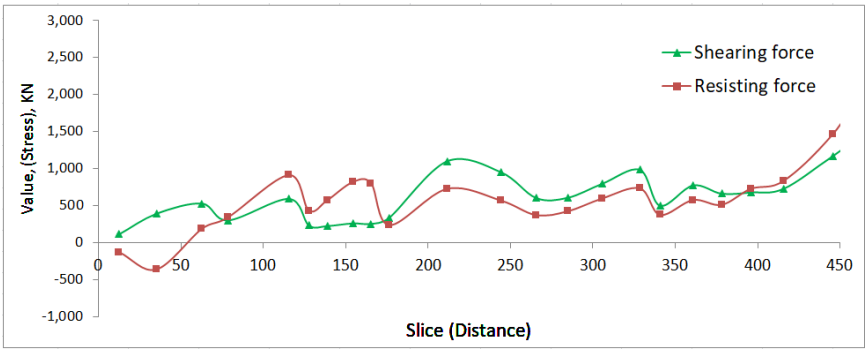

Figure 6-2 Profile of resisting and driving force of slope instability along Profile 9

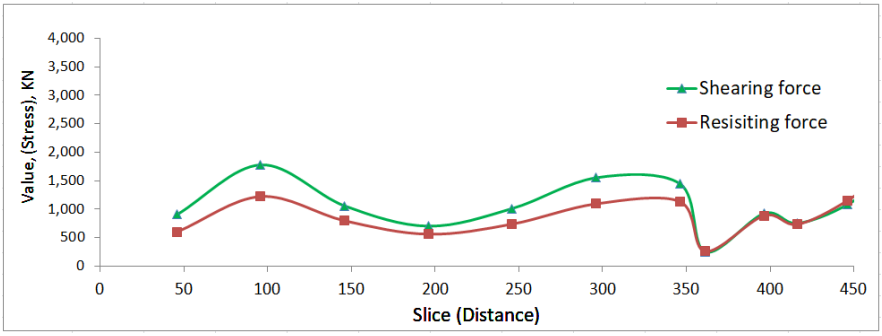

Figure 6-3 Profile of resisting and driving force of slope instability along Profile 16.

6.3 Semi- 3D stability analysis

The stability analysis utilizing the cross sectional area weighted individual profile evaluation for determination of semi- 3D factor of safety shows generally higher than anticipated. The

factors of safety at the reference initial water level and back analysed condition were consistently lower than the factors of safety along profile 8 and 9 which are the western most profiles, whereas the central and eastern profile (specially profiles 10, 14, 15 and 16) are relatively found to have lower or equal factors of safety. A number of factors can be speculated the first of which is that this approach of 3D modelling is rudimentary and might not necessarily conform to the expectation that the other robust 3D models achieve in a much more constrained and quantified approaches. On the other hand the issue of obtaining shear strength parameters can be viewed with mixed success specially looking at the obtained cohesion values where higher than zero values are reported in this study for a reactivated recurrent slide surface. The situation might be improved if smaller and well established slip surface continuity can be ensured and also where alternative back analysis can be used. The best scenario with regard to the higher factor of safety than the 2D slope profiles is that of the case where water level is raised by 50% from the reference initial condition. Except profiles 8 and 9, the other profiles gave lower factor of safety than the 3D factor of safety. On the other hand further increment to fully saturated condition of 100% increment resulted again in lower 3D factor f safety than most of the 2D factors of safety.

Such success and the nature of the sliding material poses problem in arriving at reliable back analysed values as can be seen in the back analysis. Nevertheless, it lacked the expected more conservative estimate. Another factor can be the approach of the area calculation in excel which is limited to approximate determination based on slices resolution (spacing) which is weighting parameter for the factor od safety. It should also be considered that other weighting mechanism might be more appropriate in the simpler approach using such spread sheet programs to account more reliably the factor of safety in semi- 3D models.

It also is meant to appreciate the limitations and opportunities in the implementation of semi-3D modelling in more controlled and easy to manipulate environment. With the exception of the initial cumbersome steps to create the slope model from various sources, the data processing and analytical results has been quite manageable.

6.4 Sensitivity analysis

The analysis of sensitivity analysis followed the course of changing the shear strength parameters and evaluating the imposed change on the compute factor of safety for both the 2D and 3D cases. These introduced changes and results are summarized in Table 6-1 for the

impact of variation in water table and in Table 6-2 for the shear strength parameters influence.

Table 6-1 Change in semi- 3D FoS as water level is varied uniformly across all profiles

	Water level (initial)	Water level (+10%)	Water level (+30%)	Water level (+50%)
Water level (%)	0	10	30	50
Semi- 3D FoS	0.95	1.02	1.15	1.28
Semi- 3D FoS (Change %)	0	7.4	21.1	34.7

Table 6-2 Change in semi- 3D FoS as shear strength parameters are varied uniformly across all profiles

	Scenario 1		Scenario 2		Scenario 3		Scenario 4	
	C (+0%)	φ (+0%)	c (+30%)	φ (+30%)	c (+50%)	φ (+50)	c (+100%)	φ (+100)
Profile 8	2	6	2.6	7.8	3	9	4	12
Profile 9	1.4	9	1.82	11.7	2.1	13.5	2.8	18
Profile 10	0	15	0	19.5	0	22.5	0	30
Profile 13	0	11	0	14.3	0	16.5	0	22
Profile 14	0	16	0	20.8	0	24	0	32
Profile 15	0	11.7	0	15.21	0	17.55	0	23.4
Profile 16	0.7	11	0.91	14.3	1.05	16.5	1.4	22
Semi- 3D FoS	**0.95**	**0.95**	**0.96**	**1.25**	**0.96**	**1.46**	**0.97**	**2.01**

In the case of profile 8, sensitivity of factor of safety to changes in cohesion, friction angle and water level changes are compared. The changes are tested by keeping two of the parameters constant while changing one of them. Maximum sensitivity has been obtained mainly in response to changes in internal friction angle, which improved the stability. The factor of safety is also sensitive to change in water level.

In the case of Slope Profile 14

In slope profile 16, it can be seen that the factor of safety is slightly more sensitive to change in internal friction angle than change in water level while the sensitivity is very low for the change in cohesion. This signifies that the intervention most effective might be to implement measures that have the effect of increased internal friction angle accompanied with water level reduction. The effect of internal friction angle is seen to be most important among the three considered parameters of slope stability: cohesion, water level and internal friction angle. The stability is less sensitive to changes in cohesion which might be logical as the materials are observed to be in residual state and hence have very low to zero cohesion. On

the other hand, the residual friction angle can be noted to have the most influence on the stability of the slope. The factor of safety was significantly changed with slight change in internal friction than with the change in cohesion.

the effect of water level change on the central part of the landslide (represented by Profile 14) is found to be more significant than the friction angle unlike other most cases. Similar situation is observed where the impact of the water level change is found to be closer to the effect of the change in friction. This variation in influence is important to note as we are considering variation with regard to 2D stability analysis. The role of water level variation appears to have significant control on changing factors of safety next to internal friction angle. From practical point of view variation in friction angle are less commonly achieved and hence the water level being most variable, would be expected to have the real influence more than the friction angle.

Nevertheless the water level is found to lie above the slip surface even under lowest depth considered in the sensitivity analysis (*Figure 6-4*. This signifies the demanding task of achieving stability by lowering of water level as it requires numerous mechanisms and extensive work to withdraw enough water to stabilize the landslide. On the other hand the consequence of environmental impact could be even worse than the landslide problem in this case. An example from Profile 10 (*Figure 6-4*) shows the water level still above the slip surface even after uniformly reducing the level by 50%. Therefore it is worth consideration to what extent the counter measures will be effective when recommending measures.

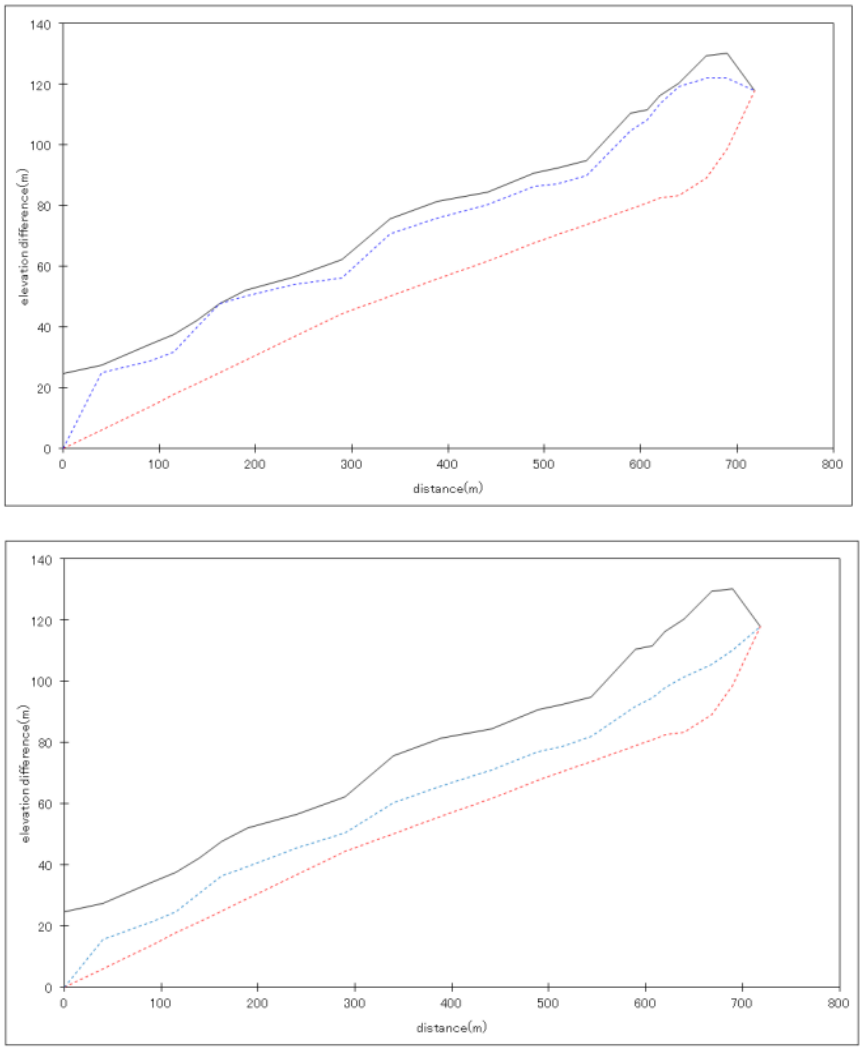

Figure 6-4 Water table reduction in the slope profile No. 10 from original level (left) to less than 50% of its original level (right). Red line is extrapolated slip surface; blue line is water level.

In similar manner the sensitivity of the semi- 3D factor of safety to the considered parameters of shear strength and water level variation showed considerable variation (Figure 5-2). The sensitivity range of the semi- 3D factor of safety to the change in internal friction can be seen to be much higher than that of change in cohesion which reflects the overall trend in the individual profiles (Profile, 8, 14 and 16). It is again shown that the role of cohesion is almost nil for the integrity of the material to be stable under the configuration of the slope model. This again might lend to the fact that the behaviour is reflecting conditions on failure as theoretical value which cannot be captured by the physical test conducted under different conditions than actual landslide moment. Nevertheless the very low value of cohesion cannot be ruled out and suggest reliance on internal friction angle in terms of effective remediation.

7. Conclusion

Slope stability analysis following classical 2D stability models has been carried out and extended to semi- 3D model. It has been implemented in Microsoft Excel spread sheet program and has given satisfactory result for carrying out analysis of various scenarios of the slope conditions. The site chosen for testing of the methodology is located in the Abay Gorge along the main road from Gohatsion to Dejen at 28 Km distance from Gohatsion. The Slope stability model of simplified Janbu's method has been followed as it assumes non-circular slip surface shape which is appropriate for the studied landslide on the one hand and also more efficient and convenient for implementation in a simple spread sheet program.

The landslides in Abay Gorge are part of the lasting history of geomorphic processes associated with uplifting and incision by River. The succession of cretaceous and tertiary volcanic series by the Blue Nile gorge has given way to opening of the Valley with in short span of time. The recent and historical landslide history of the area has attracted attention of many researches on various aspects of the landslide problem resulting in perhaps the most studied landslide zone in the country. The availability of such relatively higher number of studies offered an opportunity to test possibility to implement semi- 3D stability analysis as demonstrated in this thesis.

The landslide are complex and have more or less planar slip surface with annual cycle of recurrent movement following rainy season with instruments recording abrupt changes in phreatic water level and associated slightly delayed displacement suggesting direct impact of the water precipitation on the stability of the slope. Ass also seen from the monitoring data and the sensitivity analysis of step wise uniform phreatic water level reduction, all the profiles which were previous highly unstable were seen to have factors of safety greater than 1. Based on this it can be concluded that temporary water level rise might be associated with the type of perched water aquifer which lasts shorter time but had detrimental impact on slopes when it is saturated during and immediately after rainy season. The effect is also reflected in the sensitivity analysis of the 3D model where uniform reduction of water by as little as 10% in all profiles had resulted in bringing the semi- 3D factor of safety unity.

A back analysis and sensitivity has also been carried out in the spread sheet program. The inputs were generated from geometric construction of slopes based on investigation of JICA AND GSE (2012) and field reconnaissance. In addition, the physical characteristics of the

sliding mass are well constrained from the monitoring data of the same study (JICA AND GSE, 2012). The method of integrating multiple slope profile stability analysis into a 3D model of computing factor of safety has then been implemented for the whole of the site.

The shear strength parameters involved in the landslide have been determined by back analysis. The landslide is found to be highly in unstable condition in most scenarios. The resulting factor of safety as changes in shear strength parameters and water level change are compared suggests controlling role of internal friction angle and water level. Cohesion is found to have less influence on factor of safety. The semi- 3D factor of safety is found to be only higher two profiles and lower than five individual slope profiles analysed in the classical method of simplified Janbu's method. In the best case scenario the 3D factor of safety gave higher value of factor of safety than five slope profiles while two profiles gave greater factor of safety than the 3D Factor of safety. Nevertheless, the factor of safety should not always be taken measure of success or performance, whether it gave a conservative or non-conservative factor of safety. It might have real physical bearing to have given a result contrary to expectation although certain doubt cannot be ruled out in the process of the analysis.

The lab tests should rely on residual shear strength values rather than the peak strength when dealing with recurrent landslide problem which otherwise leads to overestimation of factor of safety and significantly increase risk of running slope failures.

The following points can be drawn from the study on the methodological aspect as well as the landslide characteristics. The possibility to fully implement stability assessment in simple spread sheet programs has been tested and gave insight into characteristics of the landslide. Basic and interactive spread sheet programs allow more intuitive approach to the analysis compared to commercial software's which usually have underlying working modifications of the basic classic models of slope stability analysis that are usually not obvious for most of the user.

Mainstream 3D slope stability models involve use of highly specialized numerical computations which almost reduces the physical meaning of the problem at hand to greater extent. A rather intuitive approach, with increased number of more sensible and simpler 2D slope stability models integrated into reasonable semi- 3D model, can offer an alternative far easier to understand. On the other hand the cumbersome task of geometric construction and elaborate field and test data requirement is a setback in carrying out such 3D models. Hence

it still needs an easier and better way for practical application other than basic research as it proved in this study, requiring still heavy reliance on use of other commercial software's such as ArcGIS® and AutoCAD®.

The set out objectives of the study has been fully met but the findings were found to be not conclusive enough as expected or hypothesized. This might be due to two factors where the first one is lack of relevant data especially on the material properties to carry out more robust back analysis for the shear strength parameters. The second is the uncertainty in assigning the slip surface continuity across the whole landslide body. As the available well constrained profiles were limited in the study area, consideration was given to the wider and deeper seated slip surface where multiple profiles traversed it creating the opportunity to develop semi- 3D spatial models. This on the other hand led to increased uncertainty of the identified slip surfaces in the deeper level in all sections to be continuous.

Nevertheless, despite the subjectivity and limitations in assumptions made and availability of data to constrain findings, the developed model can be seen to have served to process and deliver outputs that can be utilized for various design or intervention effectiveness checking. The inputs and the models are also subject to easy manipulation and changes giving it flexibility to some extent. The developed method can be seen to give at least an insight and an option for undertaking certain aspects of instability evaluation using Janbu'simplified approach. It is believed the attempted modelling will trigger more onterest in the application of 3D models in slope stability analysis in our country in more robust and sound theoretical bases of numerical models.

References

Abramson, L.W., Lee, T.S., Sharma, S., Boyce, G.M. (1996). "Slope Stability and Stabilization Methods" John Wiley and Sons, N.Y

Agam, M.W., Hashim, M.H.M., Murad, M.I., Zabidi, H. (2016). Slope Sensitivity Analysis using Spencer's Method in Comparison with General Limit Equilibrium Method. Procedia Chemistry 19, 651 – 658

Albataineh, N. (2006). Slope stability analysis using 2d and 3d methods. Master's Thesis. The University of Akron, 143 pp.

Almaz Gezahegn and Tadesse Dessie (1994). Report on Engineering geophysical investigation of the Blue Nile basin for rerouting of the main road. Ethiopian Institute of Geological Survey.

Anderson, M. G. & Richards, K. S. (1987). Slope Stability: Geotechnical Engineering and Geomorphology. John Wiley and Sons, N.Y.

Atalay Ayele (2017). Probabilistic seismic hazard analysis (PSHA) for Ethiopia and the neighboring region. Journal of African Earth Sciences, Volume 134, Pages 257-264.

Bishop, A.W. (1955). The use of the slip circle in the stability analysis of earth slopes. Géotechnique, 5(1): 7–17.

Bisrat Yifru and Fenta Ayehu. (2017). Prediction of Groundwater Level Fluctuation towards Rainfall Induced Landslide: Case of Blue Nile Gorge, Central Ethiopia. Open Journal of Modern Hydrology, **7**, 274-297.

Chen Z., Mi H., Zhang F., Wang X. (2003). A simplified method for 3D slope stability analysis. Can. Geotech. J. 40: 675–683.

Cheng, G., Jiang, P. (2012). Sensitivity analysis of factors affecting soil slope stability. Applied Mechanics and Materials, Vol. 170-173, 1072-1075.

Cheng, Y.M., and Yip, C.J. (2007). Three-Dimensional asymmetrical slope stability analysis extension of Bishop's, Janbu's, and Morgenstern–Price's techniques. Journal of Geotechnical and Geoenvironmental Engineering, 133(12): 1544–1555.

Cori, S., Raki, D., Hadzi-Nikovi, G. and Vlajkovic, V. (2015). Three dimensional approach to stability analysis of landslide Mokra Gora. Proceeding of the 2nd regional symposium on landslides in the Adriatic – Balkan Region, Belgrade, Serbia.

Coric, H., Rakic, D., Hadz-Nikovic, G., Vlajkovic, V. (2015). Three dimensional stability analysis of the "Mokra Gora" landslide. Proceedings of the 2nd Regional Symposium on Landslides in the Adriatic – Balkan Region, Belgrade, pp 62-65.

Cornforth, D. H. (2005). Landslides in Practice, John Wiley & Sons, New Jersey.

Cruden, D.M. and Varnes, D.J. (1996). Landslide Types and Processes. In Turner, A.K., Schuster, R.L. (eds), Landslides: Investigation and Mitigation, Transportation Research Board, Special Report, 247:36-75.

Duncan J.M. and S.G. Wright, (2005). Soil Strength and Slope Stability. John Wiley and Sons. NY.

Duncan, J. M. (1996). State of the Art: Limit Equilibrium and Finite-Element Analysis of Slopes. J. Geotech. Eng. 122:577-596.

Duncan, J. M. and S. G. Wright, (1980). The Accuracy of Equilibrium Methods of Slope Stability Analysis. Engineering Geology, 16: 5-17.

Fekadu Kebede and Laike Mariam Asfaw (1996). Seismic hazard assessment for Ethiopia and the Neighboring countries. Sinet – Ethiopian Journal of Science, 9(1), 15-50.

Filz, G. M., Brandon, T. L., and Duncan, J. M. (1992). Back analysis of the Olmstead Landslide using anisotropic strengths. TRANSPORTATION RESEARCH RECORD 1343, 72-78.

Fredlund, D. G., and Krahn, J. (1977). Comparison of Slope Stability Methods of Analysis. Canadian Geotechnical Journal, Vol. 14, No. 3, pp. 429-439

Gani, N., Abdelsalam, M.G., Gera, S., Gani, M. (2009). Stratigraphic and structural evolution of the Blue Nile Basin, Northwestern Ethiopian Plateau. Geol. J. 44, 30-56.

Gani, N.D.S, Gani, M.R., Abdelsalam, M.G. (2007). Blue Nile incision on the Ethiopian Plateau: Pulsed plateau growth, pliocene uplift, and hominin evolution. GSA Today, Vol. 17, no. 9, 4-11.

Gani, N.D.S., Abdelsalam, M.G. (2006): Remote sensing analysis of the Gorge of the Nile, Ethiopia with emphasis on Dejen-Gohatsion region. Journal of African Earth Sciences. 44, 135-150.

Getaneh Assefa (1980). Stratigraphy and sedimentation of the type Gohatsion Formation (Lias-Malm) Abay River basin, Ethiopia. Ethiopian Journal of Science (Sinet) 3, 87–110.

Getaneh Assefa (1991). Lithostratigraphy and environment of deposition of the Late Jurassic–Early Cretaceous sequence of the central part of Northwestern Plateau, Ethiopia. Neues Jahrbuch fur Geologie und Paleontologie Abhandunglen 182: 255–284

Griffiths, D.V., and Marquez, R.M. (2007). Three-dimensional slope stability analysis by elasto-plastic finite elements. Géotechnique, 57(6): 537–546.

Guo, T., and He, Z.M. (2011). Comparison of Factor of Safety of a Roadway Slope Based on the Limit Equilibrium Method and Shear Strength Reduction Method. Slope Stability and Earth Retaining Walls, pp: 34-40.

Henok Woldegeorgis, Raghuvanshi, T.K., and Balemwal Atnafu (2014). Landslide Hazard Zonation Using Expert Evaluation Technique: A Case Study of the Area Between Gohation Town and the Abay (Blue Nile) River, central Ethiopia. SINET: Ethiopian Journal of Science. 37(2): 75-94.

Huang, C.C., Tsai, C.C. (2000). New method for 3D and asymmetrical slope stability analysis. Journal of Geotechnical and Geo-environmental Engineering, 126(10), 917-927.

Hungr O., Leroueil, S., Picarelli L. (2013). The Varnes classification of landslide types, an update. Landslides, Review, 28 pp.

Hussain, M., Stark, T.D., and Akhtar, K. (2010). Back-Analysis Procedure for Landslides. Proceedings of the International Conference on Geotechnical Engineering, Lahore, Pakistan.

Ismail, Elamin H.D. (2013). Regional geomorphic analysis and GIS susceptibility mapping of landslides in the Blue Nile and the Tekeze River Basins of Ethiopia. Missouri University of Science and Technology. Doctoral Dissertations, 1832.pp. 236.

Janbu, N. (1954). Application of composite slip circles for stability analysis. In Proceedings of the Fourth European Conference on Stability of Earth Slopes, Stockholm, Sweden, pp: 43–49.

Jemal Saed. (2005). Slope Stability Studies along Gohatsion-Dejen Road. Master's Thesis, Addis Ababa University, Ethiopia.

Jepson, D.H., Athearn, M.U. (1962). East-West Geologic Sections, Blue Nile river Basin, Ethiopia. Addis Ababa: Department of Water Resources.

JICA and GSE (2012). The Project for Developing Countermeasures against Landslides in the Abay River Gorge. Japan International Cooperation Agency and Geological Survey of Ethiopia. Technical Report, 348 pp.

Kalatehjari, R., Ali, N. (2013). A Review of Three-Dimensional Slope Stability Analyses based on Limit Equilibrium Method. Electronic Journal of Geotechnical Engineering, Vol. 18, 119-134.

Karikari Y.O., Gyasi A.Y. (2000). Stability of slopes characterised by colluvium: investigation, analysis and stability. Melbourne, Australia, Geo.Eng.Technomic, 105.

Kim, U., Kaluarachchi, J. J., Smakhtin, V. U. (2008). Climate change impacts on hydrology and water resources of the Upper Blue Nile River Basin, Ethiopia. Colombo, Sri Lanka: International Water Management Institute. IWMI Research Report 126, 27 str.

Laike Mariyam Asfaw (1996). Catalogue of Ethiopian Earth Quakes, Earth quake parameters, strain release and Seismic Risk. Geophysical Observatory, Faculty of Science. Addis Ababa University, Ethiopia.

Lambe, T.W., Whitman, R.V. (1969). Soil Mechanics. John Wiley & Sons, New York. ISBN 47151192 7, pp 553.

Lulseged Ayalew, Moeller, D., Reik, D. (2009). Geotechnical Aspects and Stability of Road Cuts in the Blue Nile Basin, Ethiopia. Geotech Geol Eng 27:713–728.

Lulseged Ayalew, Yamagishi, H. (2004). Slope failures in the Blue Nile basin, as seen from landscape evolution perspective. Geomorphology. 61:1-22

Luo, Z., Jiang, Q., Zhang, J., Wan, L., Xu, X. (2017). Sensitivity Analysis of Factors Affecting Slope Stability Research and Application.Revista de la Facultad de Ingeniería U.C.V., Vol. 32, N°15, pp. 01-11.

Masao, Y., Kensuke, I., Takeshi, K., Tomonari, T., Atsushi, N. (2013). The Interpretation for Landslide Mechanism and The Proposal of Landslide Countermeasures in Abay Gorge in Ethiopia. In *K. Ugai et al. (eds.), Earthquake-Induced Landslides, Springer-Verlag Berlin Heidelberg, pp* 405-416.

Mengesha Tefera, Tadiwos Cherner, Workineh Haro (1996). Geological Map of Ethiopia. IEGS.

Meten, M., Prakash Bhandary, N. and Yatabe, R. (2015). Effect of Landslide Factor Cobinations on the Prediction Accuracy of Landslide Susceptibility Maps in the Blue Nile Gorge of Central Ethiopia. GEOENVIRON DISASTERS 2:9. https://doi.org/10.1186/s40677-015-0016-7

Morgenstern, N.R. and Price, V.E. (1965). The analysis of the stability of general of slip surface. Géotechnique, 15(1): 79–93.

Neng-pan J., Huang, J., Huang, R., He, C., Li, Y. (2015). A Real-time monitoring and early warning system for landslides in Southwest China. Journal of Mountain Science 12(5):1219-1228.

Nermeen Albataineh. (2006). Slope Stability Analysis Using 2D And 3D Methods. Unpublished University Master Thesis. The University of Akron. USA.

Rahardjo, H., Satyanaga, A. and Leong, E. C. (2012).Unsaturated soil mechanics for slope stabilization. Geotechnical Engineering Journal of the SEAGS & AGSSEA, March, 43(1), 48-58.

Reyes, A. and D. Parra (2014). 3D slope stability analysis by the using limit equilibrium method analysis of a mine waste dump. Proceedings Tailings and Mine Waste. Keystone, Colorado, USA.

Rotaru, A., D. Oajdea and P. Răileanu. (2007). Analysis of the Landslide Movements. International Journal of Geology. Issue 3, Volume 1, pp. 70-79.

Samuel Molla. (2011). Slope Stability Analysis for a selected slope section along the road Gohatsion-Dejen. Unpublished Msc thesis. Addis Ababa University, Ethiopia, 118 pp.

Savvaidis, P. D. (2003). Existing Landslide Monitoring Systems and Techniques. From Stars to Earth and Culture. School of Rural and Surveying Engineering, the Aristotle University of Thessaloniki. pp. 242-258.

Seleshi Awulachew, McCartney M., Steenhuis T., Ahmed A. (2008). A review of hydrology, sediment and water resource use in the Blue Nile Basin. International Water Management Institute, Colombo, Sri Lanka.IWMI Working paper 131, pp.

Shiferaw Ayele, Raghuvanshi, T.K., and Kala, P.M. (2014). Application of Remote Sensing and GIS for Landslide Disaster Management: A Case from Abay Gorge, Gohatsion-Dejen Section, Ethiopia. In: Singh, M., Singh, R., Hassan, M., (eds) Landscape Ecology and Water Management. Advances in Geographical and Environmental Sciences. Springer, Tokyo.

Skempton, A.W. (1985). Residual strength of clays in landslides, folded strata and the laboratory. Geotechnique, 35(1), 3-18.

Spencer, E. (1967). A method of analysis of stability of embankments assuming parallel inter-slice forces. Géotechnique, 171:11–26.

Stark, T. D., Choi, H., and McCone, S. (2005a). "Drained shear strength parameters for analysis of landslides." J. Geotech. Geoenviron. Eng. 131(5):575-588.

TarekegnTadesse (1993). Recent landslide and resulting damages in the Blue Nile River Gorge and its tributaries, E. Gojam Zone.Unpublished Technical Report.Geological Survey of Ethiopia.

Varnes, D. J. (1958). Landslide Types and Processes. In Landslides and Engineering Practice (Eckel, E. B., ed.), HRB, Special Rept. 29, 1958, pp. 20-47.

Varnes, D.J. (1978). Slope movement types and processes. In R.L. Schuster and R.J. Krize (eds), Landslides: Analysis and Control. Transportation Research Board, National Academy of Sciences, Washington, D.C.

Wolela, A. (2007), Source Rock Potential of the Blue Nile (Abay) Basin, Ethiopia. Journal of Petroleum Geology, 30: 389–402.

Yoseph Endalamaw. (2010). Landslide Assessment in Blue Nile Gorge, Central Ethiopia. Unpublished Masters's thesis. Gent University, Belgium.

Zaruba, Q. and Mencl, V. (1969). Landslides and their Control, Elsevier, Amsterdam – London – Wien, pp 205.

Annex

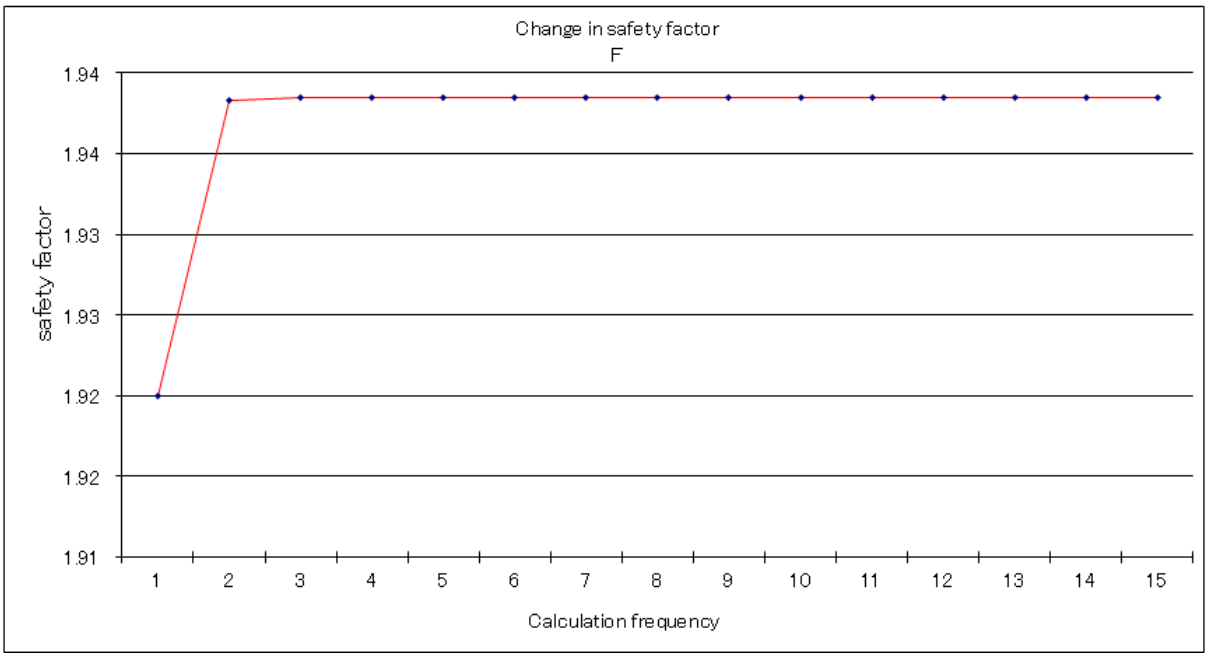

Annex 1. *Factors of safety calculated and plotted in Microsoft Excel spread sheet program according to simplified Janbu's method and corresponding landslide cross sectional area (right) for Profile 8.*

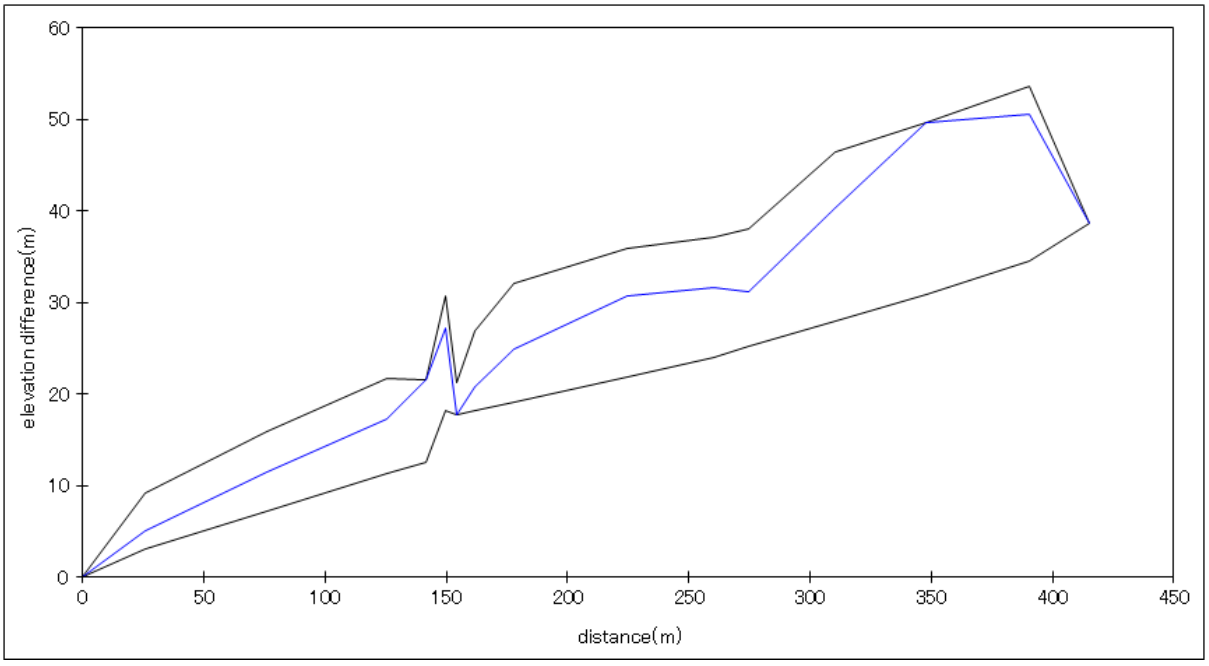

Annex 2. *Landslide cross section area of Profile 8 considered for the analysis of stability in 2D as well as semi- 3D cases.*

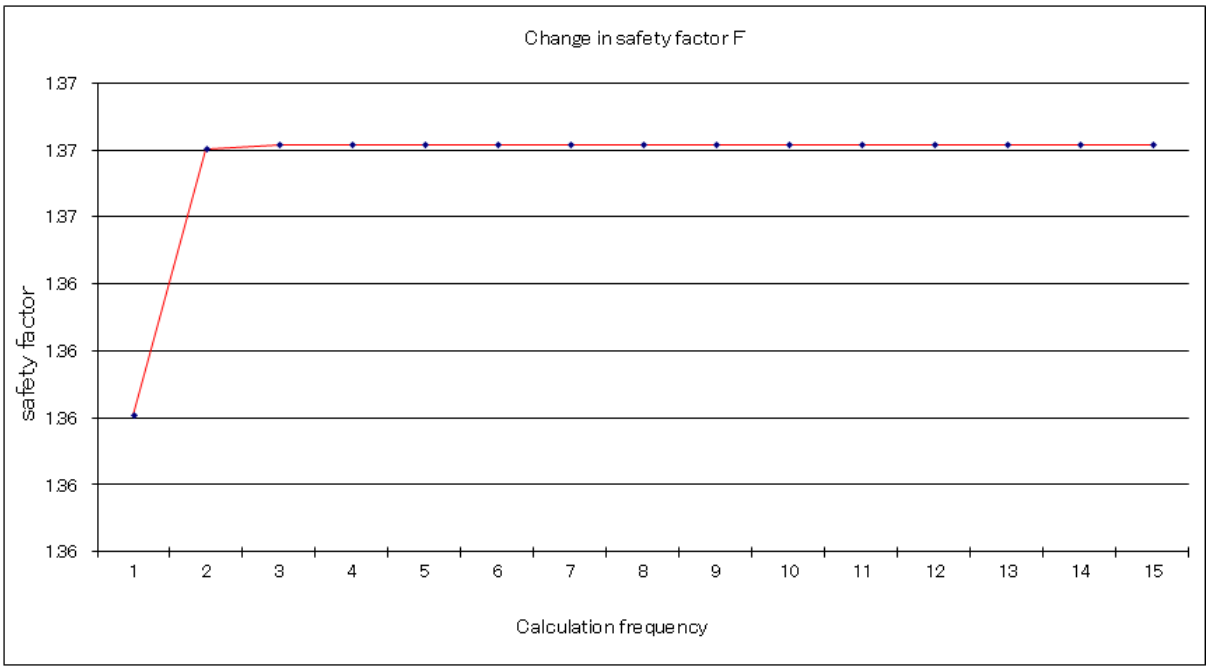

Annex 3. *Factors of safety calculated and plotted in Microsoft Excel spread sheet program according to simplified Janbu's method for Profile 9.*

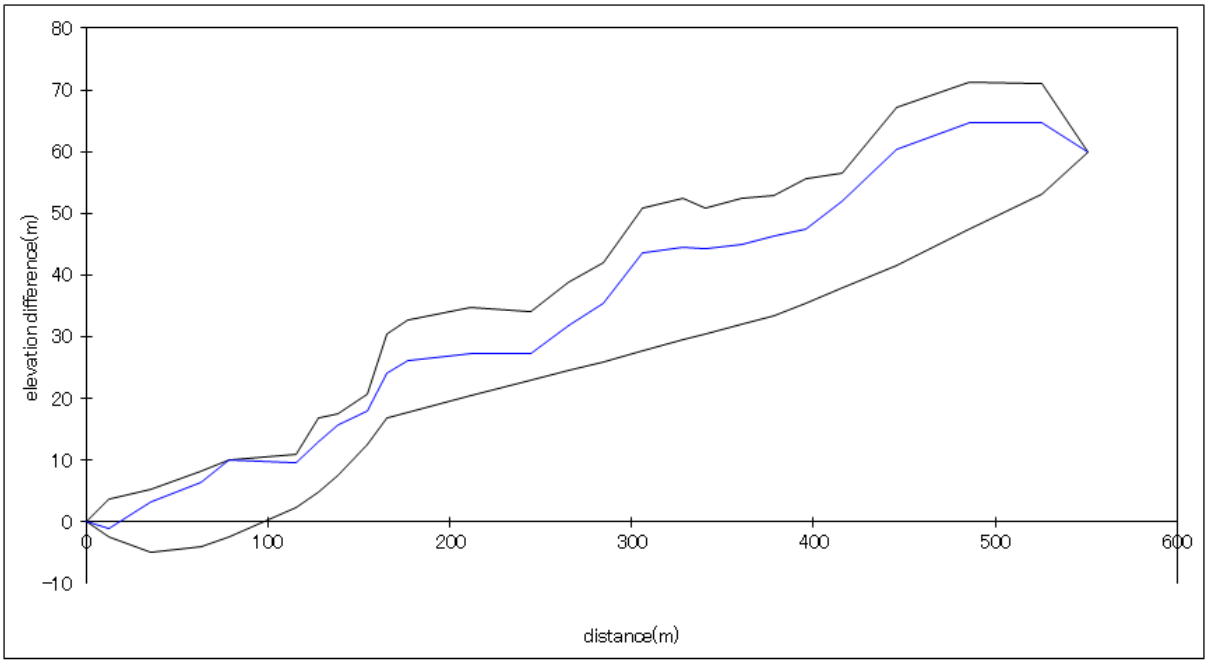

Annex 4. *Landslide cross section area of Profile 9 considered for the analysis of stability in 2D as well as semi- 3D cases.*

.

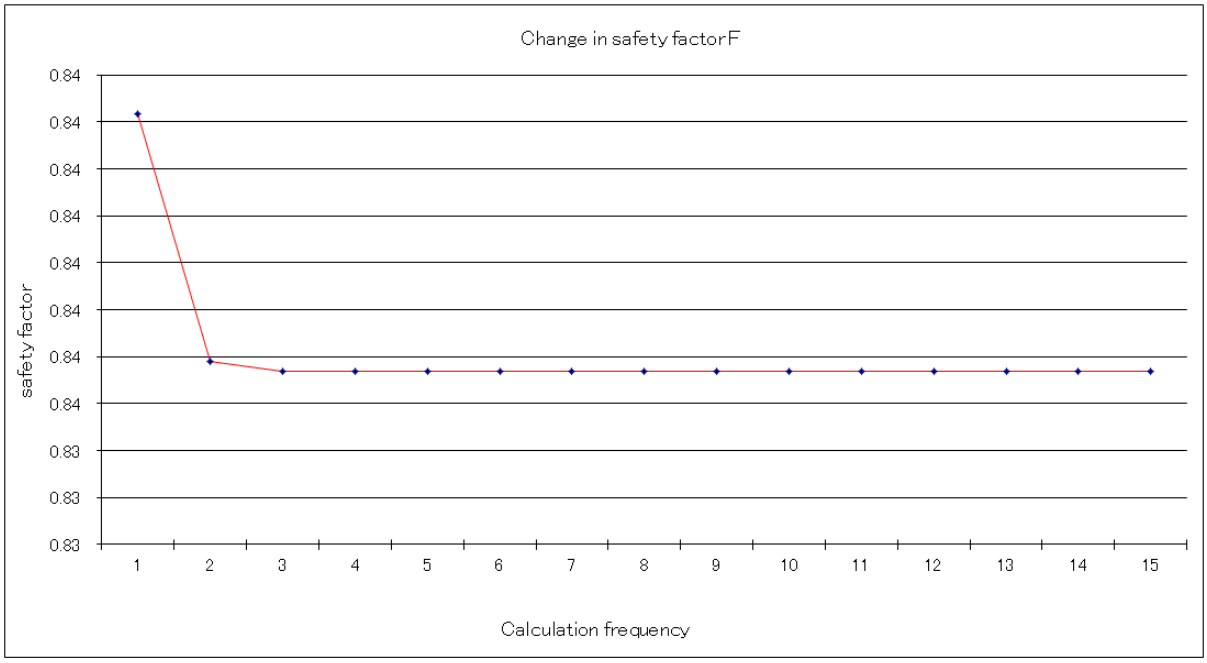

Annex 5. *Factors of safety calculated and plotted in Microsoft Excel spread sheet program according to simplified Janbu's method for Profile 10.*

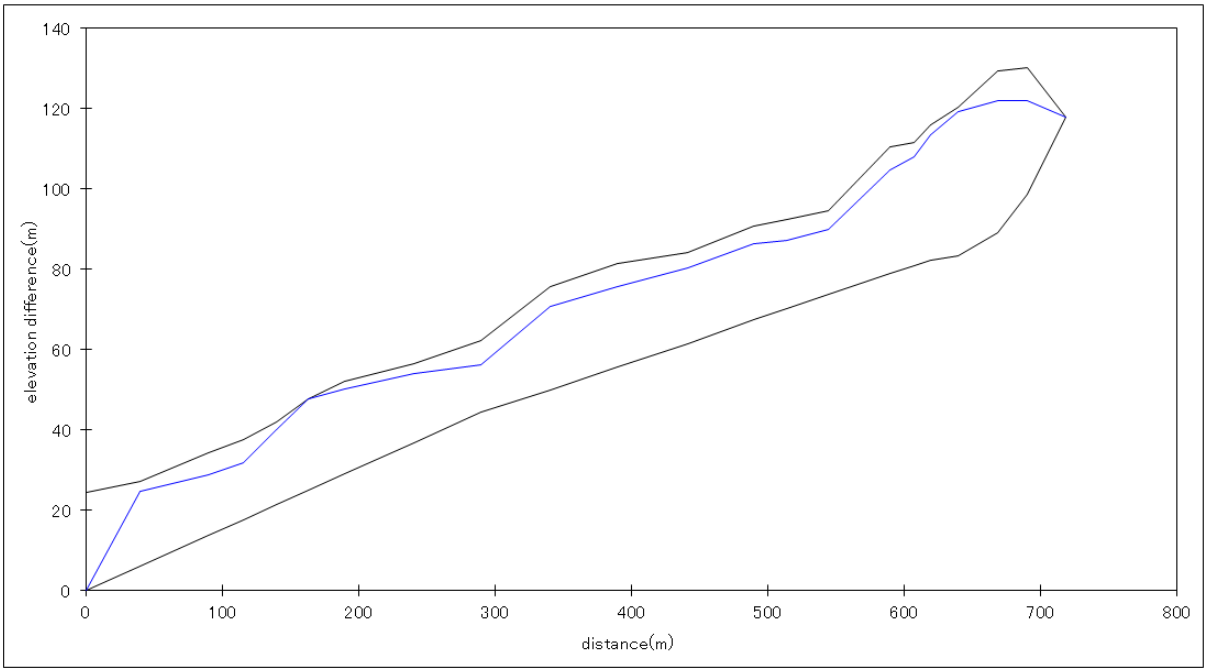

Annex 6. *Landslide cross section area of Profile 10 considered for the analysis of stability in 2D as well as semi- 3D cases.*

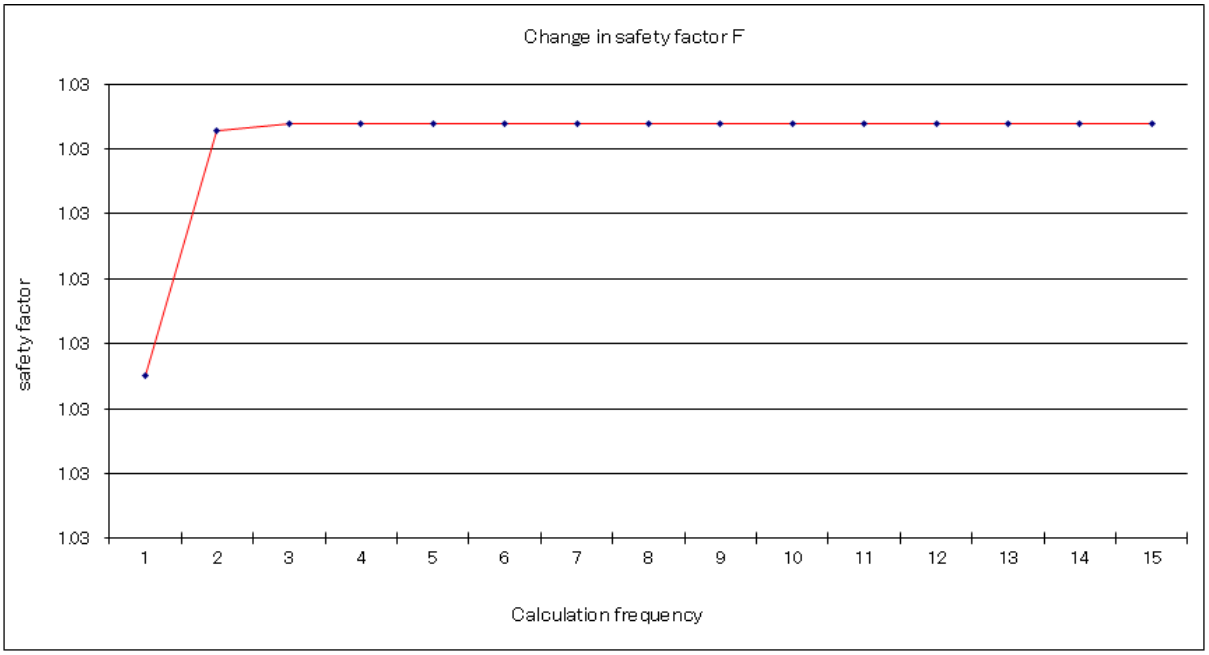

Annex 7. *Factors of safety calculated and plotted in Microsoft Excel spread sheet program according to simplified Janbu's method for Profile 11.*

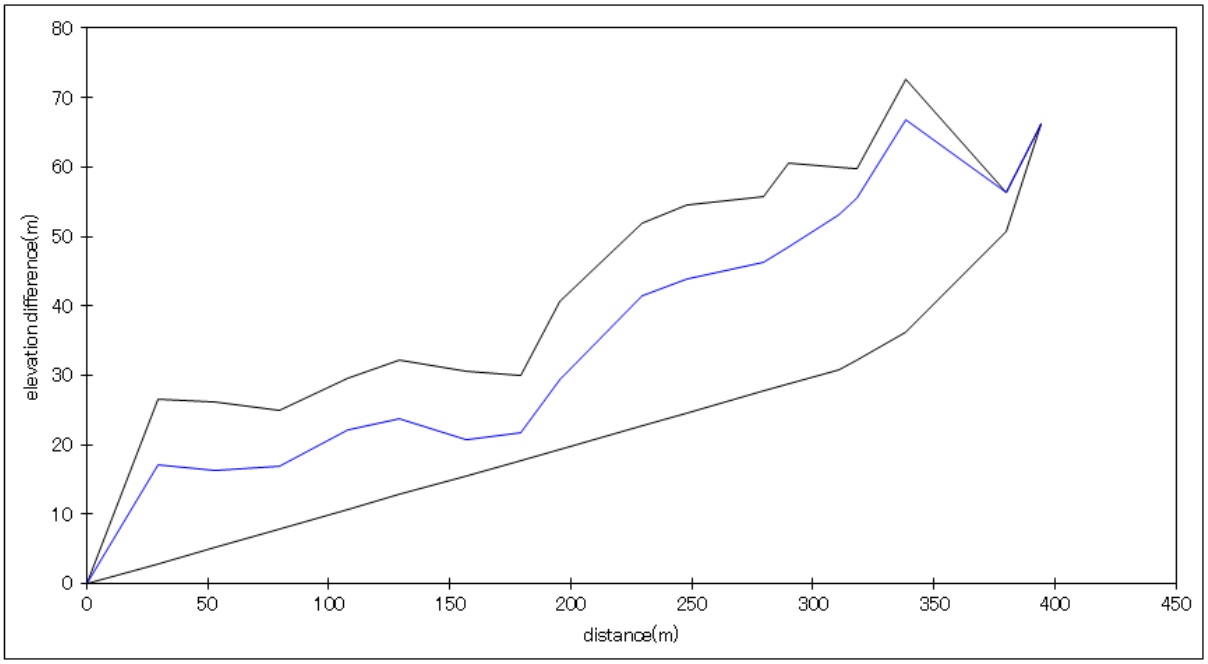

Annex 8. *Landslide cross section area of Profile 11 considered for the analysis of stability in 2D as well as semi- 3D cases.*

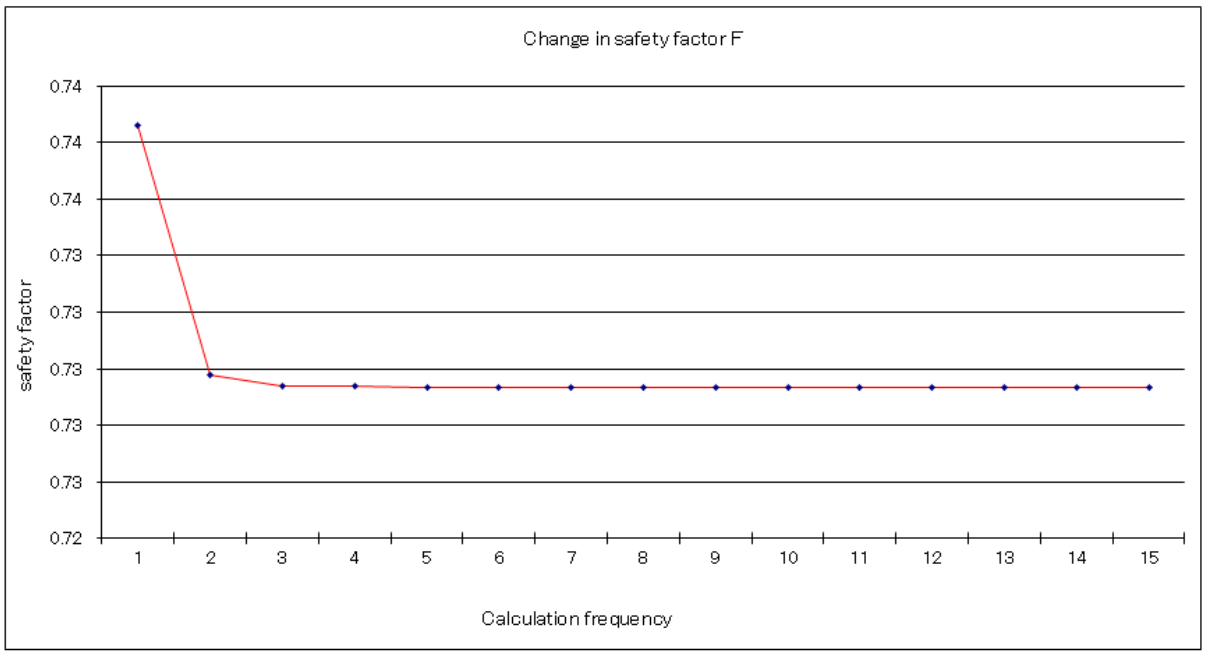

Annex 9. *Factors of safety calculated and plotted in Microsoft Excel spread sheet program according to simplified Janbu's method for Profile 14.*

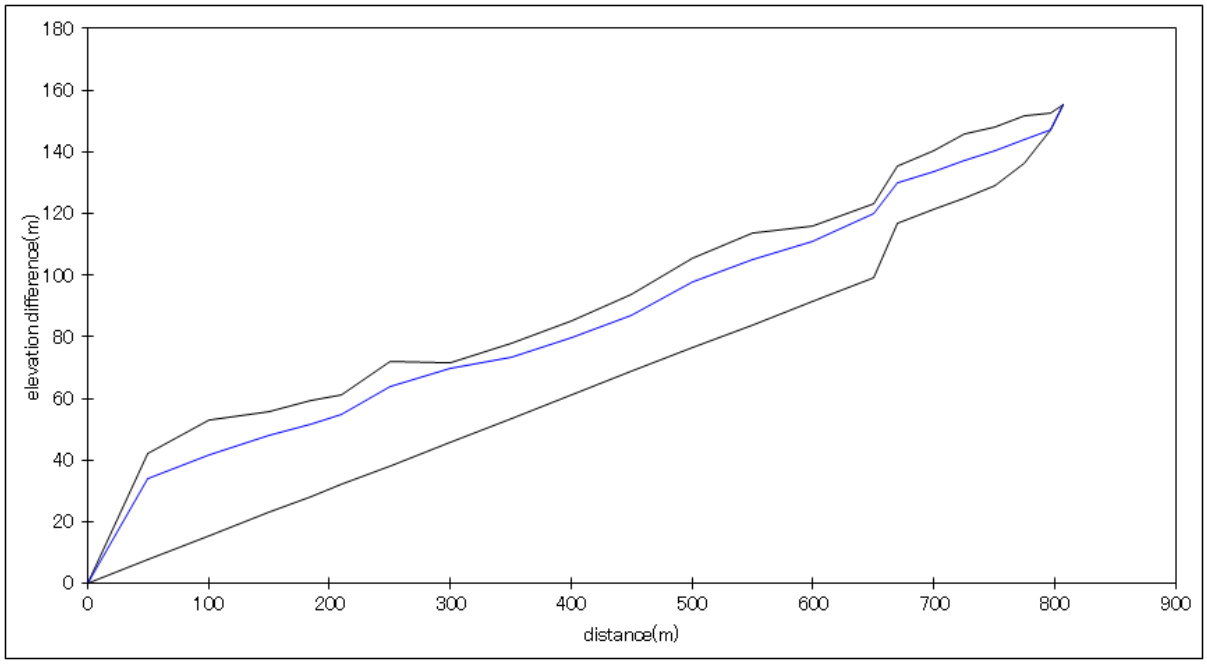

Annex 10. *Landslide cross section area of Profile 14 considered for the analysis of stability in 2D as well as semi- 3D cases.*

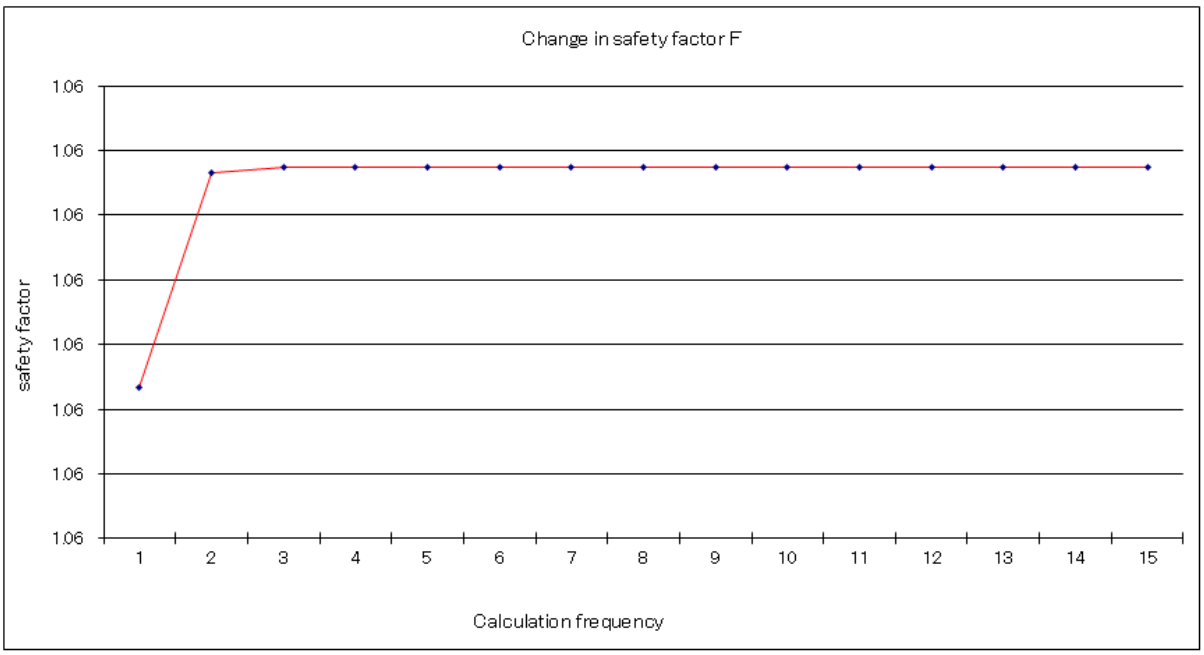

Annex 11. *Factors of safety calculated and plotted in Microsoft Excel spread sheet program according to simplified Janbu's method for Profile 15.*

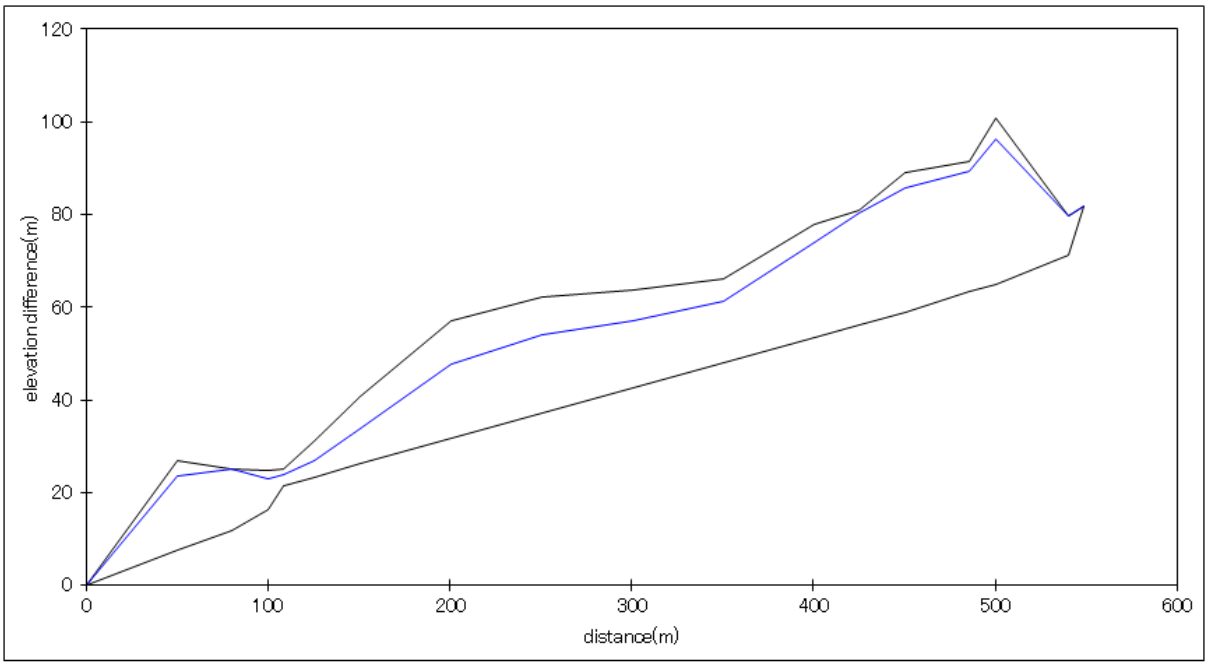

Annex 12. *Landslide cross section area of Profile 15 considered for the analysis of stability in 2D as well as semi- 3D cases.*

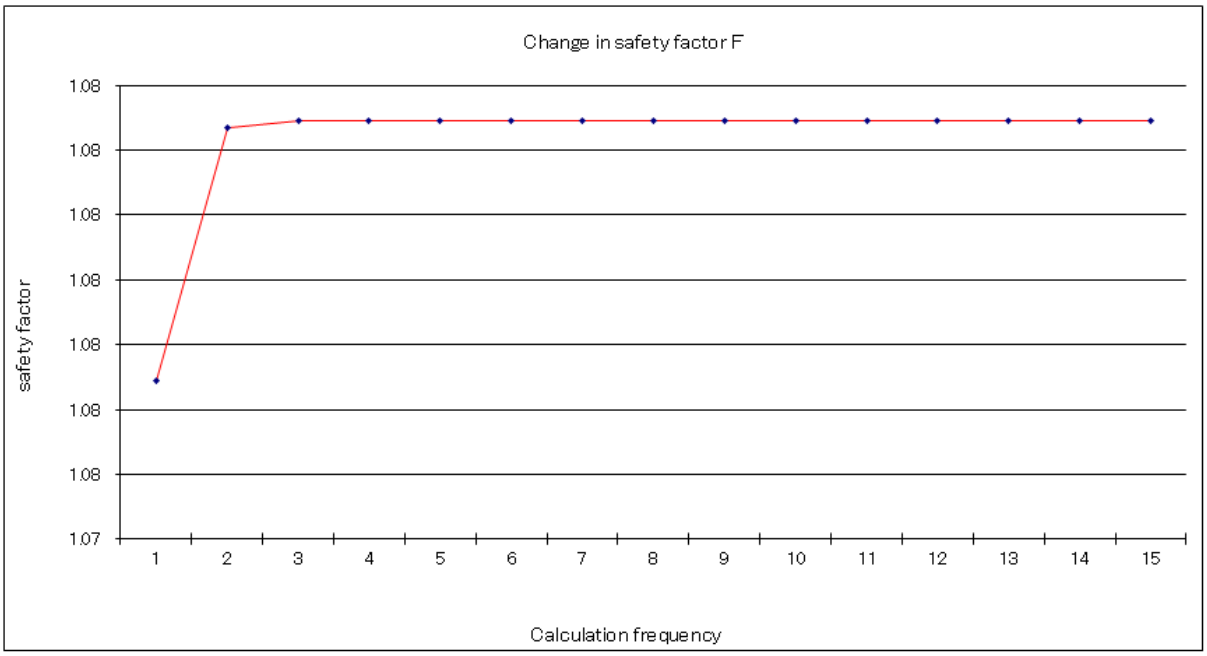

Annex 13. *Factors of safety calculated and plotted in Microsoft Excel spread sheet program according to simplified Janbu's method Profile 16.*

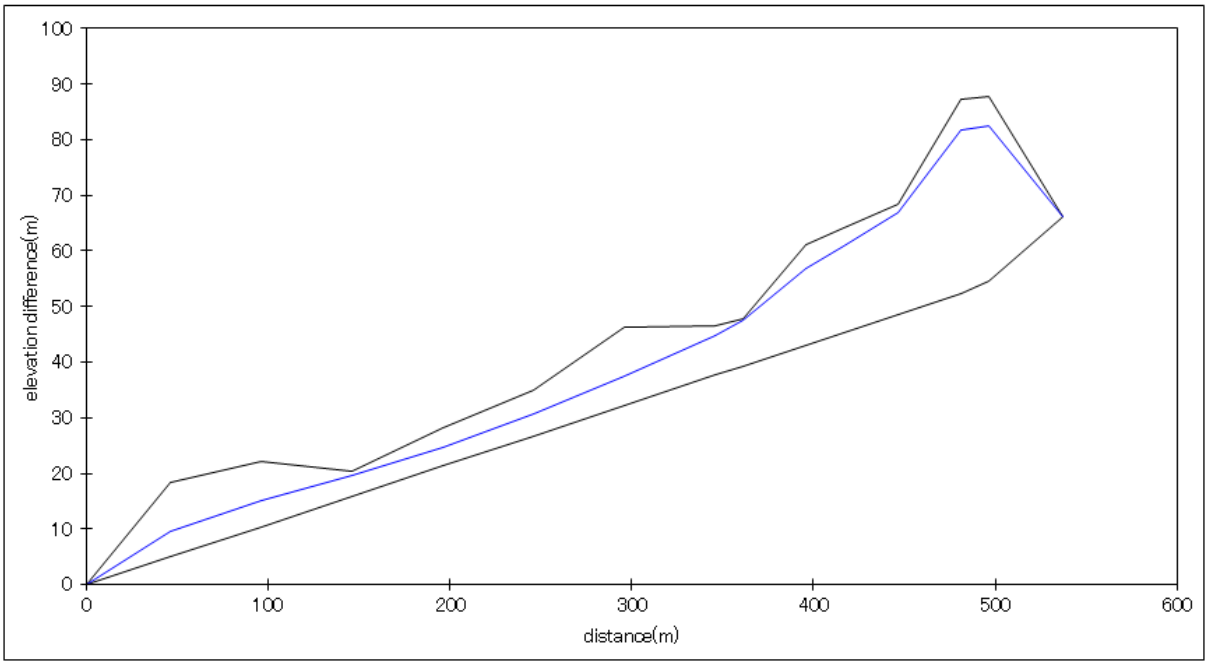

Annex 14. *Landslide cross section area of Profile 16 considered for the analysis of stability in 2D as well as semi- 3D cases.*